JOAN SEBASTIAN GARCIA VILLA

Optimization and Comparison between Polymer, Surfactant-Polymer and Water Flooding Recoveries in a Pre-salt Carbonate Reservoir Considering Uncertainties

Master Thesis presented to the Graduate Program in Mining Engineering at the Escola Politécnica da Universidade de São Paulo to obtain the degree of Master of Science.

São Paulo

2019

JOAN SEBASTIAN GARCIA VILLA

Optimization and Comparison between Polymer, Surfactant-Polymer and Water Flooding Recoveries in a Pre-salt Carbonate Reservoir Considering Uncertainties

Master Thesis presented to the Graduate Program in Mining Engineering at the Escola Politécnica da Universidade de São Paulo to obtain the degree of Master of Science.

Concentration area: Mining Engineering

Supervisors:

Prof. Ph.D. Jean Vicente Ferrari

Prof. Ph.D. Marcio Augusto Sampaio Pinto

São Paulo

2019

Este exemplar foi revisado e corrigido em relação à versão original, sob responsabilidade única do autor e com a anuência de seu orientador.

São Paulo, _____ de _____ de _____

Assinatura do autor: _____

Assinatura do orientador: _____

Catalogação-na-publicação

Name: GARCIA VILLA, Joan Sebastian

Title: Optimization and Comparison between Polymer, Surfactant-Polymer and Water Flooding Recoveries in a Pre-salt Carbonate Reservoir Considering Uncertainties

ACKNOWLEDGMENTS

ABSTRACT

GARCIA VILLA, J. S. **Optimization and Comparison between Polymer, Surfactant-Polymer and Water Flooding Recoveries in a Pre-salt Carbonate Reservoir Considering Uncertainties.** 2019. 156 p. Dissertation (Master's degree) – Mining and Petroleum Engineering Department of the Escola Politécnica of the University of Sao Paulo, Sao Paulo, 2019.

A successful Chemical Enhanced Oil Recovery (CEOR) program starts with a proper process selection for a given field, followed by a formulation of the batch components and a representative simulation step. Also, lab studies, field data, pilot testing, and economic analyses are required before project implementation. This work discusses the state of the art of the Surfactant-Polymer flood (SP) EOR technique, specifically for carbonate reservoirs, and states a methodology mixing laboratory, literature and reservoir simulation, to assess its applicability under economic and geological uncertainties. First, it is explained concepts related to the research, such as polymer, surfactant, microemulsion, functionalities of each chemical injected, advantages, and disadvantages. Second, a state of the art is developed about recent SP advances. Third, it is described the laboratory method being used to evaluate some properties of the chemicals injected for the Polymer flooding (PF) and SP flooding. Later, the simulation study step being conducted is explained, which will define the volume recovered and Net Present Value (NVP) obtained for the PF, SP injections and water flooding, in different economic and geological scenarios for two models resembling carbonate Brazilian reservoirs. Finally, it is discussed the results obtained, future researches that could be performed, and the respective bibliography. As part of this research, it was verified the Xanthan gum shows adequate results at different concentrations; that a surfactant specifically selected for a carbonate rock with low Interfacial tension and low adsorption is required; also that for the Lula based model although the polymer flooding and Surfactant-Polymer simulation brought some benefits, when compared with the waterflooding, on different economic scenarios and geological models, the high cost associated to the chemical handling facilities and volume spent do not make favorable its application in any scenario. On the contrary for the Cerena I field model, it was found the SP and Polymer flooding on all cases brought better results when compared with the water injection. Concluding that the performance and success of a CEOR program require finding the correct slug

characteristics for the unique conditions of each reservoir. In this research the reservoir with higher production rates made possible the use of Chemical EOR presenting better results than a water injection however in the smaller model they were not economically viable due to the additional associated prices.

RESUMO

GARCIA VILLA, J. S. **Otimização e comparação entre recuperação por injeção de Polímero, Surfactante-Polímero e Água num reservatório carbonático do Pré-sal considerando incertezas.** 2019. 156p. Dissertação de Mestrado – Departamento de Engenharia de Minas e Petróleo da Escola Politécnica da Universidade de São Paulo, 2019.

Um programa bem-sucedido de recuperação melhorada de petróleo por método químico (CEOR) começa com uma seleção precisa do processo para um determinado campo, seguido pela formulação dos componentes e uma etapa de formulação representativa. Adicionalmente, testes laboratoriais, dados de campos, testes pilotos e análises econômicas são necessárias antes da implementação de um projeto. Este trabalho discute o estado da arte da técnica de recuperação melhorada de petróleo (EOR) pela injeção de surfactante-polímero (SP), especificamente para reservatórios carbonáticos e, utilizada uma metodologia baseada em dados de laboratório, literatura e de simulação de reservatório para avaliar sua aplicabilidade sob incertezas econômicas e geológicas. Primeiramente, são explicados conceitos necessários a este trabalho relacionados com polímero, surfactante, microemulsão, funcionalidades de cada produto químico injetado, vantagens e desvantagens. Em segundo lugar, um estado da arte é desenvolvido sobre os avanços recentes do SP. Após, descreve-se os métodos laboratoriais utilizados para avaliar algumas propriedades dos produtos químicos usados nas injeções de Polímeros (PF) e SP.

Posteriormente, é explicada a etapa do estudo de simulação, que definirá o volume recuperado e o *valor* presente líquido (NVP), obtidos para injeções PF, SP e água, em diferentes cenários econômicos e geológicos, para dois modelos semelhantes a reservatórios carbonáticos brasileiros. Por fim, são discutidos os resultados obtidos, sugestões de trabalhos futuros e apresentação da bibliografia. Como parte desta pesquisa, verificou-se que a goma xantana apresenta resultados consistentes em diferentes concentrações e que é necessário um surfactante especificamente selecionado para uma rocha carbonática, possuindo baixa tensão interfacial e baixa adsorção. Para o modelo baseado em Lula, embora a simulação de injeção de polímero e surfactante-polímero tenham trazido alguns benefícios, quando comparados com a injeção de água, em diferentes cenários econômicos e modelos

geológicos, o alto custo associado às instalações de manipulação química e volume gasto não favorece sua aplicação em qualquer cenário. Por outro lado, no modelo de campo Cerena I, verificou-se que as injeções de SP e de polímero, em todos os casos, trouxeram melhores resultados quando comparadas com a injeção de água. Concluindo, o desempenho e o sucesso de um programa de CEOR exige encontrar as corretas características de slugs para condições únicas de cada reservatório. Neste trabalho, o reservatório com maiores taxas de produção infere que o método químico de EOR apresente melhores resultados quando comparado com a injeção de água.

Palavras-chave: recuperação melhorada de petróleo, surfactante-polímero, polímero, reservatório carbonático, Otimização por Enxame de Partículas, valor monetário esperado

LIST OF FIGURES

LIST OF TABLES

LIST OF ACRONYMS

API:	American Petroleum Institute or API gravity
AS:	Alkaline-surfactant flooding
ASP:	Alkaline-Surfactant-Polymer flooding
BHP:	Bottom Hole Pressure
BPD:	Barrels Per Day
CEOR:	Chemical Enhanced Oil Recovery
CMC:	Critical Micelle Concentration
CMG:	Computer Modelling Group
CTAB:	Hexadecyltrimethylammonium Bromide
EMV:	Expected Monetary Value
EOR:	Enhanced Oil Recovery
HPAM:	Hydrolyzed Polyacrylamide
IFS:	Inverted Five Spot model
IFT:	Interfacial Tension
IOR:	Improved Oil Recovery
LSSVM:	Least Square Support Vector Machine Learning
MMm3:	Million Cubic meters
MMUSD:	Million dollars
NPV:	Net Present Value
OOIP:	Original Oil in Place
PF:	Polymer Flooding
PSO:	Particle Swarm Optimization
PV:	Pore Volume
PVT:	Pressure-Volume-Temperature Analysis
RF:	Recovery Factor
SP:	Surfactant-Polymer flooding
SWCT:	Single Well Chemical Tracer Test
TAN:	Total Acid Number
TDS:	Total Dissolved Solids
WCUT:	Water Cut percentage
WF:	Waterflooding
WI:	Water injection

LIST OF SYMBOLS

N_c: Capillary number

u: Fluid velocity

μ: Displacing fluid viscosity

σ: Interfacial tension

M: Mobility ratio

k_w: Water permeability

k_o: Oil permeability

μ_o: Oil viscosity

μ_w: Water viscosity

V_o/V_s: Solubilization ratio of oil

V_w/V_s: Solubilization ratio of water

c: Constant for IFT

σ_{mo}:   Interfacial tension between microemulsion and oil phases

σ_{mw}:   Interfacial tension between microemulsion and water phase

D: Number of parameters to be optimized

x_i: Particle position

N: Number of candidate solutions

X: Solutions for N candidate's population

$V_{i,t}$:   Velocity vector associated to a particle

t: Iteration of the algorithm

$P_{i,t}$:   Best solution at the iteration by the particle

$G_{i,t}$.   Global best solution of the swarm

r_1:   Random diagonals matrices of random numbers

c_1, c_2, c_3:   Constants of the PSO

NPV_i: Optimal Net Present Value per case

P_i: Probability per model an economic scenario

C_o: Initial equilibrium concentration of the adsorbate

C_e: Equilibrium concentrations of the adsorbate

M: Mass of adsorbate solution in contact with the adsorbent

g_{rock}:   Weight of the adsorbent used

η: Apparent viscosity

K: Consistency index

| n: | Flow behavior index |
| γ: | Shear rate |

SUMMARY

1. INTRODUCTION

During the primary and secondary oil recovery phase, as a result of an inefficient macroscopic sweep and a microscopic capillary entrapment, the residual oil is found in the reservoir as a discontinuous volume of droplets which can reach up to 70% of the original oil in place (HIRASAKI; MILLER; PUERTO, 2011), leaving in average only one third of crude acquirable with conventional techniques. Therefore, one of the biggest challenges the oil industry has encountered is to increment the global efficiency of oil recovery on mature reservoirs worldwide. Regarding EOR methods, the objective is to mobilize the residual oil by increasing the capillary number (Nc), which describes the ratio of viscous to capillary forces (CHO et al., 2018).

Since the higher the Nc, the lower the residual oil saturation (STEGEMEIER, 1977; AMRAN et al., 2017), the residual saturation on the reservoir strongly depends on the relationship found on the capillary number (N_c) equation,

$$N_C = \frac{u\mu}{\sigma} \qquad (1)$$

Where u is the fluid velocity, μ is the displacing fluid viscosity, and σ is the interfacial tension between displaced and displacing fluids. Regarding this equation, the increase of oil recovery can be achieved in three different ways: the first one would be an increase of displacing fluid viscosity, affecting the macroscopic sweep, but not the microscopic sweep. The second one would be a reduction of interfacial tension which does impact the microscopic sweep efficiency, possible with interfacial tension reducers and the third is by increasing the velocity of the fluid on the porous media (FARAJZADEH et al., 2012).

Between the enhanced and improved recovery methodologies being employed to increase the hydrocarbon recovery, it can be found a diverse selection of techniques in which chemical EOR methods (CEOR) are well established. The more well-known processes are polymer flood, surfactant flood, alkaline flood and any mix from the previous ones such as the alkaline-surfactant flood (AS), the alkaline-surfactant-polymer flood (ASP) and the surfactant-polymer flooding (SP). Processes where polymer has as main function to provide mobility control by viscosifying the water; the

surfactant reduces the interfacial tension and alter the rock wettability; and the alkaline reacts with the oil acids, generating an in-situ soap, which will provide an additional source for rock wettability alteration and a minor need of adding synthetic surfactant in the slug (CHANG et al., 2006; AYIRALA; YOUSEF, 2015).

However, although CEOR methods had an important growth in the 1980s, they are highly sensitive to oil prices and the chemical additive costs, if compared with other methodologies such as waterflooding, CO_2 injection, steam injection and water alternating gas (MANRIQUE; MUCI; GURFINKEL, 2007b). The techniques require finding the correct slug characteristics for the unique conditions of each reservoir. Variables such as chemical concentration, water ratio, ions presence, flow rate, and others influence the production program (OLAJIRE, 2014; SHENG, 2014). Moreover, challenges on field scale applications are also encountered: (1) operational difficulties, (2) surfactant precipitation, (3) difficulties in treating produced emulsions, (4) produced water disposal treatment, and (5) sole challenges of offshore application (OLAJIRE, 2014; SHENG, 2014).

There has been little report studying the SP injection on carbonate reservoirs, some authors when constructing screening parameters, do not include these type of rock formations, or even the SP injection because of the difficulties previously mentioned. As an example, Dickson (2010) do not include the SP injection, Taber (1997) and Al Adasani (2011) proposed screenings recompiling several parameters from other authors, where they recommend sandstones as reservoir rocks. The fact there is little report of field scale application on SP flooding, strictly speaking (no alkali injection), most of them were done before 1990, none in Latin America and only four applications on carbonate reservoirs successfully carried out in the literature between 1970 to 2018 (FOSTER, 1973; MILLER; RICHMOND, 1978; WKFMNYER, 1982; TALASH; STRANGE, 1982; THOMAS et al., 1982; RATERMAN, 1990; HOLLEY; CAYLAS, 1992; BOU-MIKAEL et al., 2000; MANRIQUE; MUCI; GURFINKEL, 2007a; ZHU et al., 2012; ZHENQUAN et al., 2013; SHENG, 2013a; AL-AMRIE et al., 2015).

In consideration of these conditions and the previously mentioned challenges, the oil industry in offshore basins and carbonate reservoirs requires designs of SP programs with the following characteristics: (1) chemicals usable in adversary reservoir conditions, (2) designs flexibles for carbonate reservoir rocks, (3) divalent tolerable

chemicals, pre-salt conditions are over 50.000 ppm (BELTRAO et al., 2009), (4) surfactants with lower precipitation tendency (with divalent ions), (5) single formulation for different field requirements, and, (6) chemicals with less environmental effects (OLAJIRE, 2014; AL-SINANI et al., 2016).

Therefore, defining the applicability of SP flooding as an alternative for a Brazilian carbonate formation requires studying a program containing surfactant and polymer injection. In this research, a preliminary selection of products available is discussed, considering the rock properties and formation fluids. Secondly, it is evaluated the laboratory information and literature data which is used on the simulation phase based on the requirements of a carbonate reservoir with conditions like an offshore pre-salt field.

The simulation study was carried by using two synthetics 3D reservoir models resembling the Jupiter Field and Lula Field. The former was related to the CERENA I, a synthetic model benchmark built by the CERENA Institute (MADEIRA, 2014) because resembles some of the common characteristics of a Brazilian Pre-Salt carbonate (medium oil, high CO_2 content, and high pressures) with a microbiolite reservoir and a non-reservoir facies. The latter was obtained and adjusted from literature data also for the Brazilian pre-salt. An evaluation of two models was selected to evaluate how, despite being two Brazilian offshore reservoirs, their characteristics differ between each other such as temperature, PVT model, wettability, pressure, and CO_2 content.

The inputs information for the simulation study regarding some physical-chemical parameters from the selected chemicals were obtained from the laboratory experimentation for the polymer (xanthan gum) and literature review for the surfactant (zwitterionic type). Concerning the surfactant, available laboratory screening tests were carried out in some available materials to guide the choice of the literature surfactant data for the simulation input. For all cases, a high salinity scenario was considered, as conditions over 50000 ppm chloride content are observed in the field (BELTRAO et al., 2009).

After analyzing the results, it is discussed if it is viable or not the injection of SP as a possible Chemical-EOR technique for further studies on Brazilian offshore conditions.

1.1. OBJECTIVES

1.1.1. General Objective

To compare the technical and economic performance of the SP flooding against a waterflooding and a polymer flooding case in both synthetic pilot numerical simulations.

1.1.2. Specific Objectives

- To evaluate the technical and economic performance of a chosen SP formulation in a numerical simulation of a synthetic 3D reservoir model with an inverted five-spot scheme resembling the Lula Field.
- To evaluate the technical and economic performance of a chosen SP formulation in a numerical simulation of a synthetic 3D reservoir model with an inverted five-spot scheme resembling the Jupiter Field.

2. FUNDAMENTALS

On an SP flood, the polymer has as primary function providing mobility control, while the surfactant reduces the interfacial tension between water and oil phases, improving the final oil recovery on the reservoir. However, it presents disadvantages such as low permeability pore plugging, high costs either by manufacturing or storage and treatment facilities, high instability in harsh conditions (such as high salt concentration and high temperature) and mechanical degradation of the polymer (SRIVASTAVA et al., 2009). Reasons why finding alternatives and improving the performance of this injection, has been crucial. Next, it is relevant to introduce some key concepts for the SP flooding, the object of this work.

2.1. SURFACTANT (S)

An amphiphilic compound, with two functional groups, where the first is hydrophilic and the second one is hydrophobic, containing then: a water-insoluble tail and a water-soluble head (OLAJIRE, 2014), an example on **Figure 2.1-1**.

Figure 2.1-1 Schematic of a surfactant structure.
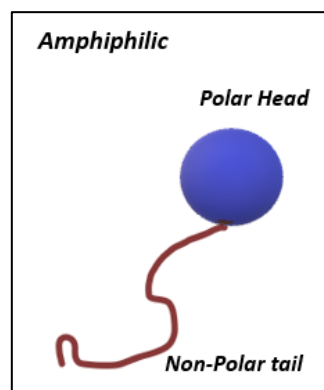
Source: Author, 2019.

Surfactants can be classified as anionic, cationic, nonionic, and zwitterionic according to the ionic nature of their head group. The anionic surfactants have a negative charge and are more widely used for EOR projects on sandstone reservoirs. Cationic ones have a positive surface-active portion and low adsorption on carbonate reservoirs but are expensive. Nonionic surfactants have no apparent ionic charge, are

more tolerable to high salinity, but they don't reduce the IFT as good as the other types, therefore are employed as cosurfactants to improve the phase behavior system. Zwitterionic have both ionic charges, have strong electrolyte tolerance (therefore salt tolerance), are thermodynamically stables, but they are not that extensively studied as the other types of surfactants (ROSEN, 2004; SHENG, 2013b).

The main objective of surfactant use on the batch is to reduce the interfacial tension (IFT) between the water and the oil, recovering, in that way, the residual oil trapped on the pores of the rocks. When the oil encounters the chemical batch, the surfactant accumulates between the fluids contact interface and it forms an adsorbed layer, which reduces the IFT. This one allows the dispersed oil droplets to be swept and produced.

Levitt et al., (2009, 2016) mentioned the formulation requirements for a surfactant being employed in an EOR method:

- The surfactant solubilization ratio ≥ 10 (explained in the microemulsion section);
- Low viscosity microemulsion phase with low apparent macroemulsion;
- A transparent solution at reservoir temperature (no oil addition conditions);
- Low adsorption on the rock surface.

2.2. POLYMER (P)

A polymer is a long chain molecule formed by the joining of smaller molecules called monomers, which results in a high molecular weight (KASIMBAZI, 2014). It is employed in EOR methodologies to increase the sweep efficiency of the injected fluid by reducing the mobility ratio defined as:

$$M = \frac{k_w \mu_o}{\mu_w k_o} \qquad (2)$$

Where M, k_w, k_o μ_o, and μ_w are mobility ratio, water and oil relative permeability at the endpoints and oil and water viscosity, respectively. The polymer, when incorporated on the water injection, increases the viscosity of the displacing fluid,

reaching then closer values to one (1), which is defined as a controlled process (Rosa, Carvalho, & Xavier, 2006).

Sheng, Leonhardt and Azri (2015) describe the sweep efficiency increasing because of reducing viscous-fingering, improving the displacing fluid injection profile due to crossflow between vertical heterogeneous layers and longest permeability reduction after the flooding of the solution containing polymer. In **Figure 2.2-1** can be observed an example of the areal sweep efficiency of a water injection compared with the one obtained with a polymer injection for an inverted five spot model. **Figure 2.2-1a** shows a simplified aerial view of how the water channels in the reservoir resulting in lower recovery efficiencies, while **Figure 2.2-1b** resembles the polymer flooding which reduces fingering issues and reaches a larger area than the first by having a more homogeneous front.

Figure 2.2-1 Areal sweep efficiency of (a) water and(b) polymer injections.
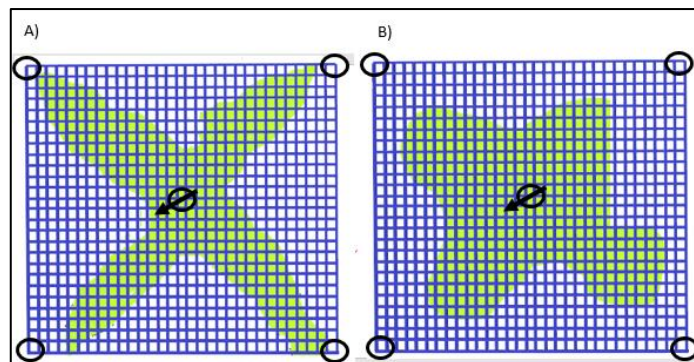
Source: Author, 2019.

Two main types of polymers are employed in chemical EOR methodologies (CEOR), synthetic polymers such as partially hydrolyzed polyacrylamide (HPAM) and biopolymers such as Xanthan gum and Scleroglucan (SHENG, 2011; KULAWARDANA et al., 2012; KASIMBAZI, 2014; MOHAMID et al., 2015). The HPAM is the most widely used because of its low costs and larger viscoelasticity than other polymers; however, it is susceptible to the brine salinity and hardness (OLAJIRE, 2014). On the other hand, biopolymers and specifically Xanthan gum are relatively insensitive to salinity and hardness, but their main disadvantage is their susceptibility to bacterial degradation (KASIMBAZI, 2014). Examples of these polymer structures can be observed in **Figure 2.2-2** and **Figure 2.2-3**.

Figure 2.2-2 Polyacrylamide and Hydrolyzed Polyacrylamide – HPAM chemical structures.
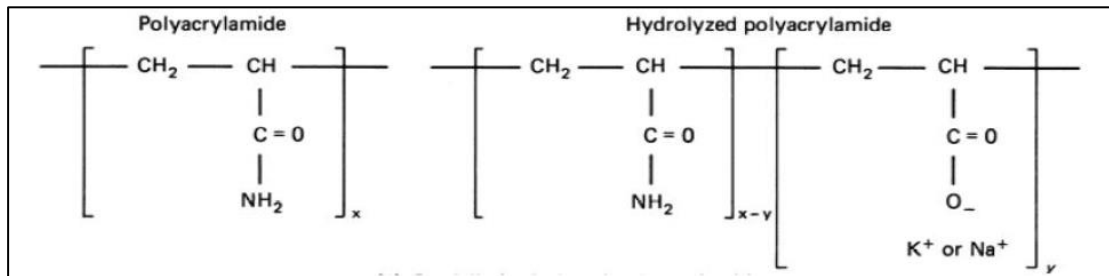
Source: OLAJIRE, 2014.

Figure 2.2-3 Example of a Xanthan gum chemical structure.
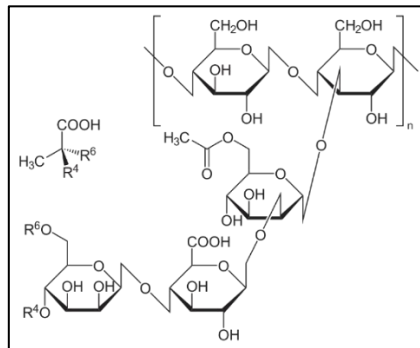
Source: OLAJIRE, 2014.

According to Levitt et al. (2009, 2016) a polymer solution for an EOR method must meet the following parameters:

a. Aggregates low or free polymer solution to ensure there are no particles capable of plugging the formation (indicated by a filter ratio test);
b. Acceptable injectivity in the reservoir;
c. Stable at reservoir temperature and ionic composition over a reservoir-residence timescale.

2.3.   MICROEMULSION TYPES

The Winsor classification (Winsor, 1954) identifies four general types of phase equilibrium for the microemulsion. On type I, the surfactant is preferentially water soluble, and the microemulsion is oil in water (o/w). In this case, the rich-surfactant water phase coexists with the oil phase, where the surfactant appears in the form of

monomers at low concentration. On type II, the surfactant appears mainly on the oil phase and the microemulsion formed is water in oil (w/o), in which, the surfactant-rich oil phase coexists with the poorest aqueous phase. On type III, a triphasic system is generated where the intermediate phase rich on surfactants, coexist with the water and oil phases, both with a low surfactant concentration. Finally, in type IV, one micellar solution phase appears, which is formed when there is enough addition of an amphiphilic volume. In **Figure 2.3-1** can be observed the schematic of how each microemulsion (ME) type behaves according to the previously discussed.

Figure 2.3-1 Schematic examples of microemulsion phase behavior types according to Winsor classification.
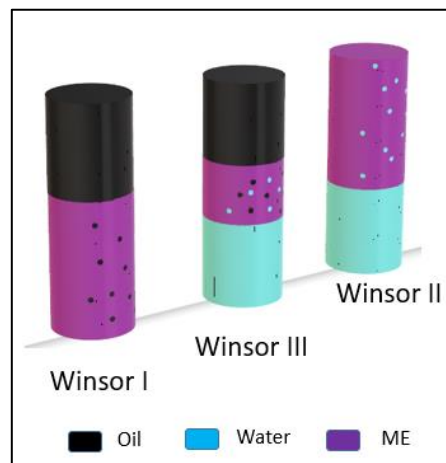
Source: SHENG, 2011.

Technically, type III is preferred, because it reaches an ultra-low IFT between the microemulsion phase and the water and oil-rich phases (equal or less than $1x10^{-3} \, mN/m$ for successful solubilization and oil recovery). It sweeps the remaining oil as one unified bank with little entrapment of the microemulsion phase, which means that there will be a larger area swept by the surfactant and a bigger volume of chemistry recovered on the surface facilities. Attention must be taken to the optimal salinity ranges where the type III microemulsion can be reached, meaning that it can be considered a crucial factor in a surfactant-based flood.

The solubilization ratio of oil is the ratio of the volume of solubilized oil to the volume of surfactant present (V_o/V_s), and the solubilization ratio of the water is calculated following the same concept for the water volume (V_w/V_s). The optimal salinity can be defined as the point where the solubilization ratios V_o/V_s and V_w/V_s are equal (ZHANG et al., 2006). Huh (1979) proposed that for a classical Winsor III

behavior the solubilization ratios between the microemulsion phase and excess oil and brine phases respectively were defined as,

$$\sigma_{mo} = c/\left(\frac{V_o}{V_s}\right)^2 \qquad (3) \qquad \sigma_{mw} = c/\left(\frac{V_w}{V_s}\right)^2 \qquad (4)$$

Where c is a constant for each system, σ_{mo} and σ_{mw} are the interfacial tension between phases on a Winsor type III microemulsion. This way, the IFT of the mixture (water, oil and surfactant) can be calculated based on experimental data of solubilization ratios.

2.4. CRITICAL MICELLE CONCENTRATION

As the concentration of a surfactant increases, molecules start to interact with each other and organize aggregates of larger numbers of molecules called micelles. In these, the lipophilic parts will associate in the interior of the aggregate, and the hydrophilic parts will face the aqueous medium. The concentration at which the molecules start to interact, and form micelles is called critical micelle concentration (CMC), and over its value, the surface tension will not be reduced any further. It depends highly on the surfactant type, while it has a smaller dependence on pressure and temperature (SCHRAMM; MARANGONI, 2001; BENT, 2014; LASKARIS, 2015). The surfactant effectiveness can be defined as how much the surface tension/interfacial tension can be reduced until reaching the CMC in the mixture. Therefore, it's a parameter which characterizes the surfactant and relates the IFT behavior, making its evaluation a detail to observe (CRAFT; ABDELRAHIM, 2012).

2.5. PARTICLE SWARM OPTIMIZATION

An optimization method was used in this research, the Particle Swarm Optimization algorithm (PSO), which will be later mentioned in the methodology section. The PSO is a global optimization method developed by Kennedy and Eberhart (1995) which can be explained by the behavior of bird flocks, where individual adjusts its fly vector according to their individual and the companion's experiences. In it, each PSO candidate, or particle, represents a D-dimensional space, being D the number of

parameters to be optimized (KEMMOÉ TCHOMTÉ; GOURGAND, 2009). Hence, the position of the particle and the population or swarm of N candidate's solutions can be described as

$$x_i = [x_{i1}, x_{i2}, \ldots, x_{iD}] \tag{5}$$

$$X = [X_1, X_2, \ldots, X_N\} \tag{6}$$

While an optimal solution is searched, the particles update their position iteratively based on the next relation:

$$V_{i,t+1} = c_1 V_{i,t} + c_2 r_1 (P_{i,t} - x_{i,t}) + c_3 r_1 (G_{i,t} - x_{i,t}) \tag{7}$$

where, $V_{i,t}$ it's the velocity vector associated to the particle, t and t+1 are two consecutive iterations of the algorithm, $P_{i,t}$ it's the best solution so far by the particle, $G_{i,t}$ it's the global best solution of the swarm, r_1 are random diagonals matrices of random numbers from a uniform distribution from 0 to 1 and c_1, c_2, c_3 are constants modulating the magnitude of the steps taken by a particle in the direction of its personal and global best solution.

2.6. EXPECTED MONETARY VALUE

According to Fraser and Seba (1993), the expected monetary value (EMV) combines quantitative probabilities (estimates) with each alternative element evaluated. This parameter is defined as the sum of the product of the probability of each outcome times the value of that outcome for all possible outcomes, so for this research purposes:

$$EMV = \sum_i \sum_j NPV_{ij} * P_i * P_j \tag{8}$$

where NPV_i it's the optimal Net Present Value for each possible case and P_i its the probability that of each the NPV's will occur.

The expected monetary value is used in this research to quantify the economic performance of the injection programs: waterflooding, polymer flooding, and Surfactant-Polymer flooding.

3. STATE OF THE ART

As described previously in the introduction, the benefits of both components on the SP method have a synergistic effect that may help to reach higher recovery factors on adequate production fields. However, the Surfactant Polymer flood is a CEOR method traditionally employed only in sandstone reservoirs and it has been less studied than ASP and Polymer floodings (TABER et al., 1997; MANRIQUE; MUCI; GURFINKEL, 2007b; ROMERO-ZERÓN, 2012; ZHU et al., 2012; OLAJIRE, 2014; SHENG, 2014).

Manrique et al. (2007) briefly explained that, although CEOR methods had an important growth in the 1980s, they are highly sensitive to oil prices and the chemical additive costs, if compared with other methodologies such as WAG, waterflooding, CO_2 flood. Moreover, they possess several issues to overcome, as described next.

Olajire (2014) resumes five challenges to overcome in order to put an ASP project in a field scale application, which can be extrapolated to an SP program: (1) operation difficulties, (2) surfactant precipitation, (3) difficulties in treating produced emulsions, (4) produced water disposal treatment and (5) sole challenges of offshore application. Meanwhile Zhu et al. (2012) describes five: (1) lack of high efficient and stable industrial surfactants, (2) lack of understanding on the oil displacement mechanism of the technique, (3) imperfect evaluation method, reflected in a non-existing standard methodology, (4) few pilot tests performed in history and (5) high technological risk. These difficulties limit the SP applicability and selection in a preliminary screening stage, but also bring forward the future developments that must be carried to make it attractive in other non-traditional scenarios.

There are few reports of field scale application on SP flooding, strictly speaking, alkali-free. Chauhan (2014) on his research reported 42 SP/Micellar Polymer flooding projects carried out worldwide until 2014, based on the Oil & Gas Journal biennially report, however, most of these projects are only mentioned on the

literature without further description of them. From this total, only 3 of the 33 projects on the U.S were performed on carbonate reservoirs, according to Manrique et al. (2007). Additionally, two more recent projects can be added to this list, the Illinois pilot (IZADI et al., 2018), and the Middle East pilot performed by Total S.A on an offshore carbonate reservoir (MOREL et al., 2016) summing up 44 projects.

From these projects mentioned previously, Sheng (2011), Zhu et al. (2012) and Manrique (2007) describe 12 of these projects, and they can be defined as the projects more documented in the literature. From this, it can be concluded: (a) most of them were done before the 1990s; (b) there are only four applications on carbonate reservoirs found in the literature, (c) there has not been any pilot or field development reported in Latin America; and (d) there is only one offshore project around the world. Some of these pilots are discussed next, including laboratory and simulation studies on carbonate rocks, high salinity brines and CEOR optimizations on reservoir simulation models. The overall distribution of these projects can be found in **Figure** *3-1*.

Figure 3-1 SP projects Worldwide status.

Source: MANRIQUE; MUCI; GURFINKEL, 2007; MOREL et al., 2008; SHENG; SHENG, 2011; ZHU et al., 2012; CHAUHAN, 2014; IZADI et al., 2018; LI et al., 2018

Next, will be introduced some field implementations, laboratory applications and simulation research relevant to this study as a guide for the work developed.

3.1. LABORATORY TESTS OF SP FLOODING ON HIGH SALINITY AND/OR CARBONATE RESERVOIRS

For the Bramberge reservoir in Germany, it was studied in the laboratory the use of an SP program with high salinity production brine, using adsorption inhibitors (TABARY et al., 2012). This onshore sandstone reservoir has high permeability, averaging 1 Darcy, low temperature (40°C), crude oil of 28.6 API, a water cut close to 95%, formation water salinity of 120 g/L and an injection brine with a TDS of 25-43 g/L. Their research focused on testing the performance of the SP program on different brine conditions, including diluting, brine treatments, and inhibitors. They concluded that despite softened water (low hardness) and its mixing can help the performance of the SP injection on a high salinity brine formation, the treatment processes required to achieve the softening makes these alternatives challenging to implement on field conditions. Concluding, of these alternatives the mixture including adsorption inhibitors was the one with the best results, as it obtained similar recoveries as the other alternatives and moreover the adsorption was reduced 50% to 70% when compared to the conventional solutions. These results showed the viability of a high salinity SP, an opportunity on unconventional scenarios.

Zaitoun et al. (2003) reported a study for the Chihuido field in Argentina of SP flooding at a laboratory scale for high salinity brine. The formation brine salinity moves close to 110.000 ppm and around 2.800 ppm TDS, which can be considered as high salinity in a sandstone formation. The rock has a porosity moving between 9 to 27 % and an average permeability of 45mD up to 400 mD, a light oil, 33 to 35 API, and 55°C. An anionic surfactant for IFT reduction and a sacrificial surfactant were evaluated on three experiments: coreflooding, static, and dynamic adsorption. The primary and sacrificial surfactant concentration was 0.125%w for each one of them, and it was obtained a final recovery of 36%, the lowest IFT measured was of

0.0036 mN/m and adsorption for the primary surfactant of 0.048 mg/g-rock. The study concluded that it is possible to use and SP injection on high salinity formations, with low surfactant concentrations and moderate adsorption on the rock.

Zhu et al. (2013) reported an ASP and SP laboratory study on a heterogeneous biostromal carbonate reservoir from Indonesia KS oilfield. The research focused on evaluating and comparing the adsorption of different surfactants and polymers and their performance under coreflooding. Five different polymers were evaluated between polyacrylamides and biopolymers, eleven surfactants, including amphoteric, anionic, cationic and non-ionic types, two alkali agents, sodium carbonate and sodium phosphate, and a crude oil sample with a TAN of 0.09 mg KOH/g. From this research can be highlighted that: (1) the best performance on the chemical slug was provided individually by the specially manufactured polymers (HPAM) with heat and salt resistances; (2) the ASP with a weak alkali and the SP flooding had similar oil recoveries over a water injection meaning that the presence of the alkali can be eliminated on a chemical flooding of these characteristics; (3) the amphoteric surfactant had one of the best performance on both injection programs ASP and SP and its adsorption was of 0.41 mg/g considered a viable loss on the reservoir during dynamic conditions.

Later Levitt et al. (2013), evaluated on a laboratory scale the challenges of SP flooding in a low permeability carbonate with high temperature and salinity conditions. The methodology consisted of the selection of polymer and surfactants, to later evaluate their performance on different core plugs: limestones, sandstone, and original reservoir cores. The results pointed out that: (1) there was emulsion production while at the same time a build-up pressure was encountered on limestones, which did not appear on sandstones, a possible reason was the formation of in-situ macroemulsion or capillary pressure in the same order of magnitude as the low gradients in the coreflooding test; (2) on laboratory scale exists a dispersity effect only obtained on original reservoir core plugs, which affects the oil bank formation of the SP flooding directly, resulting in lower recovery factors than the expected (a solution may be the use of longer cores); (3) the predictions of the

capillary desaturation curves are not representative of laboratory data, which reaches oil recoveries over 90%, a possible reason is oil solubilization rather than mobilization of the trapped oil.

Also, there have been researches employing chemical for the SP flooding from a biological origin. Hongyan et al. (2016) studied the performance of a betaine surfactant derived from an oleic acid product of vegetable oil and later compared with two surfactants. The study was carried out in a sandstone rock at 85°C, containing a low salinity brine 1270 mg/L and crude oil of 36 API gravity. Among the tests results, it can be highlighted that the interfacial tension reached desirable values, $1x10^{-3}$ mN/m, and this was conserved even after 90 days; showing the efficiency of the biosurfactant. The remaining saturation of coreflooding test was measured using Dean-Stark apparatus and a Soxhlet Extractor. The incremental recoveries for two runs of an SP slug were of 16.03% and 14.43% for medium and high permeability sandstone cores respectively.

Another research regarding biochemicals for SP flooding was done by Saudi Aramco, where a biosurfactant, four biopolymers, and one HPAM polymer were tested in carbonate reservoir sample (ALANIS et al., 2015; ALZAHID et al., 2016). The fluids were a crude oil of 30 API, formation brine of 229 g/L TDS and an injection brine of 57 g/L TDS, while the rock samples had an average porosity of 19.6% and 26.1 %. The surfactant had low adsorption of 0.65 mg/g, 0.04 mN/m at a 0.2wt% concentration which did not change drastically after long thermal exposure at reservoir conditions and resulting in an incremental recovery of 17%. From the five polymers, three of them were pre-selected after the compatibility test with the formation brine, a Xanthan gum, a Diutan gum, and a HPAM benchmark not disclosed. Both biopolymers reached the viscosity target despite some affecting by the salinity of the brine, the filtration ratio was acceptable for a polymer concentration of 0.1wt%. However, with lower values the filtration was higher than the ones obtained with the benchmark; regarding the long-term stability, the Diutan gum required higher concentrations as to obtained in the similar long-term characteristics as the benchmark while the Xanthan gum maintained its properties. Finally, the

biopolymers adsorption was lower than the one encountered in the benchmark, and the SP coreflooding test had similar results as the HPAM but slightly lower, obtaining in an SP flooding 15.5% of incremental recovery only 2.5% lower than the benchmark. These results showed that it is feasible using biopolymers and biosurfactants for chemical EOR programs and that they can achieve good results.

Later, Levitt et al. (2016) reported the following step of the previous research, which was the evaluation of SP formulation for the Middle East pilot. The formulation was designed and optimized by performing close to 5000 microemulsion pipette tests, more than forty coreflooding tests, and several thermal stability evaluations as to find the best mixture of chemicals. The main requirements for the chemical formulation were high salinity and high-temperature tolerance, field injectivity, stability at reservoir conditions, and chemical retention on an economic level. The reservoir conditions were 83°C, formation brine salinity of 258 g/l, and a carbonate rock with 1 to 200 mD. The final formulation contained a manufactured surfactant on Total Research labs, and it was an Ethanol ester sulfonate and partially hydrolyzed polyacrylamide polymer with calcium and temperature tolerance. Such chemical batch obtained on coreflooding tests residual oil saturation of 1 to 8%, which proved economically viable.

A laboratory study was performed by Jabbar et al. (2017) to evaluate the applicability of an SP and ASP flooding on an offshore giant carbonate field in the Middle East development plan for CEOR injection, which could have pilot development on 2018-2019. This research had two objectives: (1) Identifying a chemical formulation stable at high salinity (~200000 ppm TDS), low permeability (<10 mD) and high temperature conditions (100°C), found on this reservoir; (2) evaluating this formulation performance on coreflooding test with representative crude oil and rock samples. During this laboratory phase, thermal stability, polymer rheology, and microemulsion phase behavior were evaluated. From the evaluated polymers, despite salt resistance and adequate rheology results, their thermal stability did not show the long thermal stability necessary. On the other way, the phase behavior tests (more than 100 were carried out), found optimal formulations

with high optimal salinities, for the SP 63000 ppm TDS and the ASP 57000 ppm TDS, the surfactants were large hydrophobe alkoxy carboxylate and sulfonates. Finally, the coreflooding results were encouraging, with a final recovery for the SP injection of 97% and 93.5 for the ASP, however more studies were decided as to improve the high surfactant adsorption which was considered not economically viable.

3.2.   OFFSHORE STATUS

On the literature as described previously, the number of SP projects is not large, and there has been only one report of SP flooding implementation in an offshore reservoir. In this section is described some offshore ASP projects which can serve as a reference of the challenges a mixed chemical flooding at offshore conditions can encounter, and their corresponding performance.

On the Bob Slaughter Block (ADAMS; SCHIEVELBEIN, 1987; MANRIQUE; MUCI; GURFINKEL, 2007b), there were reported two pilots of SP flooding in the '80s specifically in the San Andres dolomite reservoir. The reservoir has an average depth of 5000 ft and 109°F, it had a crude oil of 31°API, and it was under water injection 21 years approximately when two SP pilots were performed. Both configurations consisted of two-well patterns, and their formulations consisted of the injection of petroleum sulfonates and a biopolymer. The first pilot began at April 1981, and it had a mixture of petroleum sulfonate and alkyl ether sulfate, injected on a period of 171 days and a displacing batch of polymer solution mixed with fresh water for almost 140 days, having a final recovery of 77%. The second pilot had a formulation of petroleum sulfonate and an alkyl ether sulfate, injected by 61 days and later a polymer slug for 45 days, with a final recovery of 43% considered promising.

The Sabiriyaj Mauddud carbonate reservoir, in North Kuwait under waterflood development, was screened at the 2000s for EOR techniques that were possible to

implement. A six steps program was carried out to find the most adequate technology to be implemented: (1) sector model simulation, evaluating competing EOR processes, (2) laboratory studies on surfactant and polymer floods, (3) UTCHEM simulation, replicating lab results, (4) migration from UTCHEM results to a 3D sector model, (5) fine grid simulation study for the pilot area and (6) Single Well Chemical Tracer tests (SWCT). During the first step, it was found that an SP injection was favorable and could increase 41%the recovery factor. In the second step, it was established the most effective chemical formulation for the rock and reservoir fluid samples, using those results as input for the phases 3 to 5. Later, the SWCT was carried out, for this, it was selected the wells with assuring the most representative and with better benefits. The SWCT consists shortly of soaking some meters of the formation with the chemical formulation and keeping it closed for some days, later back producing the well which recovers higher volumes of oil due to the chemicals in contact with the formation. Preliminary it was obtained an increment of 20% of oil recovered. Due to the results of the laboratory, simulation phase, and the SWCT, an inverted five spot model was planned to be carried out in 2016/2017 (ZUBARI; SIVAKUMAR, 2003; CARLISLE et al., 2014; ABDULLAH; TIWARI; PATHAK, 2015; FORTENBERRY et al., 2016).

Regarding offshore applications of ASP projects, Chaco et al. (2003) describe the design of an ASP system for La Salina Field, Venezuela and, although there are no reports of application, it is worth noticing that it was a complete study covering from laboratory design, numerical simulation and facilities design for an offshore field. A sandstone reservoir presenting a medium gravity crude oil of 25°API, 18000 ft depth, with a history production of more than 60 years and a water injection plan of more than 20 years. On the laboratory phase, 23 surfactants, two alkalines (sodium hydroxide and sodium carbonate) and five partially hydrolyzed polyacrylamide polymers were evaluated with softened water and crude oil from the field (a Total Acid Number – TAN of 0.56 mg KOH/g). In this lab phase fluid compatibility, interfacial tension screening, phase behavior, polymer rheology, adsorption behaviors, and radial coreflooding tests were performed to obtain the optimal chemical injection for the reservoir formation (La Rosa). The final formula

consisted of 0.75%w/w of Na_2CO_3, 0.1%w/w alkyl aryl sulfonate and 800mg/l HPAM. Regarding the numerical simulation, a history match for waterflooding (real field data) and chemical flooding (radial corefloods and fluids data) was performed for 24 wells (producers and injectors) considering different forecast. The injection order was first waterflooding, later ASP solution, followed by a polymer drive, and lately water. All estimates got an incremental oil production of at least 31%. About the facilities design, it was considered a three years pilot, having as main construction requirements: (1) a dissolving, mixing and injection plant according to the chemical volume need planned on the laboratory phase, (2) a water treatment plant, (3) an appropriate tubing array to transport the mixture from plant to injectors and (4) the offshore platform with capacity to hold the ASP and water treatment plants. Their main conclusions were: (1) the oil recovery increment in the laboratory was significant, (2) fluids behavior and screening tests are required as primordial for the economic viability of the pilot, (3) the numerical simulation showed good performance of the ASP method for different well scenarios and (4) the design and construction of the offshore plant must follow the recommendations of the lab and simulation results.

The St Joseph offshore field in Malaysia is another offshore ASP system project found in the literature (CHAI et al., 2011; DU et al., 2011). The pilot study was focused on reservoirs containing a medium gravity oil and a chemical injection using an already existing waterflooding project from which facilities could be reused. The evaluation was performed on a numerical simulation basis, where both polymer and ASP flood were evaluated versus the water injection program already done (with gas injection). For the chemical EOR parameters, such as IFT, adsorption, and rheology, some generic set was used and later, a sensitivity study brought the polymer constraints, chemical slug size. A previously 3D model history matching was employed for the evaluation and run on a Shell in-house reservoir simulator. Additionally, some redevelopment activities were simulated: (1) rim infill wells to accelerate oil production and improve project economics, (2) stopping of oil migration into attic region (reduced by gas injection stopping and increasing pressure by fluid injection). The corresponding increment in Recovery Factor by infill wells was 7%,

polymer 13%, and ASP 20%. On their study, they describe the equipment required to implement, on a full field scale, and resembles the one mentioned previously for La Salina field. Moreover, some risks and challenges associated with the EOR technique and the offshore implementation were: (1) logistical challenges related to the supply chain of chemicals, (2) operators require training regarding the EOR method, (3) the waterflood infrastructure is relatively old, so rejuvenation and integrity maintenance is needed, (4) emulsion handling and disposal, including back produced chemicals on the facilities, (5) chemical discharge associated to produced water, (6) high adsorption of chemicals, (6) localized heterogeneities affecting the objective observation of the results, (7) unconstrained fracture growth on the rock (more viscous fluid injected) and (8) measuring the saturation of oil accurately on the observation well during the pilot phase.

A joint Shell and PETRONAS evaluation of the technical challenges of implementing an ASP flooding in three offshore producing fields in northern Borneo with a focus on space solution (KOVALEV et al., 2016). For it, four anchor cases were detailed and analyzed: (1) high injection, (2) medium injection, (3) low injection, and (4) only polymer. For the first case, the chemical delivery system was based onshore, with a water intake for the water treatment plant from the nearshore area and the ASP mixture prepared and transported to injection points by pipelines. The second was based on a floater concept, where the chemicals are supplied from manufacturers to the Chemical Delivery System and stored in a vessel hull. The third was based on two injection hubs; the first only focused on one field and a second supplying the chemicals to the other two. The fourth case was based solely in polymer reducing costs, intermediate chemical storage onshore, and ASP mixture delivered only for two fields and no cocktail injection on the third one. For all three fields were fixed alkaline, polymer and co-solvent, while the surfactant may vary between fields. A simulation phase was performed using geological and fluid models, to understand and evaluate the field dynamics, production profiles, and injection rates using the in-house reservoir simulator MoRes. Regarding the facilities scope, the two focuses were the Chemical Delivery System (CDS) and Produced Fluid Handling, the first treats and prepares ASP mixture while the second one break

downs the emulsion and treats oil and water. The CDS brought to the analysis the necessity of higher power demand (which means that a fuel source is needed, either gas or other), a pneumatic conveying system to load/offload the chemicals required and a structure and weight capacity increase. The production facilities must handle the presence of chemical back produced, which will affect the performance of the surface facilities by forming very stable microemulsions, polymer viscosifying the produced water, foam generation by residual surfactant and chemical toxicity. Concluding, new technologies regarding water treatment, capable of reducing water and energy consumption; a single chemical formulation is preferable, so no additional storage facilities are needed, currently polymer makes 10% of the chemical cost, while surfactant and alkaline cover the other 90% which brings cost issues deepen if the design does not cover the possible adsorption of the chemicals on the rock.

Another field test was performed by Total S.A in the Middle East in 2014, which was the first offshore pilot on an offshore carbonate reservoir with high salinity formation brine of 230g/L, high temperature (80-90°C) and low permeability ranging from 30-100 mD (AL-AMRIE et al., 2015; MOREL et al., 2016). The formulation employed consisted of an SP slug of 1.35%w active surfactant in an 80 g/l brine and a polymer drive with softened seawater. The well configuration selected was a one-spot, after evaluating time for drilling (not required), workovers (only one needed), pilot duration (30 days), relative costs and overall complexity (confinement and no platform difficulties). Despite the laboratory design, there were risks which could result in the failure of the project or its modification accord to the planes and countermeasures studied; they were: Well integrity failure, Single Well Tracer Test failure, SP/P failure, and chemical quality-related risks. The second risk was materialized due to poor injectivity, resulting in a change of the program to a surfactant plus brine injection after back producing the SP batch. Despite the challenges and risks, it was categorized as a success as safety was maintained during all the project, a significant oil desaturation was achieved, the tracer injection was a success as it helps evaluate the uncertainties on porosity channels, residual

oil saturation, and reservoir dispersity. It was reporting a reduction of oil saturation of approximately 4 units of saturation within 1 meter around the well.

Izadi et al. (2018) reported a technically successful SP injection on a pilot scale on the Illinois basin. The pilot had four injectors and nine producers, where oil production increased up to twenty times in offset producers. The development of the pilot followed a laboratory study, a numerical simulation model and implementation of the pilot. The chemical blend was made up of an HPAM polymer at 2500 ppm and a blend of three anionic surfactants at 0.7%w. This article was the following part of the laboratory research explained in section 3.1.

As was observed in this state of the art, there are various opportunities relating the SP flood on carbonate rock in offshore reservoirs. Among them, finding chemicals appropriate to those conditions is needed; evaluating their performance only in the laboratory is not enough, a simulation phase composed of global sensitivity analysis and optimization taking into account the variables interacting such as concentrations, injection profiles and economic scenarios can bring answers more realistic to, how feasible this type of program in no traditional scenarios which are the offshore fields and carbonate reservoir exploiting.

3.3.   NUMERICAL SIMULATION

In the literature, there are some simulation-based studies for SP flooding, evaluating the economic viability, the finding of optimal parameters and conditions for its application, by using different optimization techniques and sensitivity analysis, some of them are detailed next. There are other simulations works having as scope ASP, AS, Surfactant and polymer optimization and evaluation, but studying them is not within the objectives of this research, therefore are not described here.

A sensitivity and optimization of a quarter spot model were performed for an SP, and ASP injections in mixed-wet dolomite, where the optimum design was selected based on the net present value (ANDERSON et al., 2006) and the input

data was obtained from previously performed tests. The reservoir had water cut about 98%, average porosity of 16%, average permeability of 156 mD, a 31°API oil and brine with 60315 ppm of TDS. Sensitivity analysis was based on 21 simulation runs where it was analyzed the slug size, chemical concentrations, salinity, polymer mass, surfactant and polymer adsorption, heterogeneity, and the capillary desaturation curve. All the previous runs were later analyzed using the concept of discounted cash flow analysis, where crude oil price and surfactant cost were varied as to obtain different NPV and subsequently selecting the two optimal. These were the cases where low surfactant adsorption was selected, and a higher polymer concentration as defined.

Later, Mollaei et al. (2011) performed a global sensitivity analysis of the SP process, using an analytical chemical flood predictive model which calculates the ultimate recovery efficiency as a product of volumetric sweep efficiency, displacement efficiency and the efficiency of the mobility buffer. A database of 1381 onshore fields was collected and used for this study and the results of each case on the analytical model. Their research used a sensitivity analysis called Winding Stairs which requires a smaller number of runs than a Monte Carlo method and identifies the individual and total effect of each parameter studied on the sensitivity, helping to identify the interrelations between variables and their respective uncertainty. For this study, the settings studied were: surfactant concentration, surface density, pattern, interfacial tension, rock density, adsorption, water viscosity, oil viscosity, net thickness, heterogeneity, residual oil saturation, and porosity. It can be highlighted of their research that the previously mentioned parameters (permeability, porosity, heterogeneity, and oil viscosity) brought the higher uncertainty either individually or by interacting with others on the performance of the SP flooding. Nor economic variables were studied, and neither offshore fields were evaluated on the original database.

One year later, Alsofi et al. (2012) performed a similar study also using coreflooding test data for a carbonate sample, followed by sensitivity analysis and an optimization process was carried out as to evaluate the performance of and SP

flooding on a 1D model resembling the coreflooding. The rock and test condition were: 90°C, pore pressure of 21MPa, 0.2% of polymer and surfactant concentration, and brine with 84715 ppm of TDS. The methodology followed was: (1) laboratory design, (2) model construction based on laboratory data, (3) base runs, (4) tuning and history matching of the coreflooding, (4) sensitivity analysis and (5) numerical optimization. The sensitivity analysis evaluated different parameters on the UTCHEM software used for the simulation of the numerical models; while the optimization was performed by running ten scenarios where chemical concentration, slug sizes, and chemical consumption were performed. It was found that the simulation run could not obtain the asymmetrical oil banking profile observed in the laboratory test; the sensitivity test showed that the oil recovery of the SP injection varied greatly as the IFT is modified and the optimization phase indicated that a high polymer to surfactant concentration ratio could bring more effective results.

Alsofi. Liu and Han (2013) studied the SP flooding numerical simulation using laboratory data experiments on a carbonate rock. The study was based on five coreflooding tests where slug size, chemicals concentrations, and brine salinity were evaluated at reservoir conditions 21 MPa and 90°C. After it, a simulation model was constructed, and history matched as to reflect the injection and later optimized by simulating 10 cases varying the parameters mentioned and including a chemical consumption. It was found: (1) despite a reasonable consistency between simulation and experiment was found, the model could not model the oil banking profile; (2) there is a direct relationship between the IFT reduction and higher recovery volumes; (3) the slug size affected the final oil recovery however it varied only between 3-1%; and (4) optimal results were found on high Polymer to surfactant ratio concentrations.

Al-Dousari and Garrouch (2013) introduced an artificial neural network model for SP flooding evaluation based on 18 dimensionless parameters defined on another research and the associated results of 624 model runs. In their study is explained how the proposed model was constructed looking for the optimal selection of hidden layer and neurons, and later a training phase with a set of 499 simulated

responds and 125 field cases to validate its results. Concluding that the model it's an alternative to evaluate the oil recovery of SP injections with less computational cost as the traditional simulators.

Bahrami et al. (2016) proposed Genetic programming as a methodology to estimate the RF and the NPV in an SP flooding and later optimizing it based on selected parameters. The methodology followed the compilation of 202 data points of a sandstone reservoir and their corresponding economic evaluation. The parameters used as input variables for the Genetic Programming were slug sizes, chemical concentrations, salinity, and the ratio between vertical and horizontal permeabilty having as output the RF and the NPV. Their algorithm picked 161 data for training and 41 for testing the program, and two models were developed one for the RF and another for the NPV. It was presented for both models an accuracy of 0.963 and 0.946 on their residual square, showing a high correspondence; with this result and the advantage of not requiring a fundamental description of the physical properties of the model makes it a possible method to evaluate the performance of injection programs. Regarding the optimized input parameters, all had a positive effect and a direct relationship with the RF model. As for the NPV, the variables of slug size and surfactant concentration had both a positive and a negative effect associated with higher recovered volumes but higher associated costs. These showed themselves effective; however, an optimization base on economic uncertainties should be considered as they also have a high impact on the project results.

Kamari et al. (2016) presented two models to evaluate the recovery factor and NPV of SP flooding for sandstone oil reservoir, obtained using the Least Square Support Vector Machine methodology (LSSVM). This methodology can be described as a supervised learning method in which a set of data is analyzed based on several input and output variables to recognize patterns and to solve classification problems with a set of linear equations. For this research, a databank of SP flooding models using UTCHEM simulator was used, this data bank included for each case seven input variables and two outputs, RF and NPV. This set was later divided into three

sub-dataset, training, validating and testing as to develop the models with the LSSVM. Their results concluded that the models for the NPV and RF brought acceptable results, and the total correlation coefficient for both of them was 0.993. Also, after executing a sensitivity analysis, they found that the slug size and surfactant concentration had the most significant impact on the RF model, while for the NPV the surfactant and polymer concentration had the most significant effect on the NPV model.

4. METHODOLOGY

The methodology followed in this research can be divided into five steps, as observed in **Figure 4-1**:

Figure 4-1 Research flowchart divided into steps
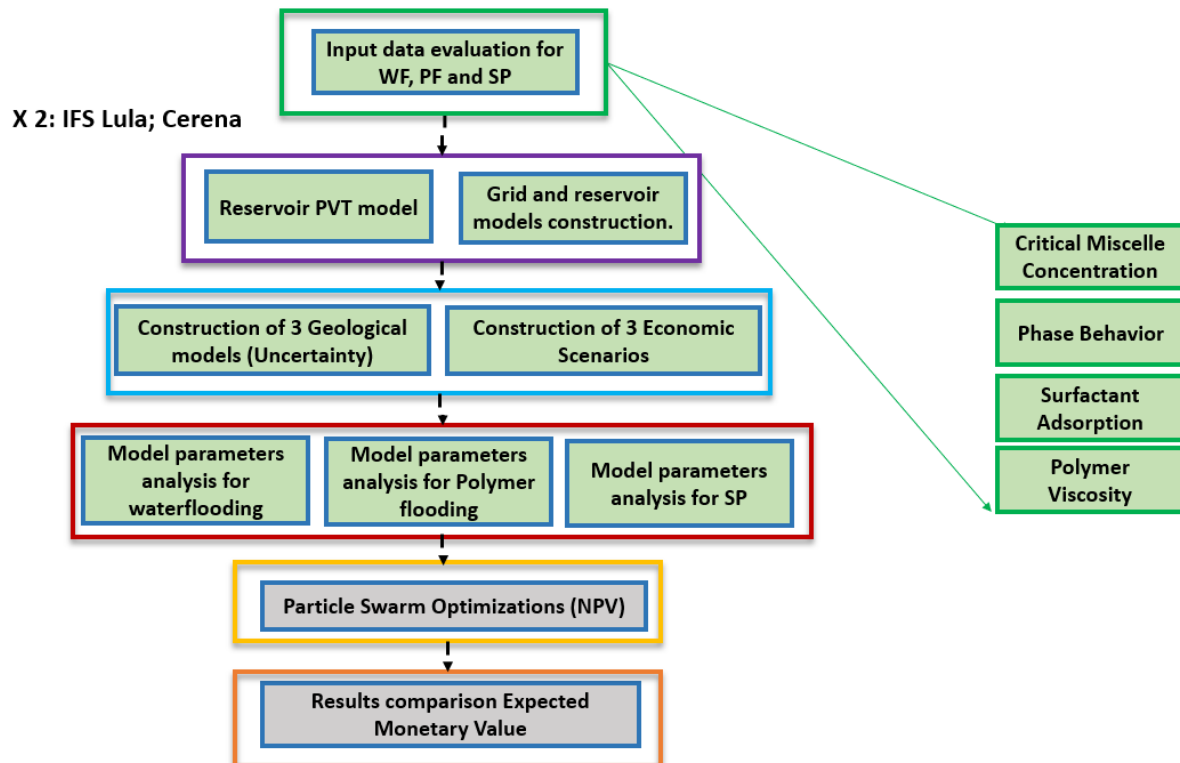
Source: Author, 2019.

1. Defining input information for waterflooding, Polymer flooding, and Surfactant-Polymer flooding from laboratory test and literature. For this research, polymer viscosity was evaluated on a laboratory level, while for the surfactant, parameters such as interfacial tension, adsorption, and CMC data was taken from the literature. A screening of three available surfactants was carried out in the laboratory, were adsorption and CMC were obtained. Having as main objective to evaluate what should be the expected behavior of different types of surfactant at this reservoir conditions and later selecting based on these results one chemical fulfilling the requirements of adsorption, CMC and IFT behavior.

2. Building and adapting the pilot reservoir models objective of the research, one based on main Lula's field properties and the Cerena-I (based on Jupiter Field)(FABUSUYI, 2015).

3. Building two additional models, low and high permeability, with the same characteristics as the two base models, having as their main difference the average absolute permeability in each direction: lower heterogeneity case and higher heterogeneity case.

4. Conducting numerical simulations for each one of them on the previous geological models to obtain the first output data. The main information for the chemical injection programs was: interfacial tension as a salinity function, adsorption as a function of the surfactant concentration, and polymer viscosity behavior (obtained from steps 1 and 2).

5. Calculate the Net Present Value (NPV) of each simulation of the previous step for each economic scenario and optimize the selected parameters for the case-scenarios using the PSO.

6. Evaluation of the optimal values/solutions in the previous step.

7. Calculate the Expected Monetary Value (EMV) for each injection program considering the maximized NPVs on steps 3 and 4.

8. Discussed and evaluate the results for all three injections on all the models, Lula based, and Jupiter based as to define how plausible it's the SP flooding in the scenarios defined when compared with other techniques.

4.1. LABORATORY PHASE

At first, it must be mentioned that microemulsion phase behavior tests or direct characterization of the interfacial tension between the aqueous solution and the crude oil is one of the inputs for the simulation and such tests were not carried

out in this laboratory work. The microemulsion phase behavior requires many tests and several screenings to select the best surfactants for the reservoir conditions, requiring, therefore, research focused on it. Moreover, the lack of dead crude oil on our facilities and equipment to measure ultra-low interfacial tensions ($\sim 1*10^{-3}$ mN/m) made its evaluation unavailable.

In this way, the CMC determination and surfactant adsorption of available surfactants in the saline medium and, also required for the simulation were used as reference parameters to search in the literature, experimental data from a chemical with similar or better performance, including, the ultra-low interfacial values.

This chapter describes the chemicals and solutions prepared to obtain the surfactant adsorption, surfactant critical micelle concentration (CMC) and polymer viscosity. This latter is also a required parameter for the simulation phase.

4.1.1. Surfactant

Three surfactants were characterized in the initial laboratory screening phase to study their behavior, in a high salinity medium, specifically regarding the CMC and adsorption behavior: anionic, cationic, and non-ionic samples.

− Anionic: Sodium C14 -16 Olefin Sulfonate, 315 g/mol, liquid at 39.1 % active.
− Cationic: Hexadecyltrimethylammonium bromide (CTAB), 364.45 g/mol, solid powder, 98% active.
− Non-ionic: Oleyl cetyl alcohol Ethylene oxide, Molecular weight not specified, solid paste, 99 % active.

4.1.2. Polymer

A Xanthan gum was selected because of its divalent cations tolerance and degradation temperature over 80°C (higher than pre-salt value). It was used for the laboratory phase a 200 mesh sample provided by Labsynth, and for the simulation phase, it was assumed a molecular weight of $2x10^6$ Da (ROSALAM; ENGLAND, 2006).

The rheological behavior of the polymer was obtained in the laboratory following a power law model, as it is described in the next sections.

4.1.3. Brine

A base high salinity synthetic brine resembling the one that could be produced in an offshore facility to be later treated and reinjected on the reservoir (**Table 4.1.3-1**) is being used for the laboratory phase of this research.

Table 4.1.3-1 Synthetic Brine composition.

Synthetic Brine composition	
Na^+ (ppm)	29505
Cl^- (ppm)	63799
Mg^{2+} (ppm)	4066
Ca^{2+} (ppm)	6993
TDS (ppm)	104361

4.1.4. Critical Micelle Concentration Determination

In order to determine the CMC of surfactant, it is employed surface tension with the methodology described by Mukerjee & Mysels (1971). This procedure bases in

measuring the surface tension of different surfactant concentrations in the same brine and later plotting the results against the logarithm of the respective concentration. A sharp decline is observed after which the curve will behave relatively horizontal (almost constant surface tension) as can be observed in **Figure 4.1.4-1**. This intersection where the curve changes of slope and starts a plateau is known as the CMC. A Du Noüy ring tensiometer – Kruss Company, model K6 was used on this research (**Figure 4.1.4-2**).

Figure 4.1.4-1 Surfactant concentration and micelle formation.
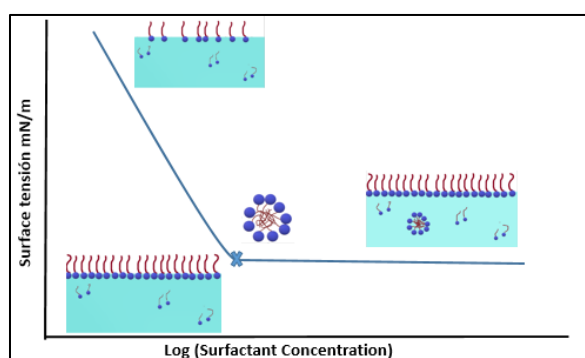
Source: SHENG, 2011

Figure 4.1.4-2 Du Noüy ring Tensiometer.

Source: KRÜSS GMBH, 2018.

Some key procedural points of the test were:

- The test was performed with two different solutions; the first was a distilled water, and the second one a brine with a NaCl concentration of 70 g/l.

- Triplicate measurements were taken, so the average and standard deviation per point could be registered in plotted graphs.

- Each CMC point was obtained intersecting the line trends and solving their corresponding equations for the two sections to get the most precise coordinate.

- Before each series of measurements, the device must be calibrated with demineralized water, so the surface tension at 20°C was expected to be 72-73 mN/m.

- The solution must be a sample from the middle of the bottle, so no excess was measured in the surface and only the bulk in the center.

4.1.5. Surfactant Adsorption

In addition to the required chemical parameters previously mentioned, the surfactant adsorption is also a parameter used in the simulation. The surfactant adsorption behavior should be reviewed as it depends on surfactant type, concentration, rock minerals, temperature, pH, the flow rate of the solution, among others (SHENG, 2011). It can be evaluated either in a dynamic or static test, however, for this research scope, only the latter one was performed (SHAMSIJAZEYI; HIRASAKI; VERDUZCO, 2013; PARK; LEE; SULAIMAN, 2015; LI et al., 2016).

For the static adsorption, the surfactants are dissolved in the synthetic formation brine at different concentrations, later rock dolomitic carbonate powder sieved in a 100-200 mesh is mixed with the solution for 24 hours in a 1:50 mass ratio at room temperature. The mixture is filtered, and the supernatant is titrated to determine the residual surfactant concentration (a potentiometric titrator version 916 Ti-Touch from Metrohm) and later constructing the adsorption curve for cationic and anionic surfactants. As for nonionic the surfactant, the methodology followed was based on comparing the surface tension of a baseline solution of surfactant and brine, against the surface tension of the supernatant fluid after being in contact with

the rock powder, a procedure detailed by Kaln (2009). The formula to find the adsorption on milligrams of surfactant adsorbed per grams of rock is the next one,

$$Adsorption = \frac{(C_o - C_e)M}{g_{rock}} \qquad (12)$$

Where C_o and C_e are the initial and equilibrium concentrations of the adsorbate, M is the mass of adsorbate solution in contact with the adsorbent and g_{rock} is the weight of the adsorbent used

4.1.6. Polymer evaluation

To evaluate the polymer, the American Petroleum Institute (API) Recommended Practice 63 "Recommended Practices for evaluation of Polymers used in Enhanced Oil Recovery Operations" was followed, in addition to other relevant literature (AMERICAN PETROLEUM INSTITUTE, 1990).

The polymer viscosity requirement was based on crude oil viscosity. So, a polymeric solution slightly above the crude oil viscosity is searched (SHENG; LEONHARDT; AZRI, 2015; LEVITT et al., 2016). Four polymeric solutions in a brine solution (Table 2) with concentrations of 500, 1000, 2000 and 3000 ppm were prepared. For each one, 4 measures of viscosity were obtained employing a model 35 Fann viscometer (**Figure 4.1.6-1**). Next, it is briefly explained the procedure followed to obtain the viscosity measurement as a shear rate function (AMERICAN PETROLEUM INSTITUTE, 1990).

1. Measure the viscosity of the solution at four rotor speeds: 100, 200, 300, 600 rpm. Starting at the lowest velocity and going upward.
2. Calculate the viscosity of each point following a Power Law model. For this research purpose, it was employed the model described by Bourgoyne et al. (1986):

$$\eta = K\gamma^{n-1} \qquad (13) \qquad n = 3.322 \log\left(\frac{\theta_{600}}{\theta_{300}}\right) \qquad (14)$$

$$K = \frac{0.0106\theta_{300}}{511^n} \qquad (15)$$

Where η, K, n and γ are the apparent viscosity, in cP, consistency index in units of pounds force per second per square feet; flow-behavior index and shear rate in s^{-1} respectively.

3. Plot the data obtained as viscosity versus shear rate, specifying the polymer concentration.

Figure 4.1.6-1 Fann model 35 viscometer for polymer evaluation.

Source: Author, 2019.

4.2. SIMULATION PHASE

In this chapter, it is shown and highlighted the main stages to build two 3D numeric models by BUILDER v.2017, later run on STARS v.2018 and GEM v.2016.2 simulators (Thermal & Advanced Process Reservoir Simulator; Compositional & Unconventional Reservoir Simulator, both from CMG). The version of GEM employed allowed the modeling of microemulsion behavior not available on their next releases.

The simulation phase was divided into several steps, as can be seen in **Figure 4.2-1**. First, the collection of laboratory and literature data from the previous phase and information required for the reservoir model construction, including fluid, rock, and chemistry characteristics. This step includes generating a model resembling the information of a Brazilian, offshore field specifically for the Santos Basin. Additionally, a second model is adapted, CERENA I model, which is a synthetic reservoir model built by the CERENA Research group to resemble the Jupiter field. From this full field model, a pilot size model was taken and adapted from Fabusuyi (2015) research. Finally, the construction of the economic model to evaluate the performance of all three injection programs: WF, PF, and SP; and selection of the output data to be analyzed in the simulations results for each inverted five spot model (IFS).

Second, the simulation of three cases was carried out for each IFS model: water flooding, as the base case, polymer flooding, as EOR comparative case; and SP flood, as the study case. For each one of the cases, an optimization of parameters was carried out, under three economic scenarios, and three heterogeneous models were the average permeability in all three directions was multiplied by a factor as to account for this uncertainty. The water cut and Net Present Value were optimized using the Integrated Analysis & Optimization Tool – CMOST, from CMG package. This phase analyses the results obtained for each case, individually, and reviews the performance to observe the advantages and disadvantages of the SP flood, on a typical water flooding and conventional chemical flooding as the Polymer injection. For this study case, it is analyzed the operation parameters and rock-fluid/fluid-fluid phenomena, inside the porous media.

Third, based on the results of both inverted five spot models, average cumulative production per well, recovery factor and optimal parameters, the water injection and the SP flood processes are evaluated. With this approach, it is possible to verify how the SP program operates in a theoretical model and a more realistic case.

The Cerena Field and the inverted five-spot model were adapted from Fabusuyi and Pinto's researches (MADEIRA, 2014; FABUSUYI, 2015) from Petrel and Eclipse to the BUILDER module from CMG, to be later simulated on the Reservoir Simulator GEM. For this work, it was assumed that the PVT results, petrophysics, and structural properties of the reservoir are well defined, and no further change or evaluation is required. The PVT data used was the same employed by Pinto's research, meaning that it was not required matching of laboratory / literature data. The inverted five spot model was used for this research to keep the benchmark of the Cerena model.

Figure 4.2-1 Flowchart of the simulation phase for both models.
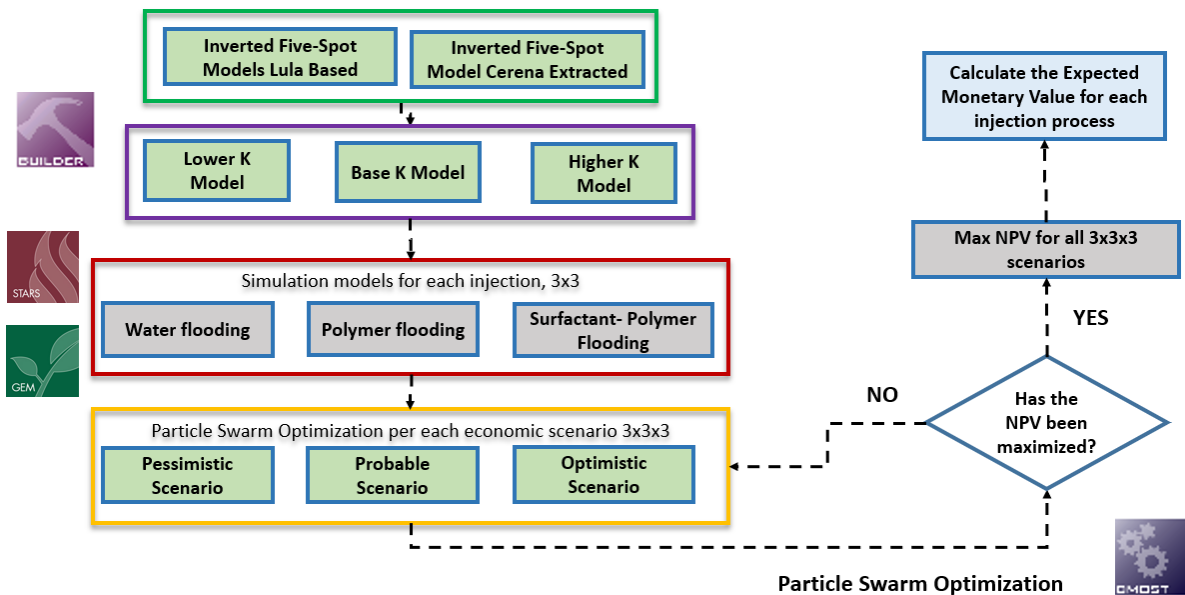
Source: Author, 2019

5. CASE STUDY

Two models were studied in this research, one constructed by taking the information of the literature of the Lula field, and a second one, more complex, extracted from a previously full field-built model based on the Jupiter field. Both studies were carried out to have a broader view of how the chemical methodologies

compare in different scenarios of the pre-salt basin. A second reason for the simultaneous study in both models, was to avoid not conclusive results regarding any of the parameters, for example, as will be mentioned later in the results section, one of the models presented injectivity problems, an issue which limited the analysis of some parameters selected.

Both models differ in properties such as API, porosity, wettability, Original Oil in Place and pressures, even when these fields are members of the same basin.

An inverted five spot configuration was selected for both models to keep the benchmark of the Cerena model carried out by other researches (MADEIRA, 2014; FABUSUYI, 2015).

5.1. INVERTED FIVE SPOT MODELS DESCRIPTION

5.1.1. Cerena-I

The Cerena-I synthetic model is a replica of some of the common characteristics of a Brazilian Pre-Salt carbonate, specifically the Jupiter field. The initial model is a corner-point grid with 161x161x300 cells, with 25x25x1m dimensions. It is composed of three blocks and two facies each, a microbiolite reservoir facie and a mudstone non-reservoir facie (MADEIRA, 2014). The porosity and permeability distributions and lateral view of the reservoir can be observed in Figure 5.1.1-1 and Figure 5.1.1-2 respectively, where can be seen the representation of the facies mentioned before with a large number of cells with low porosity and low permeability, and a smaller quantity of cells corresponding to the microbiolite facies with larger porosities and permeabilities.

Figure 5.1.1-1 Porosity distribution and lateral view of the porosity distribution of Cerena-I.
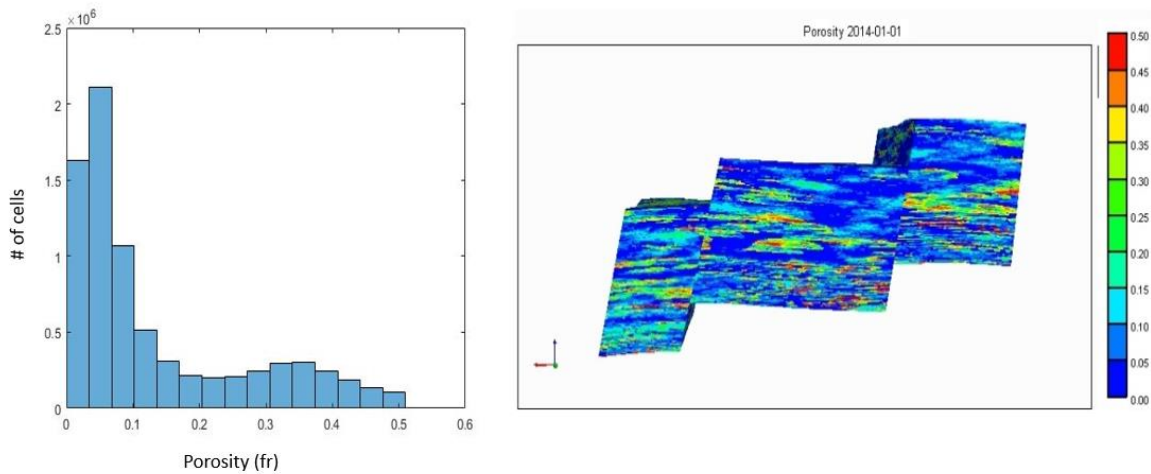
Source: MADEIRA, 2014

Figure 5.1.1-2 Permeability I distribution and lateral view of permeability I of Cerena-I.
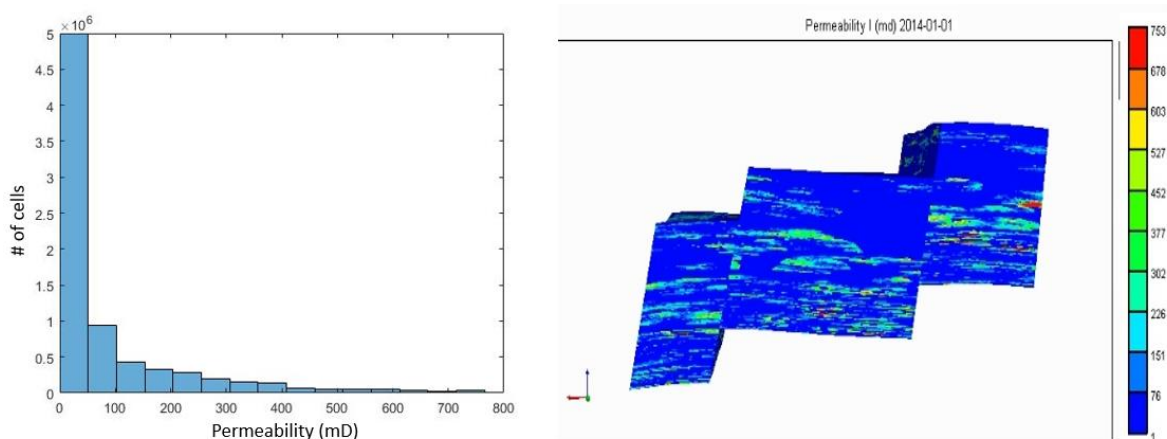
Source: MADEIRA, 2014

For the evaluation of each injection program, it was selected the sector model extracted by Fabusuyi (2015) on his research of the middle block of the Cerena model, with its corresponding characteristics worked by him. It was decided on this research to maintain the same pattern of the wells to keep the benchmark of the model for future works.

The wells positioning in the reservoir model corresponds to an inverted five-spot, this configuration has four vertical producers, and one injector in the center observed in **Figure 5.1.1-3**. The model does not present aquifer neither gas cap, formed by a 22x22x154 cells grid and 50 m x 50 m x 2 m dimensions, with porosity and permeability following the distribution found in **Figure 5.1.1-4**.

Figure 5.1.1-3 Inverted Five spot model used in this work - Permeability in I direction.
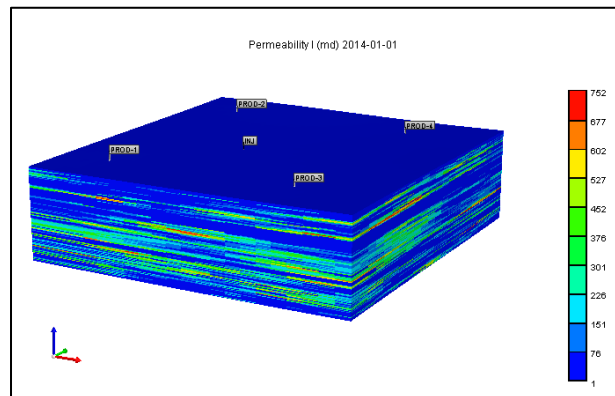
Source: MADEIRA, 2014

Figure 5.1.1-4 Histogram distribution of the inverted five-spot model Cerena-I for (a) porosity and (b) permeability I direction.
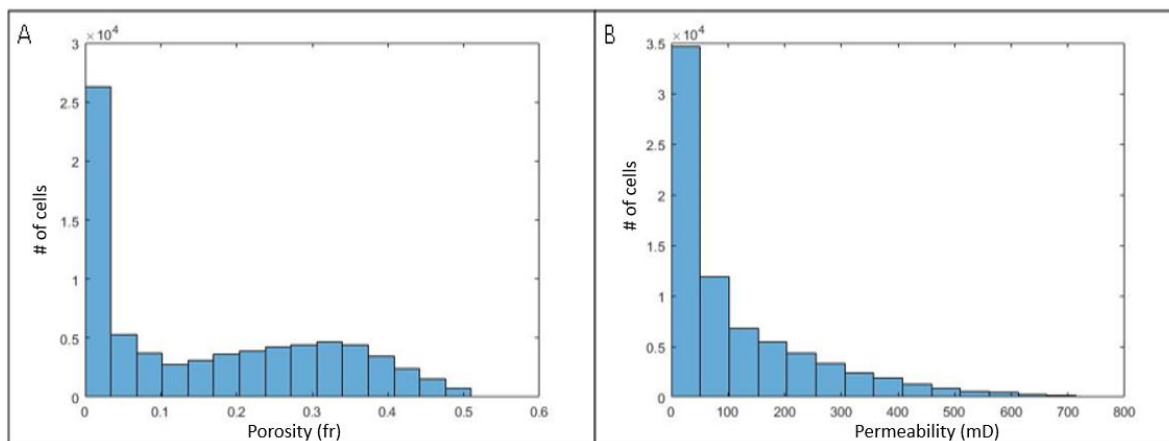
Source: MADEIRA, 2014

5.1.2. Lula based model

A 3D geological reservoir model was built in the BUILDER module, to be later simulated on the Reservoir Simulator STARS. For the builder input data, it is assumed, an entire heterogeneous reservoir saturated with oil and water, over its bubble point so that no gas phase could be encountered at the initiation of the model.

The wells positioning in the reservoir model corresponds to an inverted five-spot, this configuration has four vertical producers and one injector in the center, without aquifer and gas cap, formed by a 20x20x7 cells grid and 200 ft x 200 ft x 29 ft (**Figure 5.1.2-1**), with porosity and permeability following a normal and lognormal distribution respectively. Moreover, the properties were fixed, so it resembles a carbonate offshore reservoir with medium oil.

Figure 5.1.2-1 Inverted five spot model based on Lula Field Properties, porosity.
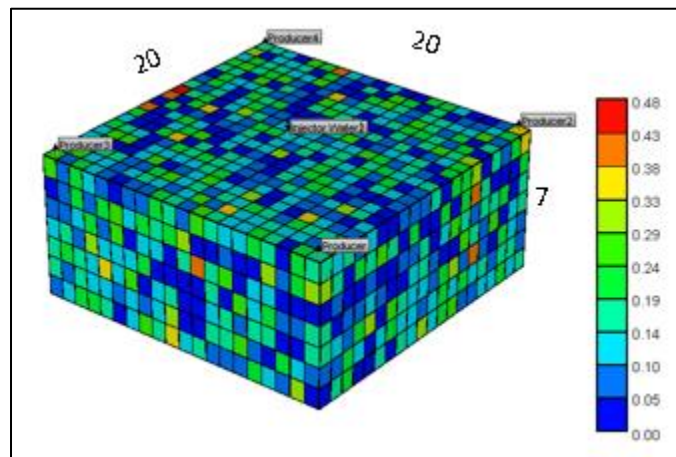
Source: Author, 2019

5.2. ROCK AND FLUID PROPERTIES

In this section, it is presented the rock and fluid properties employed as input for both models, Cerena-I and the Lula based model.

5.2.1. Cerena-I

The Cerena I field properties resemble the Jupiter field in Brazil; therefore the IFS model extracted has the same properties as for their initialization. *Table 5.2.1-1* describes these characteristics. In **Figure 5.2.1-1** and

Figure 5.2.1-2, can be found the relative permeability curves employed in the model based on Fabusuyi's work (2015). Where can be observed a medium-wet rock tendency.

Table 5.2.1-1 Reservoir model characteristics.

PROPERTIES	VALUE
Grid thickness (m)	315.91
Average porosity (%)	15.89%
Water Oil Contact (m)	300
Reference Pressure (kPa)	49299.6
Average oil Saturation (%)	28.5%
API gravity	18
OOIP (m^3)	3.08x10^8
Porous Volume (m^3)	1.35x10^9
Reservoir Temperature (°C)	100

Source: FABUSUYI, 2015

Figure 5.2.1-1 Water-oil Relative permeability curve.
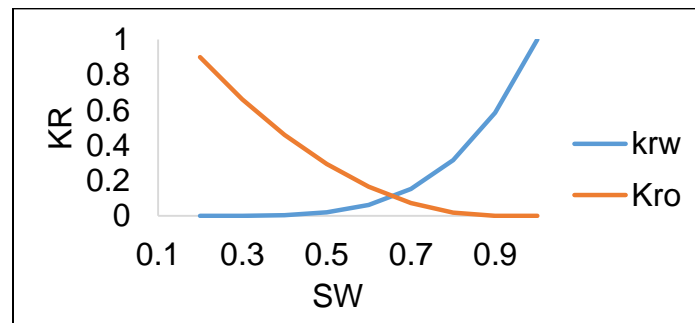
Source: FABUSUYI, 2015

Figure 5.2.1-2 Liquid-gas Relative permeability curve.
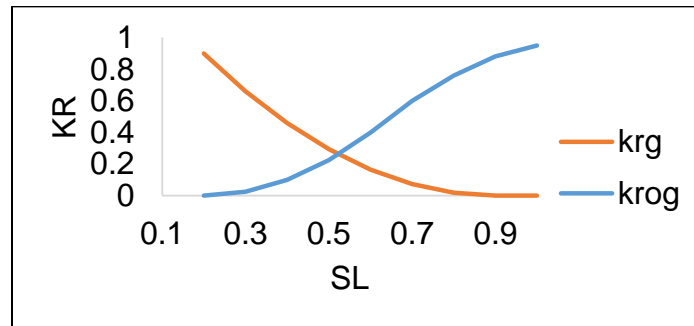
Source: FABUSUYI, 2015

To evaluate the geological uncertainty, two additional models were constructed by multiplying all the permeability distribution (i, j and k directions) of the base model by factors of 2 and 0.5 for the high and low permeability cases respectively, as described in *Table 5.2.1-2*. This was performed as to take into account, the heterogeneity uncertainties a regular EOR pilot has to encounter during its development (in this case smaller and larger permeabilities in all directions), which will affect the future expansion of the recovery technology on a larger scale.

Table 5.2.1-2 Permeability distributions for geological uncertainties, I direction.

#	Model	Permeability I		
		Avg	Max	Min
1	**Base**	113.17	751.86	1.00
2	**Low**	56.58	375.93	0.50
3	**High**	226.34	1503.73	1.99

Source: Author, 2019

5.2.2. Lula Based model

The model properties resemble the ones found in the Lula field in Brazil, *Table 5.2.2-1* describes these characteristics. In **Figure 5.2.2-1** and

Figure 5.2.2-2, can be found the relative permeability curves for a water-wet rock employed in the model.

Table 5.2.2-1 Reservoir model characteristics.

Parameter	Value
Grid top (ft)	21100
Layer thickness (ft)	203
Average porosity (%)	12
Permeability (mD)	100-1000
Reference Depth (ft)	21300
Reference Pressure (psi)	8520 @ 21300 ft
Average oil Saturation (%)	81%
API gravity	27.83
OOIP (ft3)	3.48×10^8
Porous Volume (ft3)	4.28×10^8
Reservoir Temperature (°F)	140

Source: BAKER; ZAMAN, 2010; HENRIQUES et al., 2012; PEREIRA et al., 2013; BOYD et al., 2015; MELLO, 2015; NAVEIRO; HAIMSON, 2015; PINHEIRO et al., 2015; DE MORAES CRUZ et al., 2016

Figure 5.2.2-1 Water-oil Relative permeability curve.
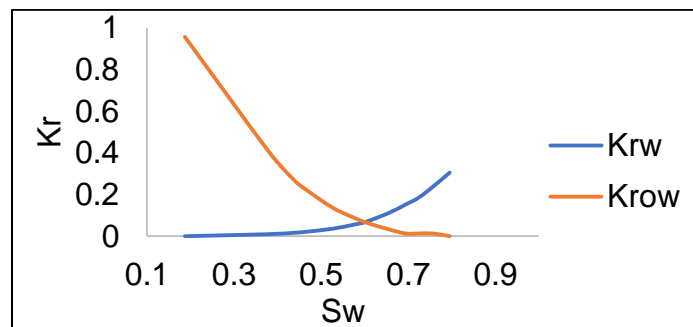
Source: MELLO, 2015.

Figure 5.2.2-2 Liquid-gas Relative permeability curve.
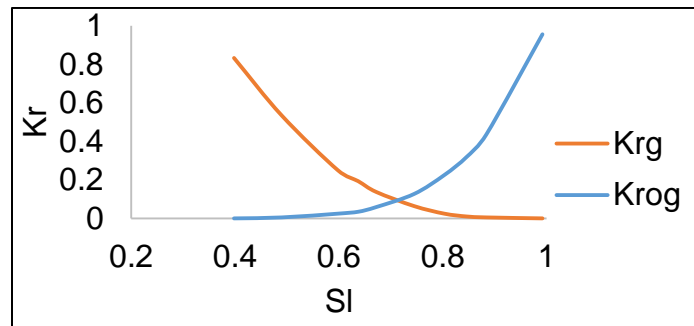
Source: MELLO, 2015.

To evaluate the geological uncertainty, two additional geological models were constructed, varying on their permeability distribution, as described in *Table 5.2.2-2*.

Table 5.2.2-2 Permeability distributions for geological uncertainties.

Distribution	Model	Mean (mD)	Deviation (mD)
	Base	500	200
Log normal	Low	200	100
	High	1000	300

Source: Author, 2019

5.3. RESERVOIR FLUIDS MODEL

5.3.1. Cerena-I

The reservoir fluid model is the one described by Fabusuyi (2015) constructed to resemble the one found in the analogs field, Jupiter. The reservoir oil composition and PVT model follows the characteristics of an 18°API oil with a high CO_2 content

close to 55% molar, and a gas cap of retrograde gas with close to 60% of CO_2. The molar percentages of the oil pseudo components are described in *Table 5.3.1-1*, and their properties in *Table 5.3.1-2*. As it was mentioned previously in this work, it was assumed that PVT, petrophysics and structure properties of the reservoir are well defined, and no further change or evaluation is required. This assumption was considered to no change the benchmark model.

The oil viscosity curve and the phase diagram can be observed in **Figure 5.3.1-1** and **Figure 5.3.1-2**. In the phase diagram, the bubble point pressure is 49300 kPa.

Table 5.3.1-1 Pseudo components oil, molar percentage.

Component	% molar
CO_2	55.00
C1	16.57
C2	4.46
C3	3.15
IC4 to C6	5.70
C7	15.12

Source: FABUSUYI, 2015

Table 5.3.1-2 Pseudo components properties.

Component	Critical Pressure (atm)	Critical Temperature (K)	Molecular Weight (g/gmole)
CO_2	117.63	250.91	44.01
C1	73.32	156.95	16.043
C2	77.39	249.11	30.037
C3	67.39	304.52	44.097
IC4 - C6 (pseudo)	56.08	380.62	70.237
C7	27.18	613.42	218

Source: FABUSUYI, 2015.

Figure 5.3.1-1 Viscosity curve at 100°C.
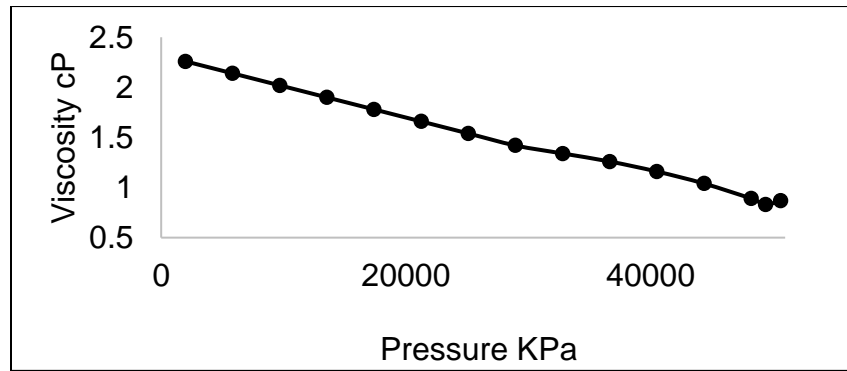
Source: MADEIRA, 2014

Figure 5.3.1-2 Phase diagram
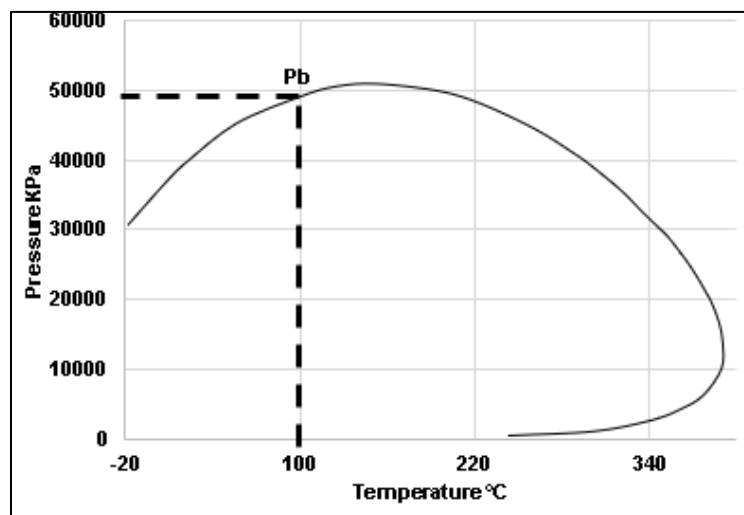
Source: MADEIRA, 2014.

5.3.2. Lula based model

The reservoir oil composition and PVT model follows the characteristics of a medium crude oil (approx. 28°API) with a high CO_2 content of 17.84%, resembling the ones found in Lula's field and described by Elias Junior (2015). The PVT and composition were input data for the Phase Behavior & Fluid Property Program called Winprop from CMG and exported into the model. It was used the component lumping option to reduce a total of 25 components to 9 pseudo components, *Table 5.3.2-1* and **Table 5.3.2-2**.

Table 5.3.2-1 PVT components oil 27.83 API high CO2 content 17.84%.

CO2	N$_2$	C1	C2	C3	IC4
0,178436	0.0020004	0.4482897	0.0528106	0.0407081	0.0010002
NC4	IC5	NC5	FC6	FC7	FC8
0,021704	0.0018004	0.0091018	0.0148030	0.0138028	0.0172034
FC9	FC10	FC11	FC12	FC13	FC14
0,014603	0.0128026	0.0116023	0.0107021	0.0112022	0.0102020
FC15	FC16	FC17	FC18	FC19	C20+
0,009502	0.0071014	0.0061012	0.0060012	0.0055011	0.0930186

Source: ELIAS JUNIOR, 2015

Table 5.3.2-2 Pseudo component after lumping.

Components after lumping (molar fraction)	
CO2	0.17843569
N2	0.0020004
C1	0.44828966
C2	0.05281056
C3	0.04070814
IC4 to NC5	0.03360672
C6 to C9	0.06041208
C10 to C14	0.0565113
C15 to C19	0.03420684
C20+	0.0930186

Source: ELIAS JUNIOR, 2015

The phase diagram and the oil viscosity curve can be observed in **Figure 5.3.2-1** and **Figure 5.3.2-2** respectively, they were based on Elias Junior's research (2015), and it was not modified as to keep the fluid properties as the original work. The bubble point pressure is 5759 psi.

Figure 5.3.2-1 Phase diagram.
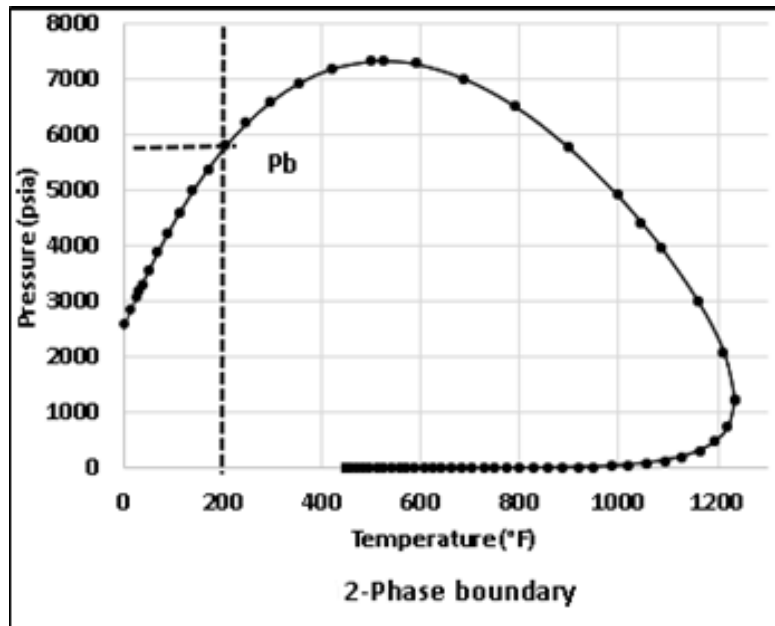
Source: ELIAS JUNIOR, 2015

Figure 5.3.2-2 Viscosity curve at 204.8°F.
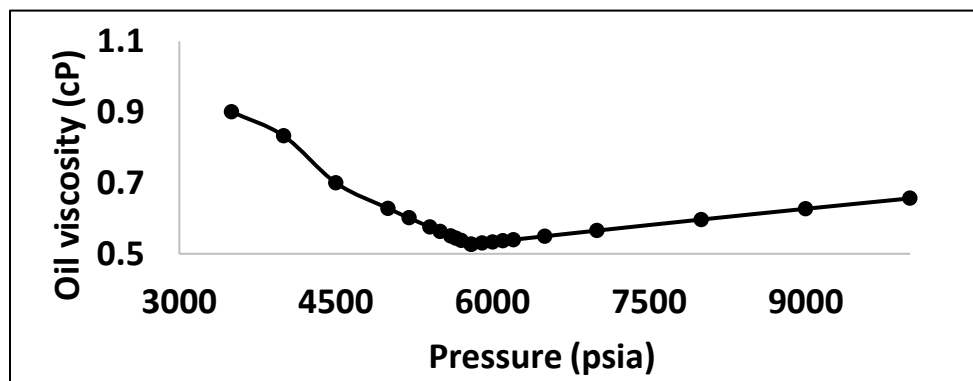
Source: ELIAS JUNIOR, 2015

5.4. ECONOMIC MODELS

All EOR methods: water, polymer and SP flooding were optimized under the water cut and NPV for both IFS models. The economic scenarios were built following a simplified Brazilian regime, having as main taxes and contribution variables presented in *Table 5.4-1*.

Table 5.4-1 Simplified Brazilian regime.

Variable	Value
Corporate tax	25%
Royalty	10%
Social contribution	9%
Social taxes rates (PIS, Cofins)	9.25%

Source: SAMPAIO et al., 2013

For all cases, the net present value was discounted by an investment covering the drilling and completion of wells, production platform, and abandonment. The economic parameters are resumed in **Table 5.4-2** and were based on the individual works of several researchers (ALSOFI et al., 2013; SAMPAIO et al., 2013; SHENG, 2014; GASPAR et al., 2015; SCHIOZER, 2015). As fior the project time a maximum of 30 years was selected for both, Lula and Cerena, however, if the shut-in constraints were reached before this limit the project was finished earlier.

Table 5.4-2 General economic parameters used economic evaluation.

Parameter	IFS Cerena	IFS Lula
Number of Wells	5	5
Investment on Platform (MMUSD)	985	305.96
Drilling and completion of vertical wells (MMUSD)	175	21.67
Investment in the exploration (MMUSD)	30	2.8
Abandonment cost	8.2% of drilling cost	
Annual discount rate	9 %	
Chemical facility Cost (MMUSD)	49.25	15.3

Source: ALSOFI et al., 2013; SAMPAIO et al., 2013; SHENG, 2014;

GASPAR et al., 2015; SCHIOZER, 2015

For the Lula based IFS, despite there are four producer's wells, it is important to highlight that each one of them is occupying only one-fourth of the well capacity. Therefore, the costs only represent the total expenditure for two wells, one injector, and one producer, the latter divided into four sections (exploration and platform investment). The platform cost depends of the fluid rates expected in the project; therefore, it was higher for the Cerena than for the Lula.

Moreover, being more specific, for the calculation of the investments abandonment and fluids related cost, it was employed the values state by Schiozer

et al. (2015). While the chemical facility cost was assumed as five percent (5%) of the platform investment base on AlSofi et al. (2013) research which employed a similar relation between both expenditures in a polymer flooding optimization. The facilities and treatment for the salinity content of the water injected was no taken into account in this research however it can increase the associated costs of the technology.

To assess the performance of the SP flooding, if compared with a polymer flooding and water injection, both optimized, an Expected Monetary Value (EMV) methodology alongside a derivation three analysis was used. For both inverted five spot models, it was considered three levels of reservoir heterogeneity and economic scenarios. These evaluation schemes can be observed in **Figure 5.4-1**. For the evaluation, each branch from the tree was assigned with a percentage weight for the final EMV calculation.

Figure 5.4-1 Derivation tree analysis for the inverted five-spot models.
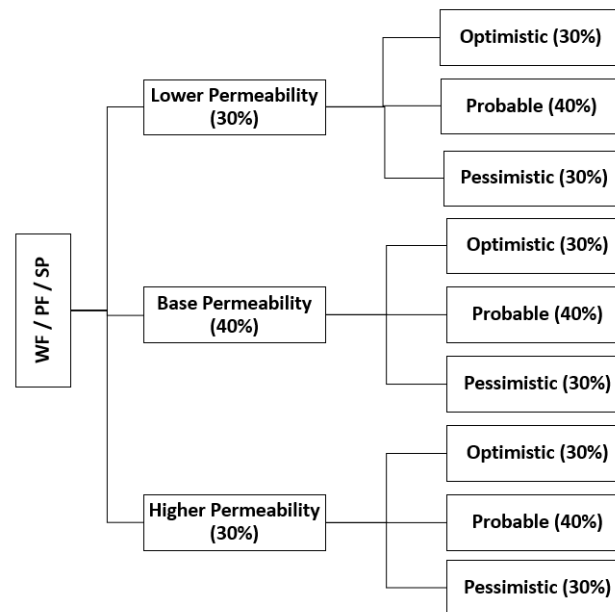
Source: Author, 2019

For the EMV, it was applied a simple multiplication between the weight percentage of the branch, the model probability (30% and 40%) and the

corresponding NPV. Finally, the results for each branch were summed up to calculate the EMV for each EOR methodology for each model, either WF, PF or SP.

The economic parameters considered for each optimization are presented in **Table 5.4-3**. Aiming at a balanced comparison between the water, polymer and SP injection programs, it was carried out optimization for all cases employing CMOST module from CMG, specifically the PSO having as objective function the NPV.

Table 5.4-3 Economic scenarios and parameters.

Scenarios	Oil Price (US$/bbl)	Oil Production Cost (US$/bbl)	Water Production Cost (US$/bbl)	Water Injection Cost (US$/bbl)	Polymer cost (US$/Kg)	Surfactant cost (US$/Kg)
Optimistic	70	10	1.1	1.1	1.05	2.3
Probable	50	9	1	1	1	2.2
Pessimistic	40	10	1.2	1.2	1.1	2.4

Source: Author, 2019

Finally, the EMV for each injection program is compared, and the highest value is the one which brings the highest added value to the reservoir production program.

5.5. OPERATIONAL CONDITIONS

In this section, it will be shown the operational conditions and constraints with each model was run in every economic scenario and IOR project.

5.5.1. CERENA-I

For this research, it is being considered the drilling of five wells for both models. In **Table *5.5.1-1*** it is shown the operational conditions assumed for the author for production and injection wells of the Cerena I - IFS.

Table 5.5.1-1 Initial operational constraints for injectors and oil production wells.

Well Type	Qty	Constraint	Value
Injector	1	Qinj max	25000 m^3/day
		BHP max	64121 kPa
Producers	4	BHP min	45400 kPa
		Qliq max	4769 m^3/day
		Qo min-Shutin	10 m^3/day

Source: Author, 2019.

For this model, the injection program starts after reaching an average pressure in all cells of 49299.6 kPa (bubble pressure). This was declared, accounting for a slower pressure decline after the bubble point.

The optimized parameters and the upper and lower limits are described in **Table 5.5.1-2**. For the IFS-Cerena, it was optimized the maximum oil rate, minimum bottom hole pressure, water cut to shut in each producer well, the minimum average reservoir pressure to begin the injection, for the chemical injections there were included, the chemical concentration and the Pore Volume (PV) injected.

Salinity concentrations are the parameter modifying the interfacial tension reduction of the surfactant in this research, as it was mentioned in section 2.3.

Table 5.5.1-2 Parameters optimized for the Cerena-IFS models and EOR methods.

Constraint	Initial	Max	Min
Min production Bottom hole pressure (kPa)	45400	50000	20000
Max Fluid production rate (m^3/day)	4769.62	6359.5	1589.87
Water cut shut-in producer (%)	99	99	70
Polymer Concentration on main slug (ppm)	1000	3000	500
Polymer Concentration on chase slug	1000	3000	500
Surfactant concentration on main slug (%)	0.5	0.5	0.05
Salt concentration main slug (ppm)	50000	100000	20000
Salt concentration chase slug (ppm)	50000	100000	20000
Minimum avg reservoir pressure to start injection (kPa)	49300	40000	50000
Pore Volumes injected: chemical batch	0.25	0.5	0.15

Source: Author, 2019

5.5.2. Lula

For this research, it is being considered the use of five vertical wells operated in an inverted five spot model. ***Table 5.5.2-1*** shows the operational conditions assumed for production and injection wells.

Table 5.5.2-1 Operational constraints for injectors and oil production wells.

Well Type	Qty	Constraint	Value
Injector	1	Qinj max	12000 BPD
		BHP max	8800 psi
Producers	4	BHP min	6000 psi
		Qliq max	3000 BPD
		GOR-Shutin	1965 ft^3/bbl
		Qo min-Shutin	100 BPD

Source: Author, 2019

The reservoir is initially developed without injection, so it resembles a common field development. After reaching an average pressure in all cells of 6000 psi, the injection phase starts, either water or chemical injection, this was declared, accounting for a slower pressure decline after the bubble point.

The optimized parameters and the upper and lower limits are described in **Table 5.5.2-2**. For the water injection exploitation program, the water cut to shut in the four wells and the minimum average pressure on all the reservoir to begin the water injection, chemicals concentration.

Table 5.5.2-2 Parameters optimized for each model and IOR method in the IFS Lula

Constraint	Initial	Max	Min
Water cut shut-in producer	0.99	0.99	0.90
Polymer Concentration (ppm)	1000	3000	500
Surfactant concentration (%)	0.5	0.5	0.05
Salt concentration of SP injection (ppm)	50000	100000	20000
Minimum avg reservoir pressure to start injection (psi)	6000	7000	5500
Pore Volumes injected: chemical batch	0.25	0.5	0.15

Source: Author, 2019

5.6. PARTICLE SWARM OPTIMIZATON

The optimization of all models and injection programs was done with the particle swarm optimization having as variable to maximize the NPV of each model by modifying the parameters mentioned previously on **Table 5.5.1-2** and **Table 5.5.2-2**. As for the parameters of the optimizer the selected ones are found on **Table 5.6-1**.

Table 5.6-1 Particle Swarm Optimization parameters

Inertia weight	Cognition Component	Social Component	Population size
0.7298	1.49618	1.49618	25

Source: Author, 2019

Each model was optimized until reaching 300 runs or until obtaining a visible plateau of maximum NPV as the one found in **Figure 5.6-1**.

Figure 5.6-1 PSO optimization example for PF probable economic scenario on the Cerena model
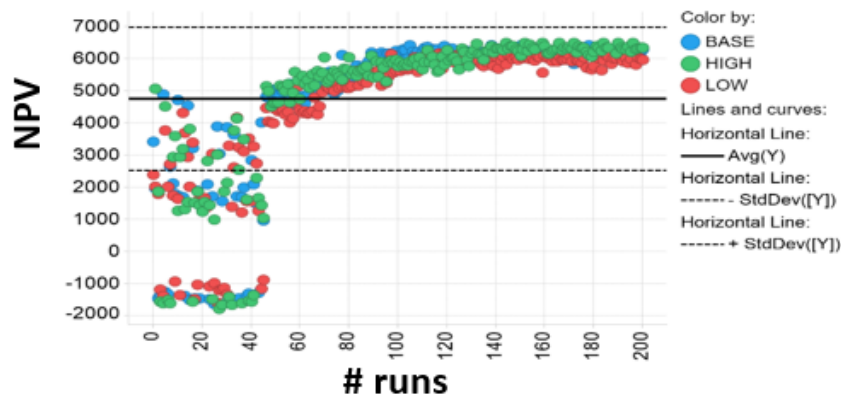
Source: Author, 2019

6. RESULTS AND DISCUSSIONS

In this section the results of the laboratory, and simulation for both Cerena and Lula models are discussed.

6.1. SURFACTANT INPUT SELECTION

The available surfactants (anionic, cationic and non-ionic) were characterized regarding their CMC adsorption in the saline medium.

Figure 6.1-1, presents the surface tension measurements for the anionic surfactant in the saline medium. It can be viewed the decreasing of the surface tension as the surfactant concentration increases and the intersection of these straight lines for the high salinity brine at 48 mg/L, which is the CMC value. The reference in distilled water of the CMC given by the manufacturer was 301 mg/L.

In **Figure 6.1-2**, it is found the curves to find the CMC of the non-ionic surfactant. There was no reference for this surfactant by the manufacturer in distilled water. The CMC was found at brine conditions as 109 mg/L.

Last, for the cationic surfactant, it was found a CMC of 300 mg/L in high brine conditions compared to 335 mg/L in distilled water given by the manufacturer. The lab plot obtained can be observed in **Figure 6.1-3**.

The difference of CMC between brine and distilled water conditions is known as "salting out" and it refers of how the salts present on the water steals the water available for polar chain hydration from the micelles resulting on lower surfactant concentrations required for the micelle concentration (HUBBARD, 2002; ROSEN, 2004).

Although at the CMC a solution attends its largest surface tension reduction, a chemical EOR method requires higher volumes to compensate for possible consumptions and losses on the reservoir due to entrapment or adsorption. Therefore, any field or simulation carried out must be over CMC concentration, and it is preferred a low CMC value, so the additional concentration does not affect the economy of any project. Similar behavior is expected in their adsorption, so no additional concentrations are added in the reservoir to compensate.

Figure 6.1-1 Anionic surfactant Surface Tension and Critical Micelle Concentration on NaCl high salinity brine, TDS 104361 ppm.
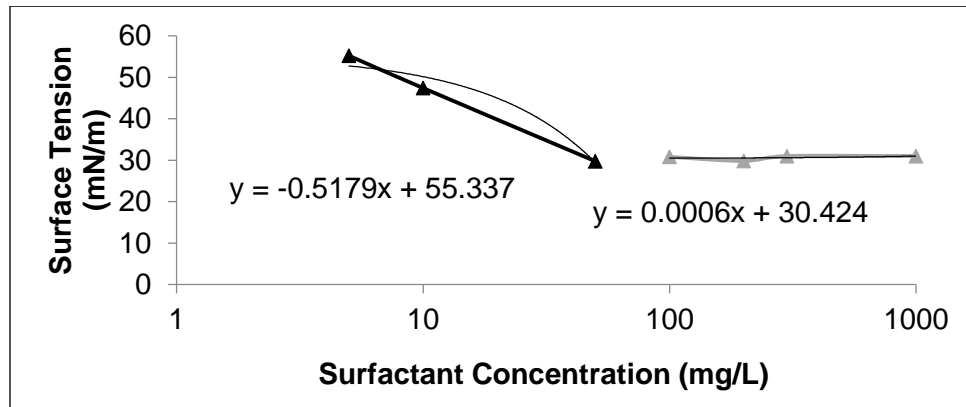
Source: Author, 2019

Figure 6.1-2 Non-ionic surfactant Surface Tension and Critical Micelle Concentration on NaCl high salinity brine, TDS 104361 ppm.
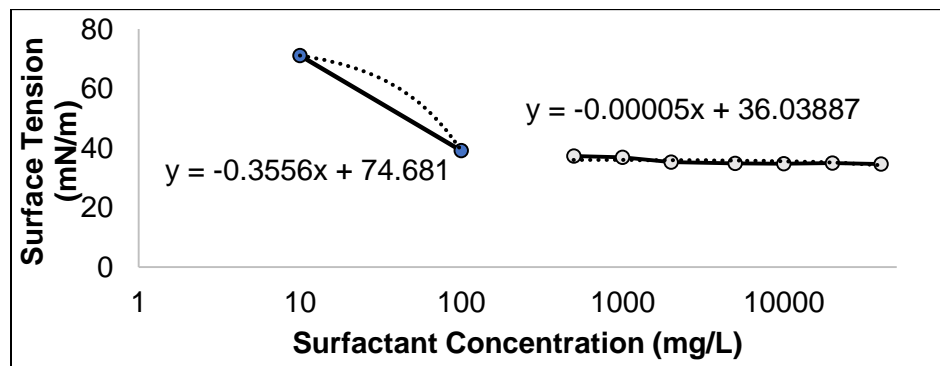
Source: Author, 2019

Figure 6.1-3 Cationic surfactant Surface Tension and Critical Micelle Concentration on NaCl high salinity brine, TDS 104361 ppm.
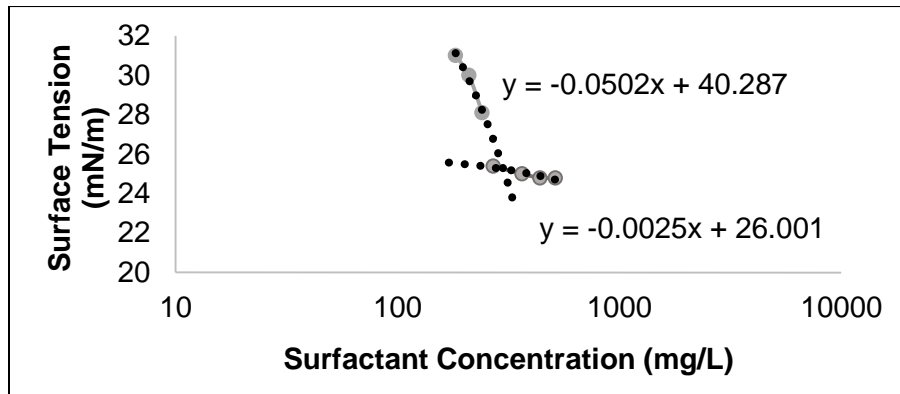
Source: Author, 2019.

Table 6.1-1 CMC for each surfactant evaluated in the laboratory.

Surfactant	CMC mg/L	Surface Tension mN/m
Anionic	48	30
Non-Ionic	36	109
Cationic	25	300

Source: Author, 2019.

Regarding surfactant adsorption, the cationic and anionic surfactant were tested as mentioned on the methodology by potentiometric titration and the non-ionic by comparing its surface tension behavior before and after rock powder presence. On **Figure 6.1-4** and **Figure 6.1-5** it can be found the adsorption curves for the non-ionic and anionic surfactants, were the plateau of adsorption was 6.3 mg/g-rock and 73.3 mg/g-rock respectively. As for the cationic surfactant its adsorption was so low that the delta between the surfactant before and after the presence of the rock after 24 hours was not perceived with the potentiometric titrator, therefore its adsorption was lower than 0.5 mg/g-rock, for this research due to the uncertainty of this measure it was selected this value reference of its adsorption. In this way, the largest consumption was on the anionic, followed by the nonionic and the cationic, behavior expected as it was mentioned in section 2.1, the surface and surfactant charges play a central role on the adsorption. In this case, the anionic with the negative charge was attracted much more by the positive surface of the carbonate generating larger adsorption. The opposite happened to the cationic surfactant.

Figure 6.1-4 Adsorption curve for the nonionic surfactant.
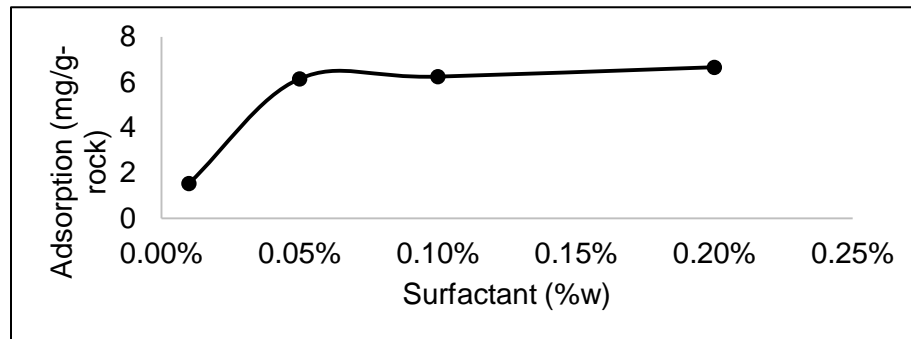
Source: Author, 2019

Figure 6.1-5 Adsorption curve for the anionic surfactant.
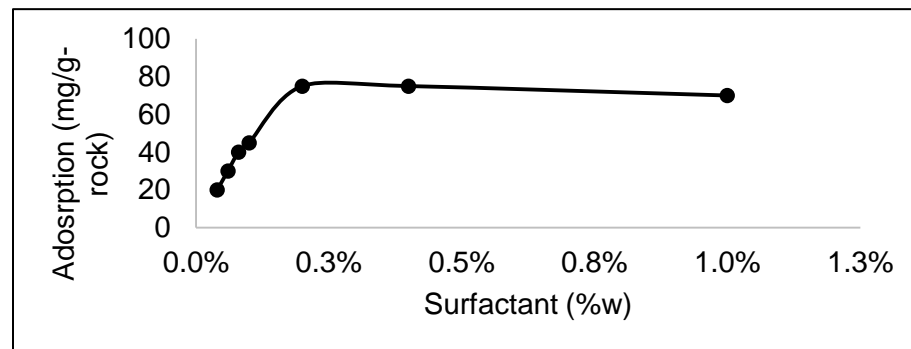
Source: Author, 2019

From these results, it was clear that it was required a surfactant with low adsorption similar to the cationic and non-ionic tested on the laboratory, and low CMC as the behavior encountered with the anionic surfactant, **Table 6.1-1**. The three surfactants did not fulfill the requirement of low adsorption and low CMC at the same time, therefore searching another surfactant was required. Additionally, as mentioned in the methodology, it was required information of the interfacial tension as a salinity function for a condition like the one encountered in the pre-salt reservoirs.

Therefore, for the surfactant, after reviewing the literature the modeling data were based on Zhang et al. (2013), using a sulfobetaine based zwitterionic surfactant with high salinity tolerance, expecting low interfacial tension (IFT) at salinity concentrations around 6% of salt content. Interfacial measurement as a function of

salinity was available at surfactant concentration ranging from 0.05% to 0.3 %, a concentration range useful to reduce the associated cost per kilogram of conventional surfactants. The interfacial tension versus total dissolved solids at different surfactant concentration is detailed in **Figure *6.1-6***. The surfactant adsorption on limestone was also considered, and it was defined as 0.72 mg/g-rock based on Zhang et al. (2013), lower than other researches (AHMADI; SHADIZADEH, 2016), and the critical micelle concentration was included on the model as the minimum concentration required to observe micelle formation, 2.65×10^{-3} g/L.

Figure 6.1-6 IFT at different surfactant concentration.
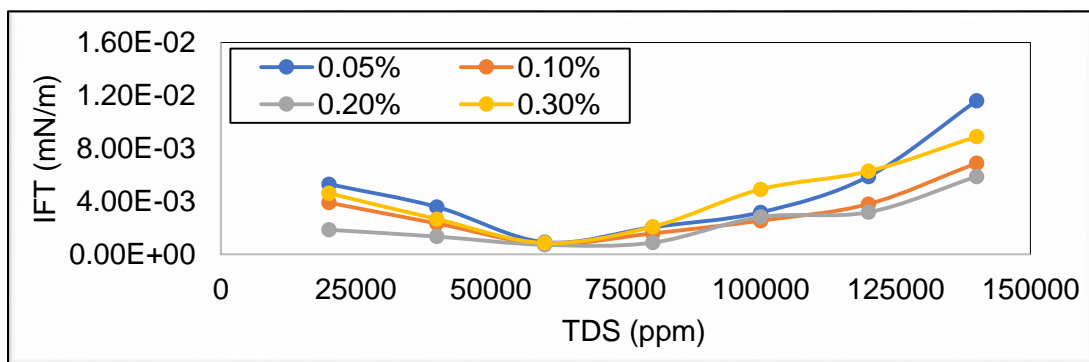
Source: ZHANG et al., 2013.

As can be observed this surfactant fulfills the behavior detailed previously, it presents low adsorption with less than 1 mg/g-rock, its CMC is placed in a low range which makes viable its use on a commercial scale, and its behavior at high salinity brines present low interfacial tension ($\sim 1 \times 10^{-3}$ mN/m). This data was the one employed as input for the simulation models.

6.2. POLYMER BEHAVIOR

The curves describing the rheology behavior of the polymeric solution test can be observed in **Figure *6.2-1***, following the procedure previously described and synthetic brine from the stock.

Figure 6.2-1 Viscosity as a function of shear rate for different polymer concentrations in a synthetic brine.
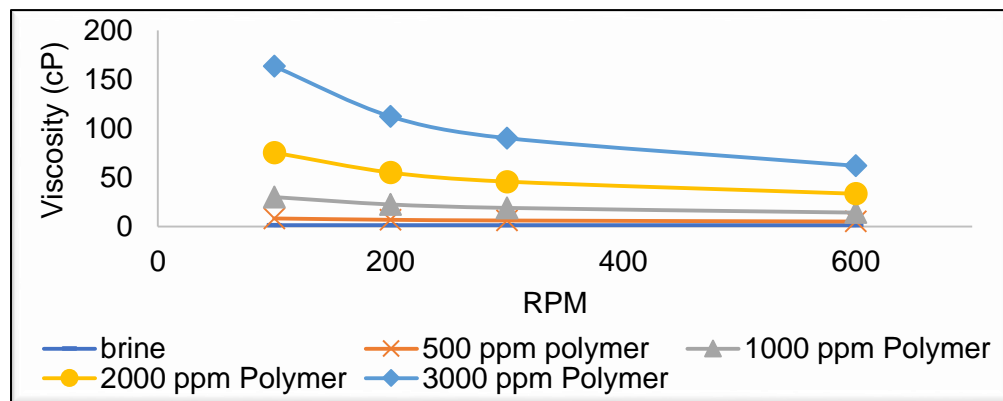
Source: Author, 2019

As discussed previously, a solution with a higher viscosity than oil was needed, >20 cP at 20°C. Therefore, polymer solutions with concentrations under 1000 ppm did not fit the requirement, so were not used preliminary (0, 500 ppm). The 1000 ppm line even when at some points w close to the oil viscosity and at very low revolutions is higher, it is discarded because these velocities are not representative of wellbore conditions, and aggressive conditions will bring uncertainties of the possible behavior of the polymer (mechanical degradation). So, the other two options are 2000 ppm and 3000 ppm, however, even when both go over the condition established, the former concentration in a preliminary screening is the option selected. The main reason is, that higher polymer concentrations represent higher costs for an EOR method, moreover, a solution with a viscosity higher than the expected can represent higher injection pressures at wellbore conditions.

It must be stated the viscosity behavior of the polymer was an input for the simulation phase, so a more precise polymer concentration is obtained under the optimization step. The tables with the laboratory measurements, n and K parameters are in the **Appendix C**.

6.3. LULA INVERTED FIVE-SPOT MODEL SIMULATION RESULTS

The main results for the inverted five-spot model, based on the Lula field case study, are detailed in the next sections.

6.3.1. Comparison between IOR methods – Economic Scenarios

In **Table 6.3.1-1** shows the results obtained for the optimization of WF, PF, and SP. It can be noticed that despite the polymer injection reduced the volume of injected and produced water, and kept the oil produced, the higher cost associated to the polymer injection reduced the NPV of the field exploitation program. As for the SP, the simultaneous injection of polymer and surfactant did increase the oil produced and the recovery factor, while at the same time the water production and water injection volumes were higher than the WF values, resulting in higher expenditures on treatment and chemical injection. Such behavior summed up to a longer production time of the model, it is reflected on a lower NPV when compared with the water injection. This behavior was observed in all three models and economic scenarios.

Table 6.3.1-1 Results for Lula IFS.

Model	Scenario	IOR	Oil Production (MMBbl)	Water production (MMBbl)	Water injection (MMBbl)	Period (Years)	Polymer Cost (MMUSD)	Surfactant Cost (MMUSD)	NPV (MMUSD)	RF (%)	Final WCut (%)
BASE	70 USD	WF	28	47	89	20	-	-	232.0	68%	96%
	70 USD	PF	29	45	87	20	4.7	-	222.8	69%	96%
	70 USD	SP	31	53	99	23	6.8	10.6	222.4	74%	95%
	50 USD	WF	28	36	77	18	-	-	52.1	67%	94%
	50 USD	PF	28	34	75	17	4.4	-	41.1	67%	94%
	50 USD	SP	30	45	90	21	4.6	10.1	41.5	73%	94%
	40 USD	WF	26	17	56	13	-	-	-59.6	63%	91%
	40 USD	PF	26	16	55	13	4.9	-	-71.9	64%	90%
	40 USD	SP	29	37	80	18	5.1	11.1	-83.5	71%	90%

LOW	70 USD	WF	26	45	83	19	-	-	192.7	62%	95%
	70 USD	PF	26	42	80	19	6.7	-	183.4	63%	95%
	70 USD	SP	28	59	101	23	10.0	21.8	177.9	68%	95%
	50 USD	WF	25	35	72	17	-	-	24.5	61%	94%
	50 USD	PF	26	35	73	17	4.5	-	13.3	62%	94%
	50 USD	SP	28	54	96	22	12.7	19.2	5.0	68%	94%
	40 USD	WF	24	20	55	13	-	-	-81.1	58%	90%
	40 USD	PF	24	21	57	13	5.0	-	-93.8	59%	91%
	40 USD	SP	26	35	74	17	11.8	17.8	-109.8	63%	88%
HIGH	70 USD	WF	30	31	75	17	-	-	255.7	72%	95%
	70 USD	PF	30	31	76	17	4.8	-	246.4	72%	96%
	70 USD	SP	34	57	107	24	9.0	10.6	236.0	82%	94%
	50 USD	WF	29	28	71	16	-	-	73.0	71%	94%
	50 USD	PF	30	25	69	16	4.7	-	61.5	71%	93%
	50 USD	SP	33	56	105	24	4.5	10.0	41.5	79%	90%
	40 USD	WF	29	23	66	15	-	-	-43.5	70%	90%
	40 USD	PF	29	22	66	15	4.9	-	-56.6	71%	90%
	40 USD	SP	32	48	95	22	6.4	11.2	-78.7	77%	88%

Source: Author, 2019

Moreover, it can be concluded that higher oil prices tend to favor the use of chemicals when observing that the exploitation period of the Probable and Pessimistic scenario were shorter than the Optimistic Scenario with higher oil prices. In years for the SP, 23>21>18 years and for the PF, 20>21>18 years, optimistic, probable, and pessimistic respectively.

For all three economic scenarios, both chemical programs proved to be not profitable even after the optimization performed. Although both presented a positive end revenue on the optimistic and probable scenarios, the chemical cost impacted the production program severally in the long run (15.3 MMUSD of chemical facilities cost at year one). However, it was proved that the PF brings lower volumes of produced water and requires lower volumes of water injected. As for the SP program, it increases the oil recovery factor by allowing longer production periods, but the cost of having longer production periods and chemical cost kept the NPV on all three scenarios at the same value of the PF, and lower than the WF.

On the other hand, it can be stated that the SP was technically speaking a success as it brought an incremental recovery ranging 5.5% to 10.3% when comparing against the WF. Proving that not all technical projects are economically viable, as in this case, the incremental was not enough to cover the chemical expenditure of injecting simultaneously surfactant, polymer and the facilities investment required for this procedure. Also, in all the six cases the final water cut was the same or lower than the ones found on the WF and PF, with longer production times, stating that the mix of surfactant and polymer at least brings the same benefits as the polymer flooding by itself.

6.3.2. Comparison of EOR methods - Geological models

For this analysis, the optimized injection programs with an oil price of 50USD/bbl were the cases taken to evaluate how the three models differ from each other for both the polymer flooding and the surfactant-polymer flooding.

In the literature can be found that a higher permeability is often desired on almost all screening criteria as described by Sheng et al. (2015) because low permeability zones often present smaller transmissibility areas where the large polymer molecules may fail to flow.

In **Figure 6.3.2-1** are represented the water cut curves for all the three models for the PF and SP injection. The uniform injection front on the reservoir results on more instantaneous water cut increment of all production wells, which is reflected on close to vertical slopes. As for the SP, the behavior is very similar; however, the water cut reaches its maximum much slower than for PF, allowing for longer production times and therefore higher recoveries. This can be also observed in **Figure 6.3.2-2** where the SP last for a longer period reaching higher recoveries than the other two methodologies.

Figure 6.3.2-1 Water cut curves for three heterogeneity models for both chemicals flooding at the probable economic scenario.
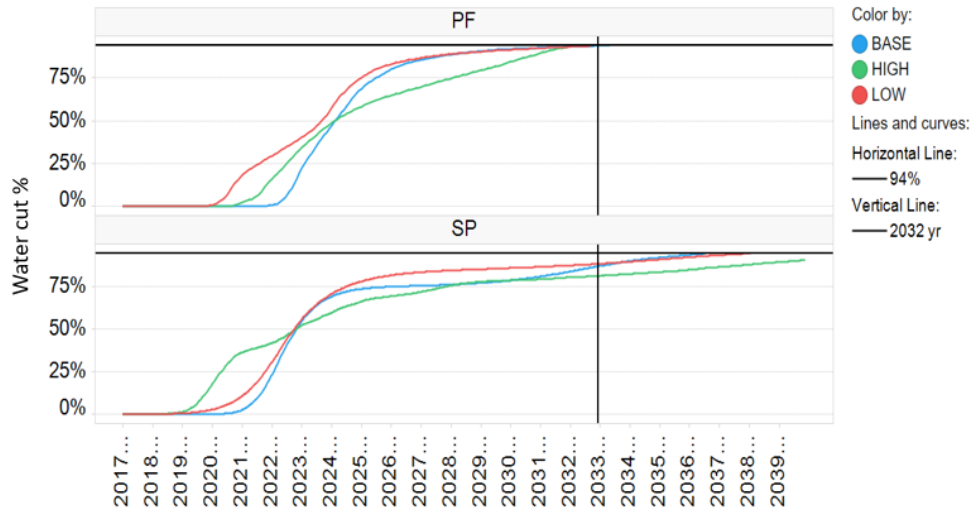
In **Figure 6.3.2-2**, it can be observed that with higher values of permeability, even when it is not a norm, higher recovery factor, therefore, larger produced volumes. On the other hand, the model with less recovery was the one with 200mD. WF and PF shut-in at earlier times in all three models which ratified the improvement in the oil sweep and incremental oil of the SP technique.

Figure 6.3.2-2 Oil recovery factor for all three heterogeneity models for all injection programs at the probable economic scenario.
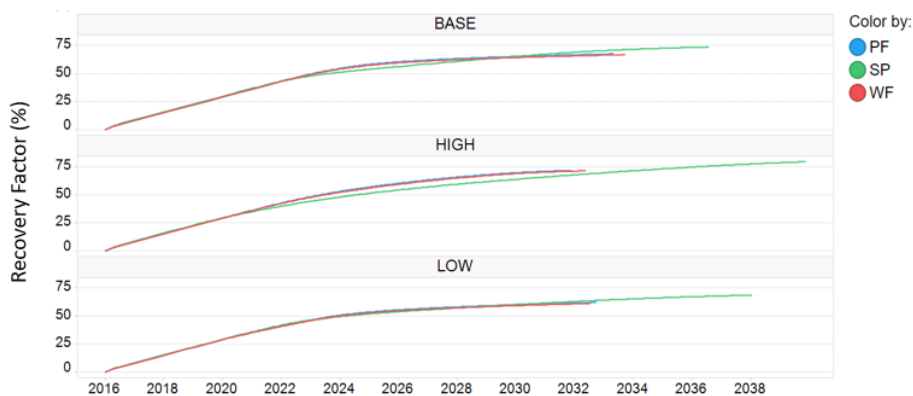
In **Table 6.3.2-1**, it can be noticed that the final results of the optimization did not lead to an apparent relation about heterogeneity and polymer consumption, nor

because it is inexistent but because the optimization followed the tendency to reduce to a minimum the chemical concentration and pore volumes injected.

Table 6.3.2-1 Polymer consumption and associated cost for each heterogeneity model.

Model	Scenario	PV	Pol Conc (ppm)	Pol Cost (MMUSD)	Pol Qty (MMlbm)
	50 USD	0.15	500	4.43	2.01
BASE	40 USD	0.15	500	4.87	2.01
	70 USD	0.15	500	4.65	2.01
	50 USD	0.15	525	4.66	2.11
HIGH	40 USD	0.15	500	4.87	2.01
	70 USD	0.15	500	4.80	2.07
	50 USD	0.15	500	4.52	2.05
LOW	40 USD	0.15	500	4.96	2.05
	70 USD	0.21	500	6.67	2.88

Source: Author, 2019

As for the SP, on *Table 6.3.2-2* can be observed that like PF, the optimization tended to the minimum injection of surfactant, as it is the highest cost material. But in this case, the tendency to have higher cost can be observed in the low permeability case, which requires larger PV injected to bring similar recoveries as to the other two models in any of their scenarios. Concluding that low permeability reservoirs required larger quantities of chemical injection and may be not the best option for a CEOR injection.

Table 6.3.2-2 Chemical consumption and associated cost for each heterogeneity model on SP flooding.

Model	Scenario	PV	Pol (ppm)	Surf Conc (%)	Pol Cost (MMUSD)	Surf Cost (MMUSD)	Pol Qty (MMlbm)	Surf Qty (MMlbm)
	50 USD	0.15	500	0.05	4.60	10.12	2.09	2.09
BASE	40 USD	0.15	500	0.05	5.11	11.14	2.11	2.11
	70 USD	0.15	701	0.05	6.80	10.62	2.94	2.10
	50 USD	0.15	500	0.05	4.53	9.96	2.06	2.06
HIGH	40 USD	0.15	630	0.05	6.44	11.16	2.66	2.11
	70 USD	0.15	894	0.05	8.99	10.55	3.88	2.08

	50 USD	0.29	724	0.05	12.66	19.23	5.75	3.97
LOW	40 USD	0.24	726	0.05	11.83	17.77	4.88	3.36
	70 USD	0.31	500	0.05	9.96	21.82	4.31	4.31

Source: Author, 2019

6.3.3. Parameters optimization

All the field development programs: water, polymer, and surfactant-polymer floodings were optimized for all economic and geological scenarios. This way, a balanced comparison could be performed between the EOR methodologies. Next, the key behaviors regarding the parameters being optimized for the PF and SP are discussed.

6.3.3.1.   Polymer flooding parameters

In **Table 6.3.3.1-1**, it can be found the optimized parameters for all geological models and all the three economic scenarios. It can be observed that despite the difference of permeability, all three models in all three economic scenarios had the smallest polymer concentration possible for this research. The main reason is the high cost associated to the chemical injection, which the optimizer reduces to improve the NPV. In other words, there was an inverse correlation between chemical concentration and NPV. This analogy can be observed in **Figure 6.3.3.1-1**, as the polymer concentration was reduced the NPV increases even going from losses to bring some profit until a plateau is reached and no further reduction alters the NPV. The situation was accrued due to the economic parameters fixed for the pessimistic scenario. Thus, the optimization model brought as optimal, the cases where a minimum of the polymer was injected, with all NPVs were negative.

As for the optimistic model, it can be highlighted that the NPV delta in the optimistic model was much less than in the other two economic scenarios, showing that higher oil prices increase the viability of using chemical EOR programs.

Table 6.3.3.1-1 Optimized parameters for PF per model and economic scenario.

Scenario	50	40	70	50	40	70	50	40	70
Parameter/Model	BASE	BASE	BASE	HIGH	HIGH	HIGH	LOW	LOW	LOW
WCUT1	99.0%	96.0%	94.9%	99.0%	90.0%	95.8%	93.4%	90.0%	95.2%
WCUT2	99.0%	98.2%	99.0%	99.0%	98.5%	99.0%	95.7%	90.3%	95.0%
WCUT3	95.2%	90.0%	97.4%	99.0%	91.3%	98.5%	94.9%	96.1%	97.5%
WCUT4	95.0%	91.5%	98.7%	94.9%	98.8%	97.8%	96.2%	97.0%	96.1%
Injection Trigger (psi)	7000	7000	7000	7000	7000	7000	7000	6879	6932
PV Injected	0.15	0.15	0.15	0.15	0.15	0.15	0.15	0.15	0.21
ppm Pol	500	500	500	525.7	500	500	500	500	500
NPV (MMUSD)	41.1	-71.9	222.8	61.5	-56.6	246.4	13.3	-93.8	183.4
% Delta NPV	-21.1%	-20.6%	-4.0%	-15.8%	-29.9%	-3.7%	-45.7%	-15.7%	-4.9%
Oil RF	67.3%	63.8%	68.7%	71.4%	70.6%	72.2%	61.8%	59.0%	62.9%
Incremental RF	0.7%	0.8%	0.7%	0.3%	0.5%	0.8%	0.9%	1.1%	0.5%

Source: Author, 2019

Based on **Table *6.3.3.1-1***, it can be noticed that with higher average permeability, the higher NPV and RF are. This statement was backed up if it is remembered Darcy's equation, in which there is a direct correlation between permeability and the oil rate, meaning that the higher permeability model is the one which brings higher recoveries. Based on **Table 6.3.3.1-1**, and relating to the Probable scenario analysis, it can be said that with higher average permeability, the higher the NPV.

Moreover, based on **Table *6.3.3.1-1***, the average water cut to shut in the well increased as the oil price did, 94.0% > 96.7% > 97.1% in order of 40USD, 50 USD and 70USD respectively. Therefore as the oil price increases, the water treatment is compensated, allowing longer periods of production and higher cost due to large water-oil ratios of fluid production. However, each well behaved differently for every geological model, so fixing one or all well to the same water cut shut in will not bring

profits without an adequate selection. It can be seen in **Figure 6.3.3.1-3** and **Figure 6.3.3.1-4** examples of this behavior.

Figure 6.3.3.1-1 NPV versus polymer concentration injected on the polymer flooding for all three geological and a probable economic scenario.
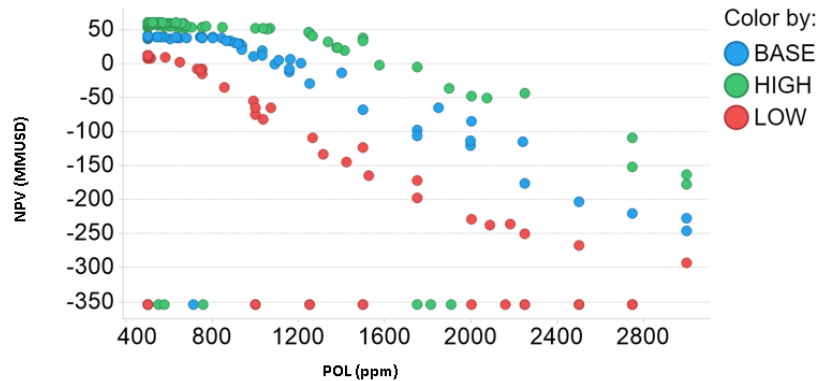
Source: Author, 2019

On the contrary, the minimum average pressure on the reservoir at which the injection well should be opened follows an opposite tendency, so a lower pressure means more time producing under no injection with the own reservoir energy. In **Figure 6.3.3.1-2**, it can be observed that the optimum moment to start the injection is in a range close to 6000 to 7000 psi. As for the minimum average pressure in the reservoir at which the injector should be opened follows the same tendency as the probable economic scenario, lower pressure means more time producing under no injection with the own reservoir energy

Figure 6.3.3.1-2 Effects of the Minimum average reservoir pressure to start injection on the NPV for all three geological models and a probable economic scenario.
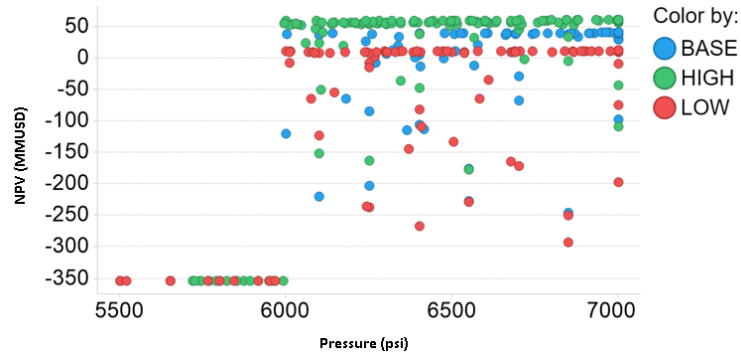
Source: Author, 2019

Figure 6.3.3.1-3 Water cut optimization at an optimistic economic scenario and three geological models for a) producer 2 and b) producer 4.
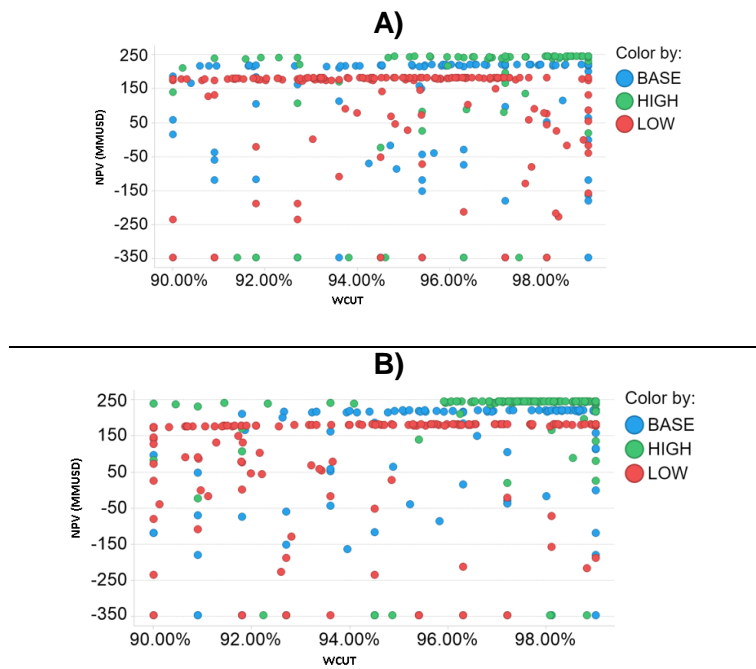
Source: Author, 2019

Figure 6.3.3.1-4 Water cut optimization at a pessimistic economic scenario and three geological models for a) producer 2 and b) producer 4.

A)

B)
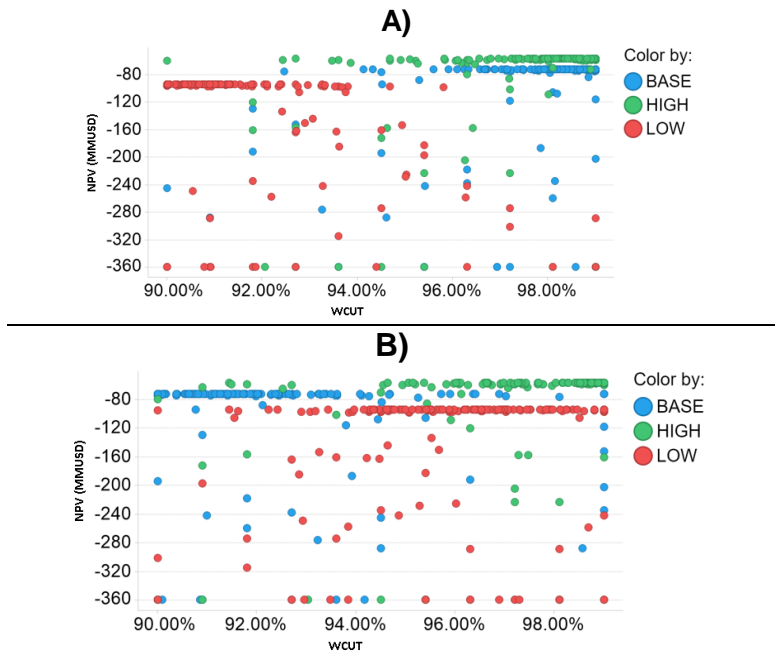
Source: Author, 2019

As for the Pore volume injected, in all three economic scenarios the tendency was to reduce it, explained as to reduce the quantity and therefore the associated cost of the chemicals, the median value of all the simulation runs per model is 15% to 16% of PV injected disregarding the economic scenario, **Figure 6.3.3.1-5**.

Figure 6.3.3.1-5 Pore volumes injected of the chemical slug for the PF per model.
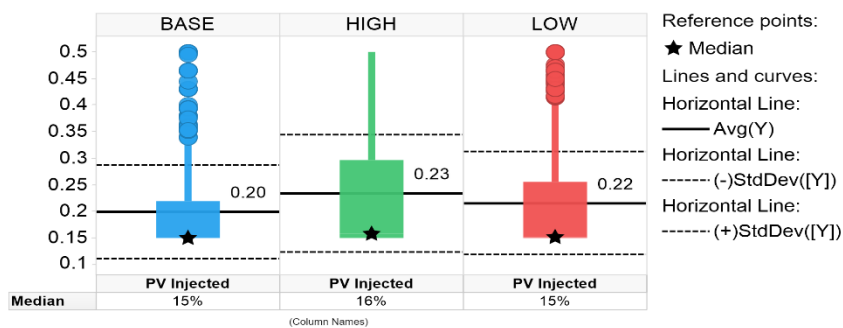
Source: Author, 2019

6.3.3.2. Surfactant-polymer flooding parameters

In *Table 6.3.3.2-1* can be found the optimized parameters for the surfactant-polymer flooding for all three modes and economic scenarios.

Regarding the production wells, it can be seen in **Figure 6.3.3.2-1** and *Table 6.3.3.2-1* that each well behaves differently in each model, as was discussed previously for the Polymer flooding cases. Arriving at the same conclusion that fixing one or all wells to the same shut-in water cut will not bring profits without an adequate selection.

Figure 6.3.3.2-1 Water cut shut-in behavior per economic scenario and every producer.
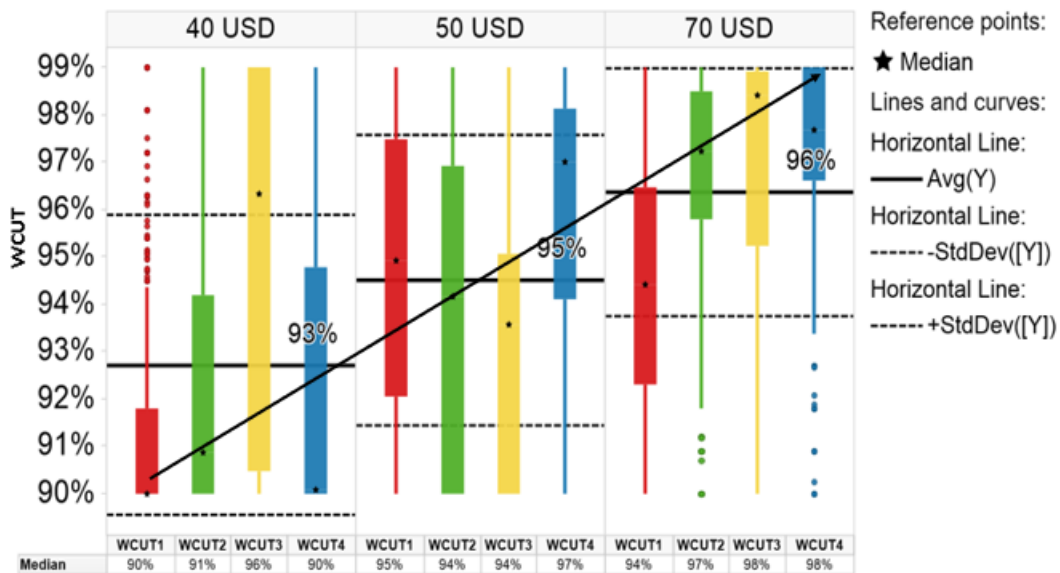
Source: Author, 2019

However, in **Figure 6.3.3.2-1** can be evaluated that as the oil price increases the water cut to shut in any of the wells increases, from 93% on the low model and 96% on the high model. Now, talking individually from each producer, the only two wells with this tendency are number 2 and 4, as their distribution moves according to the price and the median of it. This behavior reflects how at higher oil prices wells,

they have larger final ultimate recoveries because water processing costs can be compensated by the oil sells, confirmed with the values on **Table *6.3.3.2-1*** where the shut-in water cuts are lower for the pessimistic scenario and larger for the optimistic scenario, on average only for the optimized results 96.9%>94.7%>92.2% for the optimistic, probable and optimistic scenario.

Table 6.3.3.2-1 Optimized parameters for Surfactant-polymer flooding per model and economic scenario.

Scenario	50	40	70	50	40	70	50	40	70
Model	BASE	BASE	BASE	HIGH	HIGH	HIGH	LOW	LOW	LOW
WCUT1	99.0%	90.0%	94.0%	90.0%	90.7%	95.8%	94.8%	90.0%	95.2%
WCUT2	95.3%	90.0%	98.3%	90.0%	90.0%	99.0%	98.5%	93.1%	95.0%
WCUT3	94.3%	96.0%	98.6%	90.0%	90.4%	98.5%	94.2%	99.0%	97.5%
WCUT4	97.1%	96.9%	97.4%	94.6%	90.0%	97.8%	98.0%	90.0%	96.1%
Injection trigger (psi)	5500	6681	5501	6957	6864	7000	6499	5500	6932
PV Injected	0.15	0.15	0.15	0.15	0.15	0.15	0.29	0.24	0.21
Pol (ppm)	500	500	701	500	630	500	724	726	500
Salt in chemical batch (ppm)	43833	57805	48990	20000	59104	49259	44795	41969	40835
Salt pos chemical batch (ppm)	20000	100000	100000	100000	100000	20000	20000	20000	20000
Surfactant (%)	0.05	0.05	0.05	0.05	0.05	0.05	0.05	0.05	0.05
NPV (MMUSD)	41.5	-83.5	222.4	41.5	-78.7	246.4	5	-109.8	183.4
% Delta NPV	-20.3%	-40.1%	-4.1%	-43.2%	-80.8%	-3.7%	-79.4%	-35.4%	-4.9%
Oil RF	73.4%	70.5%	73.8%	79.2%	77.2%	72.2%	68.3%	63.4%	62.9%
Incremental RF	6.8%	7.6%	5.8%	8.1%	7.0%	0.8%	7.4%	5.5%	0.5%

Source: Author, 2019

Another tendency that can be observed is that the low permeability model in all cases had the larger pore volumes injected, indicating higher volumes of the chemical slug are required to achieve higher oil recoveries as the permeability is lowered.

As for polymer concentration, it was observed a similar behavior as the found for the polymer flooding, the optimal value went to the lower range, because of the high cost associated to the polymer powder, therefore, a small amount of the

chemical gives better NPV as it is reduced. This analogy can be observed in **Figure 6.3.3.2-2**, as the polymer concentration is reduced the NPV increases even going from losses to bring some profit until a plateau is reached and no further reduction alters the NPV in a range of 800 to 500 ppm. This range matched with the one in the **Table *6.3.3.2-1*** that had values slightly over 700ppm. This points to the idea that the parameters controlling the NPV of the project where the polymer concentration and the size of chemical batch injected.

Figure 6.3.3.2-2 NPV versus polymer concentration injected on the Surfactant-polymer flooding for all three geological and a probable economic scenario.
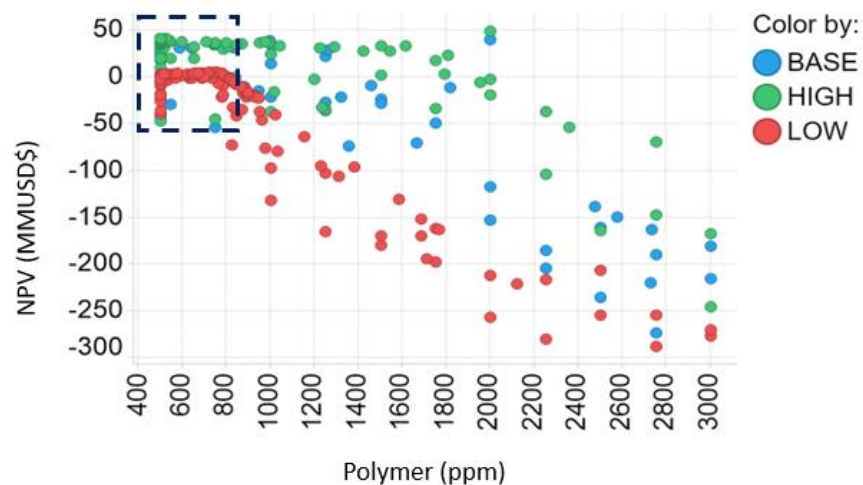
Source: Author, 2019

Based on **Table *6.3.3.2-1***, it can be noticed that higher average permeability and oil prices result in higher recovery factors. However, it also proves that higher recoveries not always do bring larger NPVs, as for this the reduction was 34.6% on average when comparing against the waterflooding. Also, the water cut to shut the wells tends to be over 94% in 9 of 12 times. However, the average water cut to shut in producers in the High model, is of 91.1%, less than the average of the other two models, 96.4%. Closing earlier the wells can be the cause of why it is presenting similar NPV that the Base case, something irregular when comparing the optimization results of the other economic scenarios and injection programs where the High permeability model is always the one with the best Cash flow. This scenario

presented a local minimum in the water cut parameters, therefore not followed the behavior expected.

Regarding the surfactant percentage, it was observed in **Figure *6.3.3.2-3*** that the tendency followed by both chemicals is the same, to reduce their associated costs. However, the interfacial tension reduction was kept as can be observed in

Figure 6.3.3.2-4 where at the beginning, a front of low interfacial tension is formed (microemulsion), and it moves across all the model until reaching the producers, which has an effect of increasing the oil recovered while moving at the same time original water saturation. This movement of oil and formation brine is what increments the water produced when compared against the polymer flooding results on section 6.3.1.

Figure 6.3.3.2-3 Surfactant concentration versus polymer concentration injected on the Surfactant-polymer flooding for all three geological and a probable economic scenario.
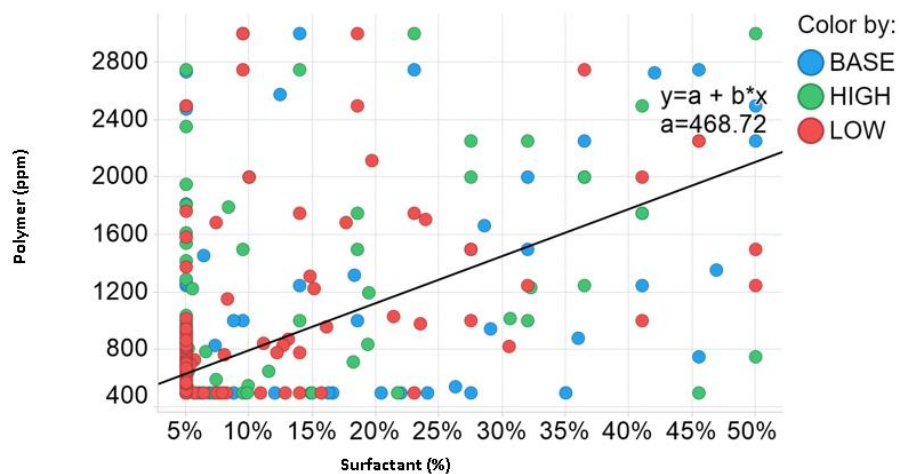
Source: Author, 2019

Figure 6.3.3.2-4 Interfacial tension o-w, two years (left) and after 9 years (right).
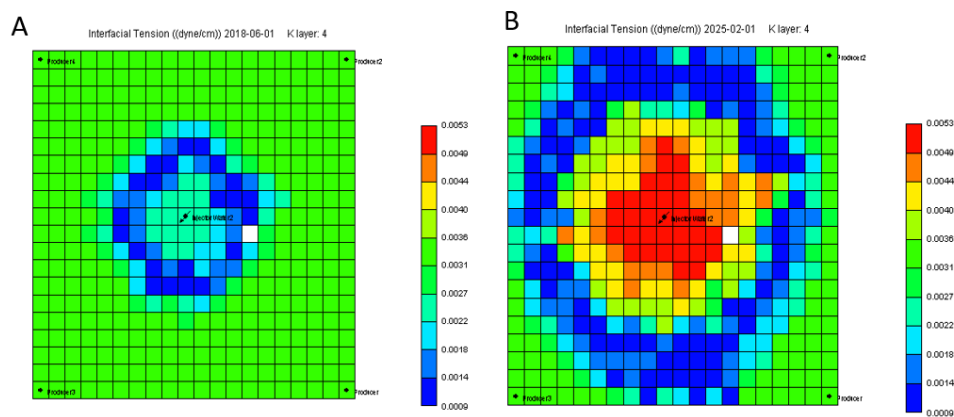
Source: Author, 2019

On the contrary, the minimum average pressure on the reservoir at which the injection well should be opened follows an opposite tendency, so a lower pressure means more time producing under no injection with the own reservoir energy. From **Figure *6.3.3.2-5***, it can be observed that the optimum moment to start the injection is in a range close to 6100 to 7000 psi, with an average of 6380 psi (***Table 6.3.3.2-1 Optimized parameters for Surfactant-polymer flooding per model and economic scenario.Table 6.3.3.2-1***), values over the bubble point pressure where the injection presents higher efficiency as does not have to fill a gas layer.

Figure 6.3.3.2-5 Effects of the Minimum average reservoir pressure to start injection on the NPV for three geological models and a probable scenario.
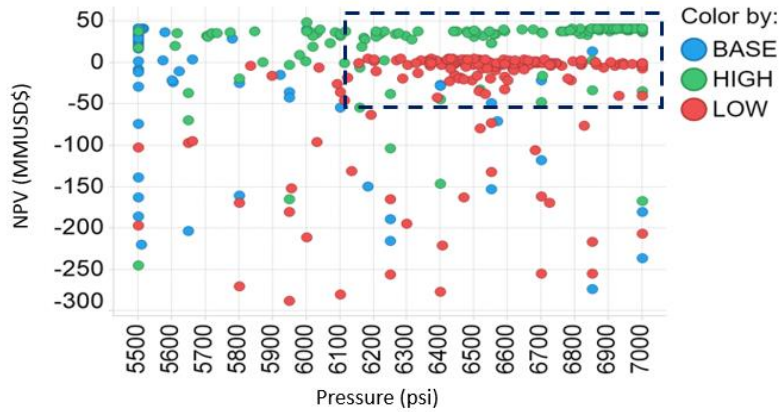
Source: Author, 2019

On **Figure 6.3.3.2-6** can be observed the box plots for each economic scenario and model for the salinity content of the chemical batch, where the tendency of the salt concentration of the brine carrying the surfactant was to go lower than the optimal value (60000ppm). Indicating the preference of a negative gradient injection program, based on the salinity content.

Figure 6.3.3.2-6 Chemical batch salt content per model and economic scenario.
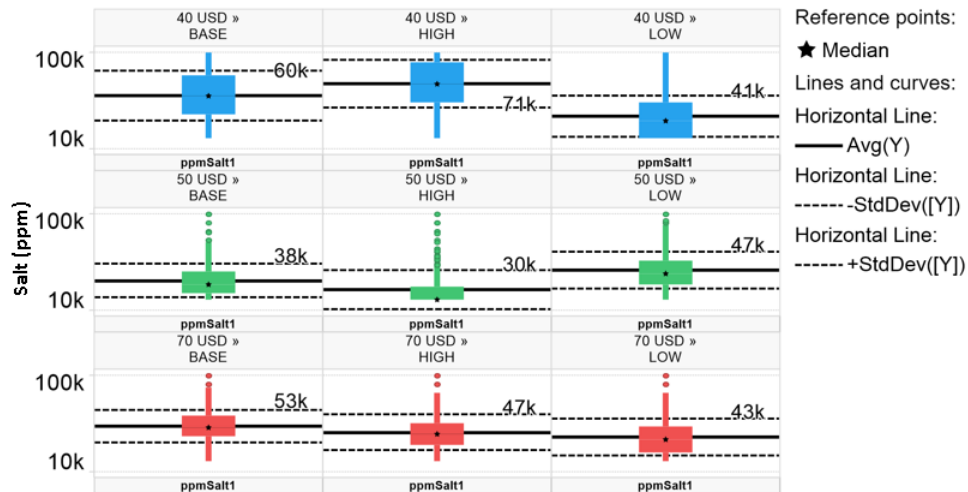
Source: Author, 2019

Moreover, **Table *6.3.3.2-1***, are found the optimized parameters for the optimistic and pessimistic scenarios. Where similar to the probable scenario, the higher the permeability the higher the NPV. Another tendency that can be observed is that the low permeability model in all cases had the larger pore volumes injected,

indicating higher volumes of the chemical slug are required to achieve higher oil recoveries as the permeability is lowered, specifically higher quantities of surfactant.

Taking into a count the optimal values of table **Table *6.3.3.2-1***, it can be observed that a negative gradient of salt injection is being followed, the first batch in 8 of the 9 cases had salt content under its optimal value of 60000 ppm, while the water injection which followed the chemical batch presented in 5 of 9 cases under optimal conditions too. This behavior is explained as in reservoir conditions the salt content of the formation brine is much higher than the optimal value; therefore the injection scheme must take into account the creation of a salinity mix between formation and injection waters (HIRASAKI; MILLER; PUERTO, 2011).

6.3.4. Expected Monetary Value (EMV) Lula

The Expected Monetary Value for the waterflooding, polymer flooding and Surfactant-polymer flooding including the NPV of all three economic scenarios and all three heterogeneous models were 69.9 MMUSD, 58.8 MMUSD, and 49.2 MMUSD respectively (**Table 6.3.4-1**, **Table 6.3.4-2** and **Table 6.3.4-3**). Therefore, with a difference of 16% and 30%, the water flooding it's the best injection program for the inverted five-spot model representing the Lula Field properties. The largest difference of 26% and 40% against PF and SP respectively is encountered on the low permeability model corresponding to a reservoir with 200mD as average permeability. Finding that matches with the common criteria that low permeability reservoirs are less preferable for chemical EOR projects that employ polymer as viscosifying agent (TABER; MARTIN; SERIGHT, 1997b; DICKSON; LEAHY-DIOS; WYLIE, 2010; AL ADASANI; BAI, 2011).

Table 6.3.4-1 NPVs and resulting EMVs for a waterflooding program

		Waterflooding NPV (MMUSD)		
Model	Probability	Optimistic 30%	Probable 40%	Pessimistic 30%

Model	Probability	Optimistic	Probable	Pessimistic	
Base	40%	232	52	-60	29
High	30%	256	73	-44	28
Low	30%	193	24	-81	13
				EMV	69.9

Source: Author, 2019

Table 6.3.4-2 NPVs and resulting EMVs for a polymer flooding program.

		Polymer Flooding NPV (MMUSD)			
Model	**Probability**	**Optimistic**	**Probable**	**Pessimistic**	
		30%	**40%**	**30%**	
Base	40%	223	41	-72	25
High	30%	246	61	-57	24
Low	30%	183	13	-94	10
				EMV	58.8

Source: Author, 2019

Table 6.3.4-3 NPVs and resulting EMVs for a Surfactant-Polymer flooding program.

		Surfactant-Polymer Flooding NPV (MMUSD)			
Model	**Probability**	**Optimistic**	**Probable**	**Pessimistic**	
		30%	**40%**	**30%**	
Base	40%	222	42	-84	23
High	30%	236	41	-79	19
Low	30%	178	5	-110	7
				EMV	49.2

Source: Author, 2019

Figure 6.3.4-1 Risk curve for all IOR methods based on the individual NPV for the Lula model.
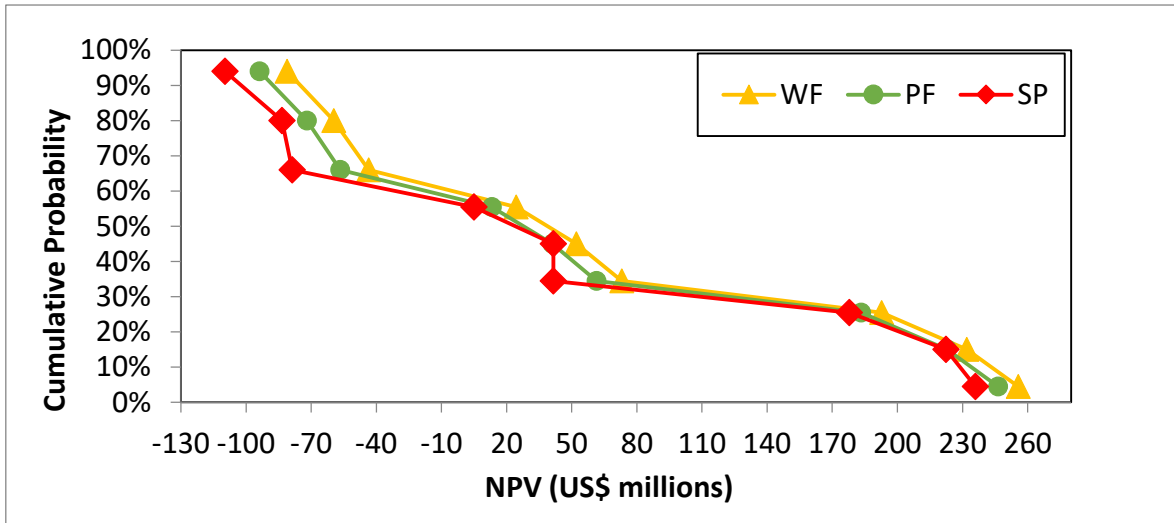
Source: Author, 2019

Evaluating the risk curve in **Figure 6.3.4-1**, there is a 45% chance of any of the projects being a failure under an economic evaluation. Moreover, the gap between technologies goes wider on negative NPVs which proves that at low oil prices the CEOR methods are not a possible selection even when higher oil RF are obtained, but they depressed even further the value of the project against WF.

6.4. CERENA I INVERTED FIVE SPOT MODEL SIMULATION RESULTS

The results for the IFS Cerena I model are detailed in the next sections.

6.4.1. Comparison between IOR methods - Economic Scenarios

In **Table 6.4.1-1** shows the results obtained for the optimization of the IOR projects. It can be noticed that both polymer flooding and surfactant-polymer floodings reduced the volume of water produced and gave an incremental on oil produced while maintaining an incremental of NPV in the project's life. The behavior of both chemical injections was similar, final water cut of the filed, oil recovery factor and total oil produced were not significantly different. Both programs, by slowing the

increment of the water phase (water cut) during the project's life, resulted in a reduction of the water treatment costs compensating the chemical investments. The similarity in their results pointed out that the surfactant was not playing a key role in the behavior of the SP flooding, despite it increased the oil recovery.

It can be observed a similar tendency as the one was presented in the previous discussion for the Lula project. Both chemical injections recovered more oil while reducing water treatment costs and injection costs, impacting therefore not only the technical performance of the field but also the economical. it was observed that in all economic scenarios both chemical methods brought higher profits than WF. Moreover, the chemical cost was compensated due to the reduction of water injection and production, both characteristics of a polymer injection. Another fact that must be pointed when comparing PF and SP it's that the individual polymer cost of the PF in 6 of 9 the cases is less than the surfactant plus polymer costs of the SP, but the NPV of the SP cases are higher, as the main factor improving it were the reduction of water injected and the water produced plus the additional recovery. Also, the consumption of polymer is less in 8 of 9 the cases for the SP than the PF, meaning that the synergy between both chemicals reduced the amount required of polymer in a Chemical EOR program. This phenomenon happened when the surfactant reduced the interfacial tension between the phases and improves the mobility of the fluid injected by altering the relative permeability curves.

Table 6.4.1-2 Results for Cerena IFS.

Model	Scenario	IOR	Oil Production (MMm^3)	Water production MMm^3	Water injection (MMm^3)	Period (Years)	Polymer Cost (MMUSD)	Surfactant Cost (MMUSD)	NPV (MMUSD)	RF (%)	Final WCut (%)
BASE	70	WF	166	113	106	30	-	-	10260	54%	74%
	70	PF	177	98.4	6	30	6.9	-	10558	58%	51%
	70	SP	180	94.7	1.54	30	2.5	2.2	10868	59%	52%
	50	WF	165	111	106	30	-	-	6226	54%	72%
	50	PF	177	98	2	30	4.2	-	6416	58%	50%
	50	SP	181	95	1.65	30	5.0	2.7	6614	59%	52%
	40	WF	151	100	115	27	-	-	3565	49%	65%
	40	PF	177	99	12	30	7.7	-	3860	58%	52%
	40	SP	180	94	0.9	30	3.0	1.1	4015	59%	51%

LOW	70	WF	167	106	76.1	30	-	-	10069	54%	60%
	70	PF	171	92.7	8.7	30	5.2	-	10258	56%	46%
	70	SP	174	88.4	0.55	30	1.7	3.9	10618	57%	48%
	50	WF	170	106	56.5	30	-	-	6175	55%	59%
	50	PF	171	93.3	2.38	30	3.6	-	6216	56%	47%
	50	SP	175	92.1	2.54	30	2.5	28.4	6458	57%	53%
	40	WF	170	106	56.5	30	-	-	3710	55%	59%
	40	PF	172	93.5	2	30	4.8	-	3723	55%	47%
	40	SP	174	88.4	0.58	30	1.9	0.7	3898	57%	48%
HIGH	70	WF	160	107	101	28.8	-	-	10239	52%	70%
	70	PF	179	99.5	2.98	30	9.35	-	10700	58%	53%
	70	SP	182	96.3	1.63	30	5.2	8.9	10954	59%	53%
	50	WF	162	112	109	29.5	-	-	6235	53%	74%
	50	PF	179	99.6	6.7	30	11.5	-	6494	58%	52%
	50	SP	182	96.3	1.87	30	5.6	8.9	6678	59%	53%
	40	WF	159	107	100	28.7	-	-	3744	52%	69%
	40	PF	179	99.5	3.2	30	8.2	-	3931	58%	53%
	40	SP	182	96.6	3.24	30	4.9	3.9	4055	59%	53%

Source: Author, 2019

Additionally, it must be noticed that for the low permeability model, the cumulative water injection tended in almost all cases and IOR projects to be reduced when compared with the other models, as the injection goes affected negatively by the polymer viscosity. Therefore, higher permeability rocks can be better objectives for a polymer-based program, either by itself or with other chemicals as a surfactant or an alkaline matching the same conclusion of the Lula model and what different authors in their screening criteria have mentioned (TABER; MARTIN; SERIGHT, 1997b; DICKSON; LEAHY-DIOS; WYLIE, 2010; AL ADASANI; BAI, 2011).

6.4.2. Comparison of IOR methods - geological models

Because low permeability zones often present smaller pore throats that may be plugged by the polymer molecules and injectivity problems due to the high viscosity of the fluid injected, reservoirs too tight are not common in the literature.

In **Figure *6.4.2-1*** are represented the water cut curves for all the three models and all three injections. As can be observed, the water cut behavior of the three models for the WF differed significantly from the chemical floodings, reaching higher points at similar production periods; moreover the rate at how the slope grew was higher for the water injection in all three models, a behavior expected when channeling and faster breakthrough happens. The breakthrough for all three models occurs between 2028 to 2032 in the WF, see **Figure 6.4.2-2**.

In **Figure 6.4.2-2** can be confirmed that low permeability models were not the preferred medium for a polymer-based injection program, as the oil production rates behaves in the same way as for the water injection, the water cut increased and the chemical addition did not generate any reduction. Also, in **Figure 6.4.2-2**, it can be observed that with higher values of permeability, even when it is not a norm, higher production rates, therefore, larger produced volumes.

Moreover, in the same **Figure 6.4.2-2**, can be observed a fall in the water rate for all the three models for the PF and SP, being more drastically in the low and base permeability models. This behavior is explained by the viscosifying action of the polymer which reduces the channeling of the water injected and reduced the water production of the more aqueous zones.

Figure 6.4.2-1 Water cut curves for all three heterogeneity models for both chemicals flooding at the probable economic scenario.

Source: Author, 2019

Figure 6.4.2-2 Oil and water rate areas per models and injection program.
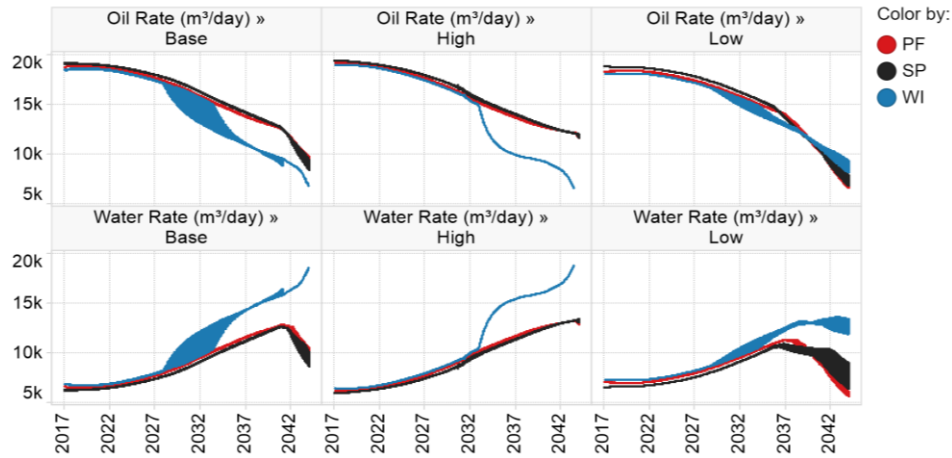
Source: Author, 2019

As shown on models **Table 6.4.2-1** and **Source:** *Author, 2019*, the pore volume injected is less than planned by the optimizer, as it will be mentioned in the 6.4.3 section. However, these volumes were still in the range of historical field test applications, based on Farouq and Thomas review (1992), which mentioned in their research a range of 0.025 to 0.4 PV. On the other hand, there was a tendency to require less chemical injected as the permeability model was smaller, the average polymer required per model was 1630<3330<5930 tons for the polymer flooding from low<base<high permeability models; the same behavior was encountered on the SP flooding. As it was reduced the chemical injected, therefore, the chemical cost followed the same behavior (**Table 6.4.2-1** and **Table 6.4.2-2**).

Table 6.4.2-1 Polymer consumption and associated cost for each heterogeneity model.

Model	Scenario	PV planned	PV Injected	Pol Conc (ppm)	Pol Cost (MMUSD)	Pol Qty (Kg*10^5)
BASE	50 USD	0.19	0.06	2023	4.2	2.8
	40 USD	0.33	0.07	612	7.72	4.3
	70 USD	0.25	0.07	1162	6.93	2.9
HIGH	50 USD	0.19	0.07	1711	11.46	5.1
	40 USD	0.39	0.06	2322	8.18	5.7
	70 USD	0.28	0.06	2994	9.35	7.0
LOW	50 USD	0.49	0.06	1524	3.62	1.4
	40 USD	0.50	0.06	2197	4.84	1.2
	70 USD	0.26	0.07	574	5.24	2.3

Source: Author, 2019

Table 6.4.2-2 Chemical consumption and associated cost for each heterogeneity model on SP flooding.

Model	Scenario	PV Planned	PV Injected	Pol (ppm)	Surf (%)	Pol Cost (MMUSD)	Surf Cost (MMUSD)	Pol Qty (Kg*10⁵)	Surf Qty (Kg*10⁴)
BASE	50 USD	0.24	0.06	3000	0.09	4.98	2.71	1.9	4.7
	40 USD	0.50	0.06	3000	0.05	2.97	1.08	0.31	3.1
	70 USD	0.21	0.06	1737	0.07	2.5	2.23	1.7	6.9
HIGH	50 USD	0.15	0.06	2993	0.35	5.63	8.9	3.8	28
	40 USD	0.26	0.06	1579	0.05	4.85	3.92	3.3	12
	70 USD	0.15	0.06	3000	0.38	5.17	8.89	3.9	31
LOW	50 USD	0.50	0.08	500	0.05	2.54	28.44	2.5	130
	40 USD	0.50	0.06	3000	0.05	1.93	0.7	0.99	0.17
	70 USD	0.15	0.06	2983	0.50	1.74	3.85	0.92	0.93

Source: Author, 2019

6.4.3. Parameters optimization

All the field development programs: water, polymer, and surfactant-polymer floodings were optimized for all economic and geological scenarios. This way a balanced comparison could be performed between the IOR methodologies. Next, it is discussed how the parameters behaved on the chemical injections.

For the Inverted five spot based on the Cerena I reservoir, the parameters in **Table *6.4.3-1*** won't be deeply analyzed on this research despite that at the beginning were selected, mainly because these parameters presented behaviors not expected and not conclusive, requiring therefore further studies.

Table 6.4.3-1 Inconclusive parameters optimized for the Cerena-IFS models and IOR methods.

IOR	Constraint	Initial	Max	Min
All	Min production Bottom hole pressure (kPa)	45400	50000	20000
All	Max Fluid production rate (m³/day)	4769.62	6359.5	1589.87
SP	Polymer Concentration **on chase slug** (ppm)	1000	3000	500
SP	Salt concentration **chase slug** (ppm)	50000	100000	20000

PF, SP	Pore Volumes injected: chemical batch	0.5	0.5	0.15

Source: Author, 2019

The first two variables on **Table *6.4.3-1***, minimum BHP and max fluid rate for each producer well, followed the same tendencies for all economic scenarios and reservoir models: maximizing the fluid rate an minimizing the bottom hole pressure. Both parameters are interdepended and were evaluated simultaneously as having the same issues. First, as the production platform cost on this economic evaluation was fixed and it did not vary depending on the fluid production of the wells, the optimizer maximizes the fluid rate without having an economic parameter that controlled its performance directly. Second, the model did not contemplate the existence of flow efficiency phenomena that affect the wells such as skin or formation damage, therefore the well followed a simplified "Productivity Index" behavior, defined as "the volume delivered per psi of drawdown at the sand face (BPD/psi)" (SCHLUMBERGER LIMITED, 2018) meaning that theoretically the maximum oil production was achieved at the largest drawdown or 0 psi of flowing pressure. For this research, the parameters always tended to the minimum bottom hole pressure of 20000 kPa and the maximum production rate of 6359.5 m^3/day.

Both tendencies can be found in **Figure 6.4.3-1** and **Figure 6.4.3-2** whereas mentioned the fluid rate tends to maximize and the bottom hole pressure to minimize following an ideal behavior.

Figure 6.4.3-1 Maximum fluid rate tendency for the Cerena-I IFS.
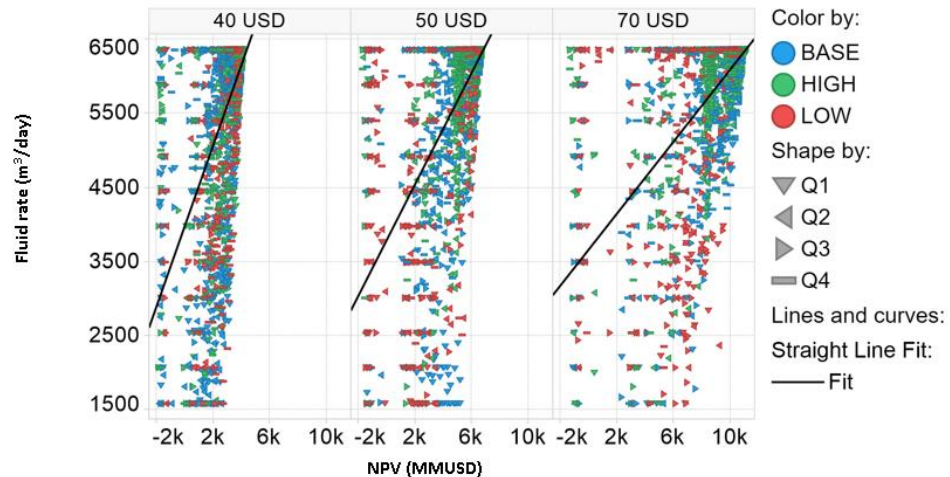
Source: Author, 2019

Figure 6.4.3-2 Minimum bottom hole pressure tendency for the Cerena-I IFS.
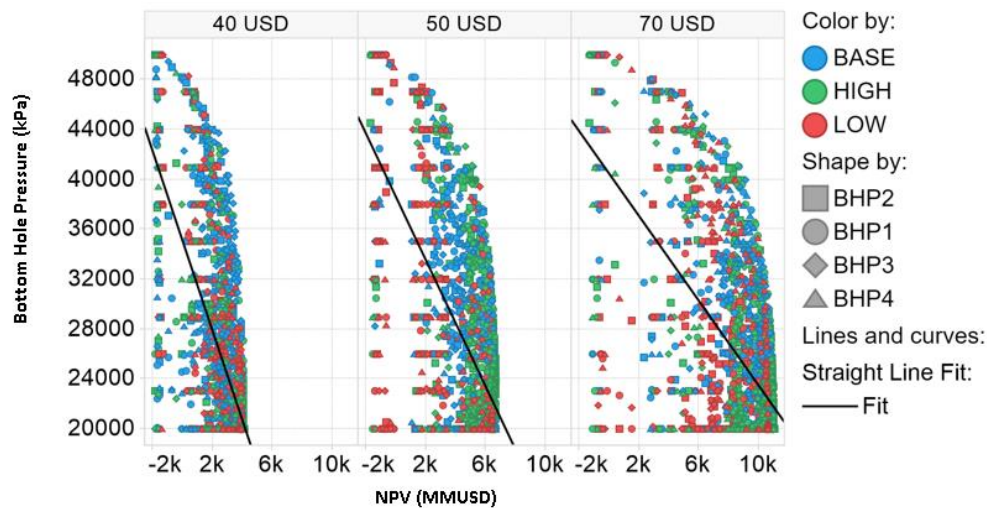
Source: Author, 2019

Regarding the other three parameters: polymer/salt concentration in the chase slug and pore volume injected, the displacing slug was not injected in any of the Cerena models, because the pore volume injected of the main slug never achieved the minimum value to start the second one. All the injections ended in less than 0.1 PV after reaching the simulation limit of 30 years.

For the PF and SP the injection rates were lower than the expected, less than ten time the water, due to the low injectivity of the formation, low permeability layers below 100 mD, and high viscosity of the fluid injected, both can be observed in

Figure 6.4.3-4 and **Figure 6.4.3-5**. The injection rate was low for the SP despite the pressure at the bottom of the hole is at its maximum, the same set as for the WF, see **Figure *6.4.3-3***.

Moreover in **Figure 6.4.3-4**, it can be noticed that the solution viscosity is higher around the injector at the end of the simulation reaching values up to 70 cp (the polymer starts to disperse and it losses the viscosity after this front) and in part "B" of the same figure, it can be noticed that the interfacial tension was reduced and it affected a large area of the sector. However, it is requiring longer PVs injected as to observe a bigger effect on the incremental oil recovery than the one presented in all the models.

Figure 6.4.3-3 Pressure and injection rate for the Base model, the probable scenario of WF and SP flooding.
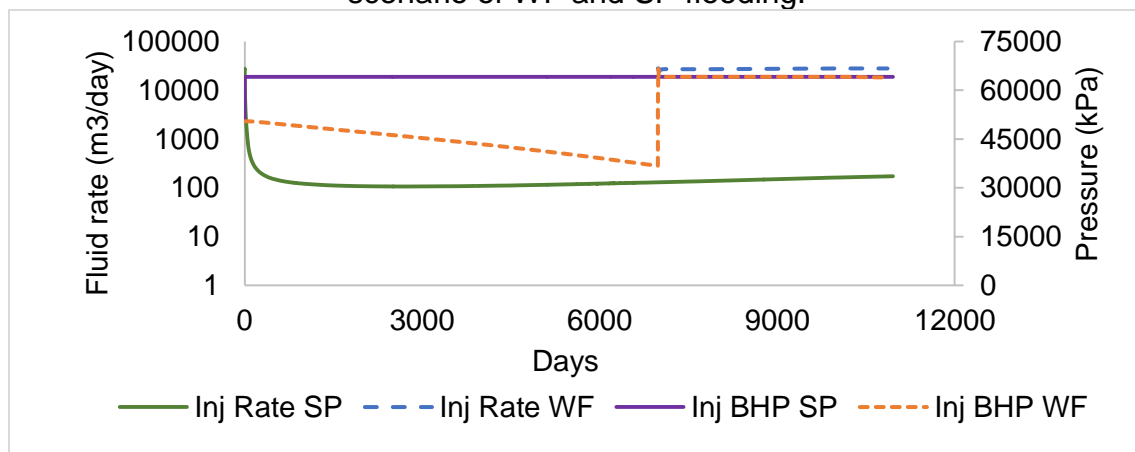
Source: Author, 2019

Figure 6.4.3-4 Properties in the High model probable scenario, end of simulation A) solution viscosity; B) Aerial view of interfacial tension layer 121.
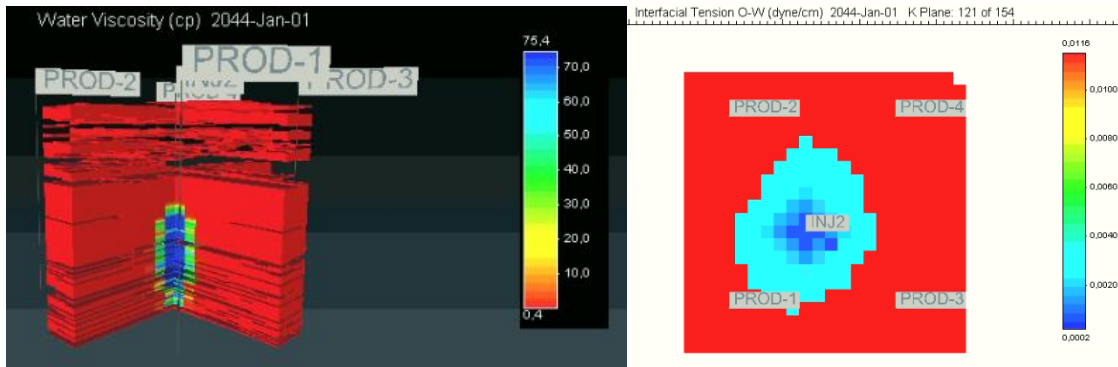
Source: Author, 2019

Figure 6.4.3-5 Permeability I md, in base model A) layer I:10 plane cut JK; B) J:10 plane cut IK
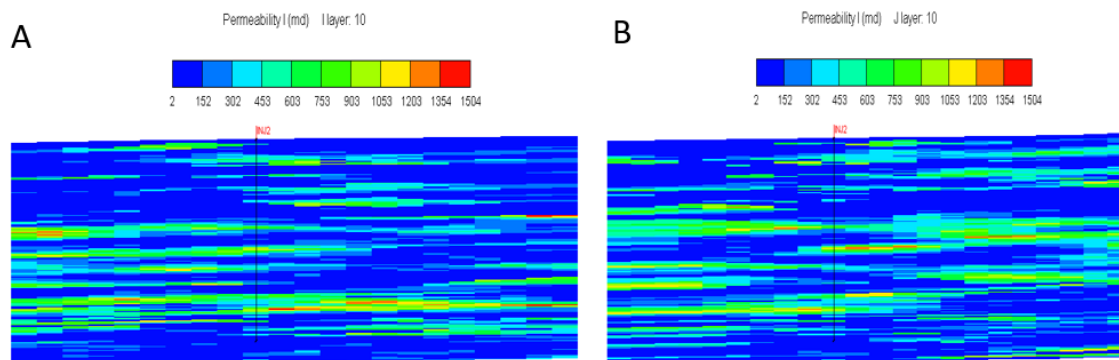
Source: Author, 2019

Also, the profile of injection despite not moving in a large area, observed an uniform vertical displacement, which has been reported in the literature for polymer injection (SHENG, 2011; SHENG; LEONHARDT; AZRI, 2015).

6.4.3.1. Polymer flooding parameters

In **Table 6.4.3-1**, it can be found the optimized parameters for all geological models and three economic scenarios. Regarding the polymer concentration, the optimal values were in the middle region of the range given to the optimizer. What matches with the section 6.4.3 analysis of the low injection rate, in this case the polymer concentration went up as to reduce the volume injected while still displacing

the oil. There was no tendency as to have lower or larger concentrations depending on the model, however, on **Figure 6.4.3.1-1** can be noticed that for all three models the range went between 1000 to 2000 ppm, where the optimal values fell. The chemical cost was paid by the incremental oil of the PF strategy, different from the observed in the Lula's model were all the values went to the low range close to 500 ppm.

Table 6.4.3.1-1 Optimized parameters for polymer flooding per model and economic scenario.

Scenario	50	40	70	50	40	70	50	40	70
Parameter	BASE	BASE	BASE	HIGH	HIGH	HIGH	LOW	LOW	LOW
WCUT1	77.3%	93.2%	84.1%	89.4%	74.1%	70.0%	94.1%	99.0%	78.1%
WCUT2	90.7%	83.3%	70.0%	82.5%	99.0%	88.0%	77.4%	77.3%	82.5%
WCUT3	87.3%	71.2%	99.0%	74.6%	70.0%	84.5%	83.1%	91.8%	74.4%
WCUT4	70.0%	91.8%	73.5%	99.0%	79.0%	70.0%	70.0%	70.0%	97.8%
Injection Trigger (psi)	40000	43350	46700	47100	40000	40000	45600	50000	46350
PV Injected	0.06	0.07	0.07	0.07	0.06	0.06	0.06	0.06	0.07
ppm Pol	2023	612	1162	1711	2322	2994	1524	2197	574
NPV (MMUSD)	6416	3860	10558	6494	3931	10700	6216	3723	10258
% Delta NPV	3.1%	8.3%	2.9%	4.1%	5.0%	4.5%	0.7%	0.3%	1.9%
Oil RF	57.6%	57.6%	57.6%	58.1%	58.2%	58.2%	55.6%	55.4%	55.7%
Incremental FR	3.9%	8.5%	3.7%	5.6%	6.4%	6.3%	0.3%	0.1%	1.4%

Source: Author, 2019

Based on **Table 6.4.3-1**, it can be noticed that with higher average permeability, the higher its NPV and RF, explained by Darcy's equation, where a larger permeability means higher fluid rates that resulted in the NPV and incremental RF observed. Also, the water cut to shut the wells varies between the models, having higher final water cuts for the High model: if a final water cut is selected for all wells, in average it would be 81.15%<81.33%<86.38% for the low, base, and high models respectively.

Figure 6.4.3.1-1 NPV versus polymer concentration injected on the polymer flooding for all three geological and a probable economic scenario.
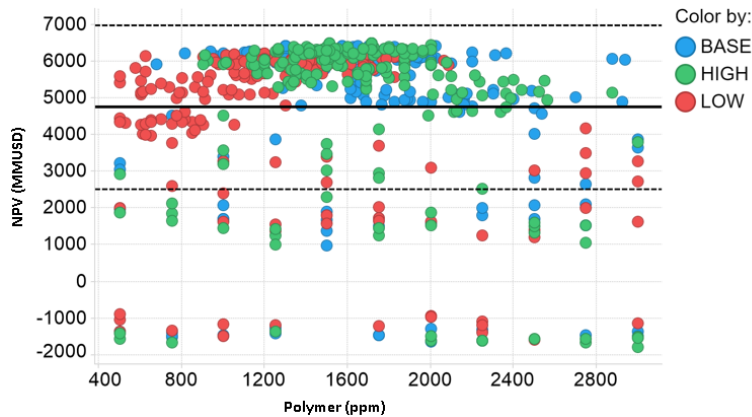
Source: Author, 2019

About the minimum average pressure on the reservoir at which the injection well should be opened has three ranges, one for each reservoir model, resulting in a range of 40000 to 50000 kPa, therefore it is a variable that must be evaluated for each case as it depends on every set of variables per model (**Figure 6.4.3.1-2**).

Figure 6.4.3.1-2 Effects of the Minimum average reservoir pressure to start injection on the NPV for each geological model in the probable economic scenario.
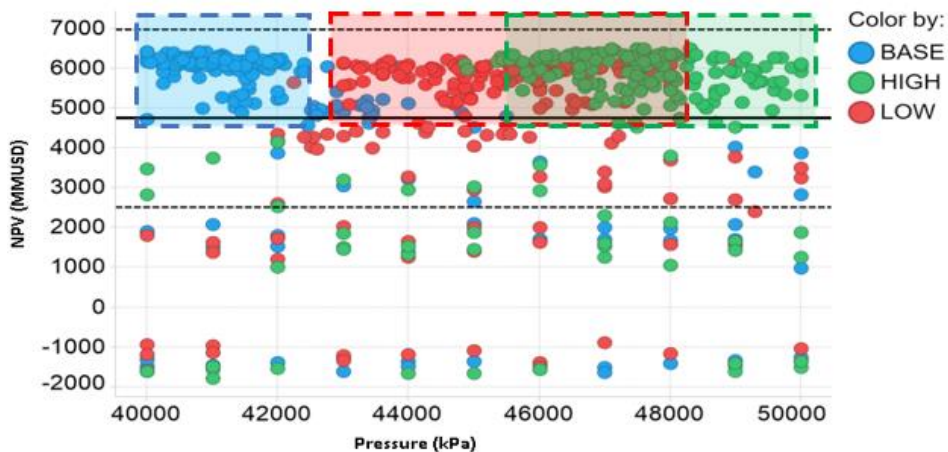
Source: Author, 2019

if needed operatively, the water cut to shut in the wells could be selected close to 83% - 84%, *Figure 6.4.3.1-3* and **Figure 6.4.3.1-4**, meaning that for any economic scenario and model this parameter could be fixed for all the well group in this range. However, as recommended for Lula's model, it is a parameter that should be

evaluated per well and operational conditions as it presented dispersion of the data from 93% to 76%.

Regarding the reservoir pressure to start the injection, all three models differ individually between economic scenarios, shown in **Figure 6.4.3.1-2**, **Figure 6.4.3.1-7** and **Figure 6.4.3.1-8**. The base model, probable and pessimistic tend to have a pressure lower than 45000 kPa; for the high model optimistic and probable tend to 40000 kPa, and the low model it's the one that has a tendency in all three economic scenarios to start the injection as earlier as possible over 45000 kPa. The last behavior can be explained, when evaluating that this model it's the one with larger problems of injectivity due to its overall lower permeability, therefore it requires to start earlier the injection as to compensate during the 30 years program the chemical investment.

The tendencies of the probable and pessimistic scenarios were similar and differ from the optimistic. Which lead to the idea that with better economic scenarios (higher oil prices) could be best to let the reservoir deplete by their own energy longer, therefore less investment, and later incorporate more reserves with IOR programs.

Figure 6.4.3.1-3 Water cut optimization at an optimistic economic scenario for all producers for polymer flooding.
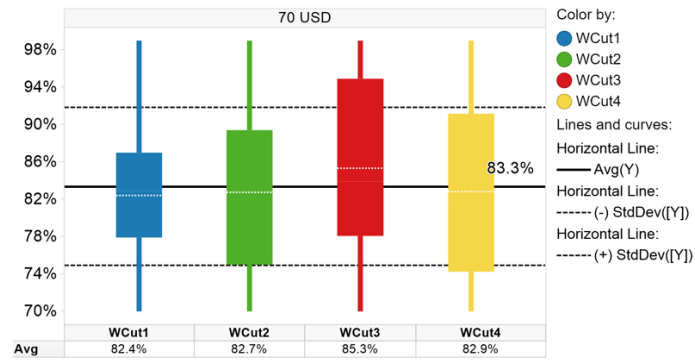
Source: Author, 2019

Figure 6.4.3.1-4 Water cut optimization at a pessimistic economic scenario on all four producers for polymer flooding.
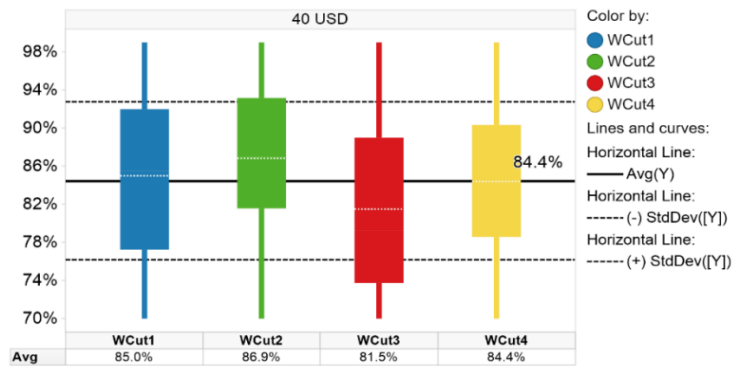
Source: Author, 2019

Figure 6.4.3.1-5 NPV versus polymer concentration injected on the polymer flooding for all three geological and the optimistic economic scenario.
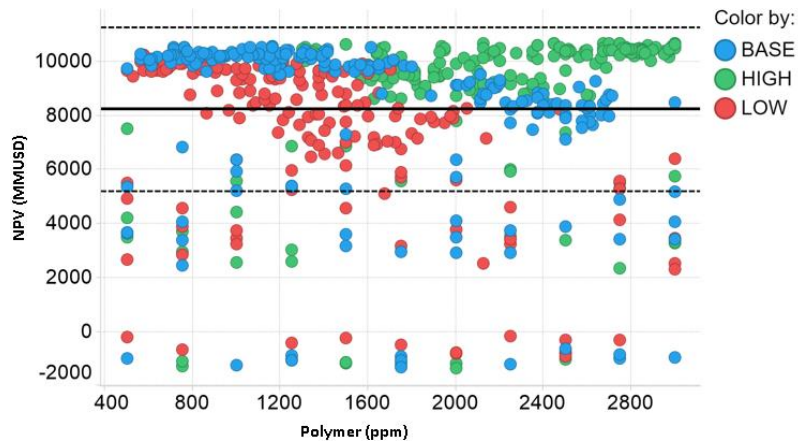
Source: Author, 2019

Figure 6.4.3.1-6 NPV versus polymer concentration injected on the polymer flooding for all three geological and the pessimistic economic scenario.
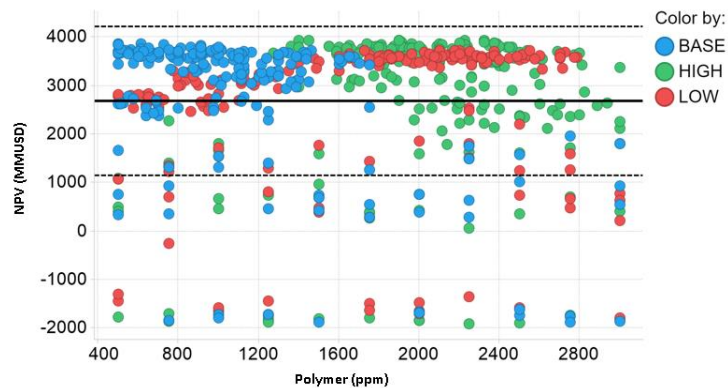
Source: Author, 2019

Figure 6.4.3.1-7 NPV versus Minimum average reservoir pressure to start injection for each geological model in the pessimistic economic scenario.
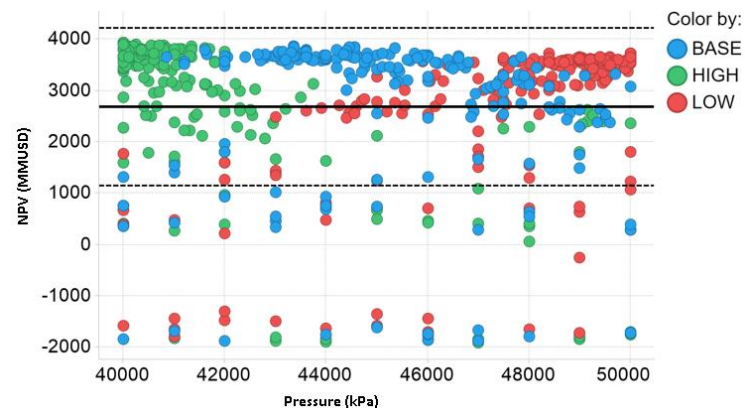
Source: Author, 2019

Figure 6.4.3.1-8 Effects of the Minimum average reservoir pressure to start injection on the NPV for each geological model in the optimistic economic scenario.
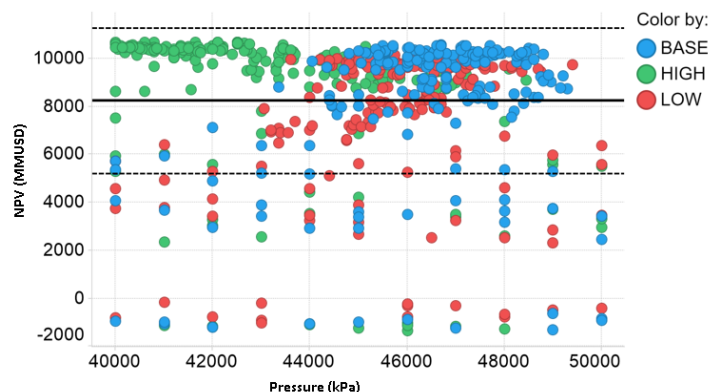
Source: Author, 2019

6.4.3.2. Surfactant-Polymer flooding parameters

In **Table *6.4.3.2-1***, it can be found the optimized parameters for all geological models for the probable economic scenario of the Surfactant-Polymer flooding. It can be observed oil RF, and the NPV increased as the permeability of the model did, while at the same time the incremental recovery when compared against the WF.

Table 6.4.3.2-1 Optimized parameters for Surfactant-Polymer flooding per model and economic scenario.

Scenario	50	40	70	50	40	70	50	40	70
Parameter	BASE	BASE	BASE	HIGH	HIGH	HIGH	LOW	LOW	LOW
WCUT1	99.0%	99.0%	99.0%	99.0%	99.0%	99.0%	70.0%	70.0%	76.1%
WCUT2	96.1%	93.8%	87.0%	73.7%	70.0%	70.0%	70.0%	71.1%	98.0%
WCUT3	96.7%	70.0%	84.9%	75.6%	98.8%	70.0%	70.0%	99.0%	70.0%
WCUT4	70.9%	84.7%	98.9%	70.0%	99.0%	70.0%	70.0%	70.0%	90.6%
Injection trigger	50000	40000	40000	41539	40788	40000	40000	40000	40000
PV Injected	0.06	0.06	0.06	0.06	0.06	0.06	0.08	0.06	0.06
Pol (ppm)	3000	3000	1737	2993	1579	3000	500	3000	2983
Salt in chemical batch (ppm)	66176	100000	20000	46611	100000	55653	20000	64778	100000
Surfactant (%)	0.09	0.05	0.07	0.35	0.05	0.38	0.05	0.05	0.5
NPV (MMUSD)	6614	4015	10868	6678	4055	10954	6458	3898	10618
% Delta NPV	6.2%	12.6%	5.9%	7.1%	8.3%	7.0%	4.6%	5.1%	5.4%
Oil RF	58.8%	58.6%	58.8%	59.2%	59.1%	59.2%	57.0%	56.6%	56.6%
Incremental FR	5.0%	9.5%	4.8%	6.8%	7.4%	7.4%	1.7%	1.3%	1.3%

Source: Author, 2019

Based on **Table** *6.4.3.2-1*, it was noticed that the polymer concentration presented one tendency to go on to the higher concentrations range from 1500ppm to 3000ppm, as happened with the PF. Explained the same way as for the PF, increasing the injected fluid viscosity reduced the fluid volume in the higher permeability layers which lower the injected fluid cost and treatment as it worked as a conformance corrector.

While the surfactant concentration was affected for the economic scenario, the lower price presented lower quantities, and the optimistic economic scenario allowed the upper concentrations. Similar to the observed in the Lula's simulations, the oil price affects the economy of the CEOR projects, but in this case as the Cerena models were able to compensate the cost, higher quantities were injected. However the tendency was not clear between models as observed in **Figure 6.4.3.2-3**, the base model tend to be on the lower range between 0.2 to 0.05 %, the high model tends to be on the upper side between 0.35 and 0.5%, while the low model does not have a range as its concentration moves between all the range defined for the optimization, 0.05% to 0.5%.

The salt concentration based one more time in **Figure 6.4.3.2-3**, had a tendency to be injected in lower concentrations (under 60000 ppm) for the low and high model, while the base goes in all the range optimized. Leading to the idea that the salt it's a parameter with interaction effects as its tendency was not marked between models. Moreover, the low model tended to have local extrema issues on this variable as in this graph the points stay in a straight line the same in all the range; therefore it was not conclusive and led to question the result for the surfactant concentration as it depended significantly on the salt content.

Focusing on the average reservoir pressure to start the injection, almost in all the scenarios the optimal value was the lowest reservoir pressure constraint, 4000 psi. This strategy reduces the quantity of chemical injected and then reduces the costs in the long run of the project, **Figure** *6.4.3.2-4*.

Regarding the water cut to shut in the wells, when observing the optimized parameters in **Table *6.4.3.2-1***, the idea of early closing the wells was supported as 8 of the 12 water cuts is lower than 75%. However, in **Figure *6.4.3.2-5*** the tendencies can be divided, the wells 3 and 4 benefited of earlier closures while the producers 1 and 2 tended to be on a larger range; therefore, they must be evaluated individually and their interactions with polymer and surfactant concentration.

Figure 6.4.3.2-1 Effects of the Minimum average reservoir pressure to start injection on the NPV for each geological model in the pessimistic scenario.
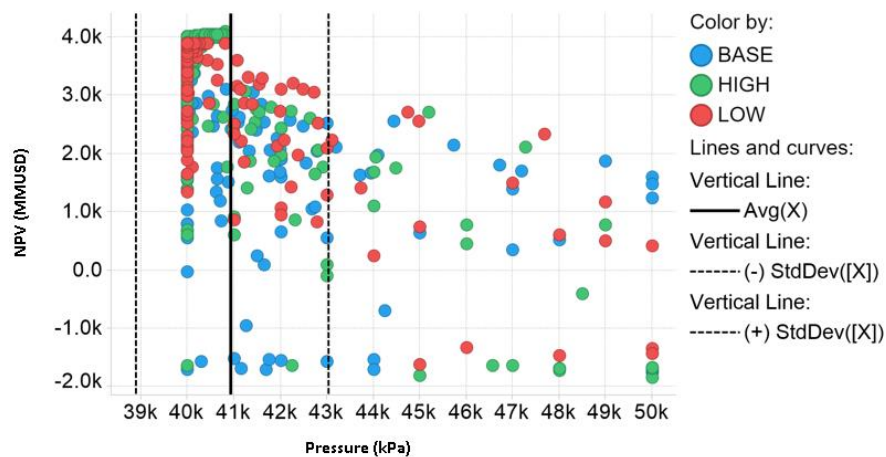
Source: Author, 2019

Figure 6.4.3.2-2 Effects of the Minimum average reservoir pressure to start injection on the NPV for each geological model in the optimistic economic scenario.
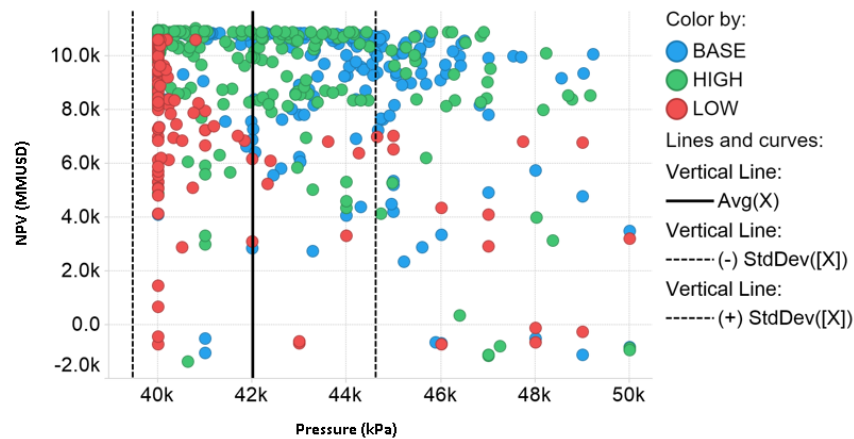
Source: Author, 2019

Figure 6.4.3.2-3 Surfactant concentration versus salt concentration injected on the SP flooding for each geological model in the probable economic scenario.
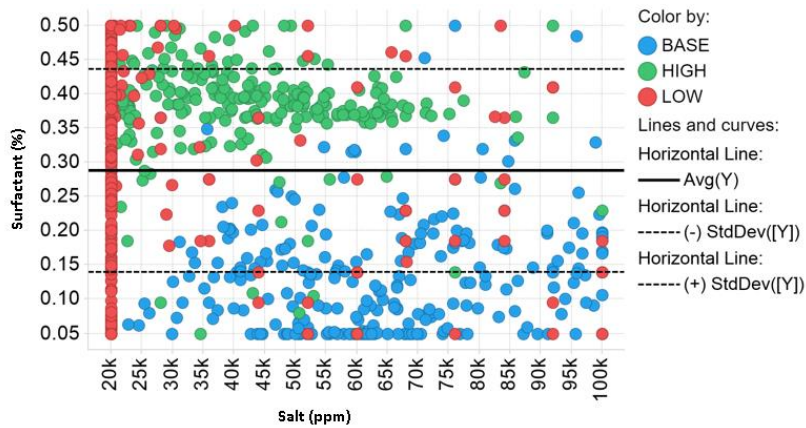
Source: Author, 2019

Figure 6.4.3.2-4 Effects of the Minimum average reservoir pressure to start injection on the NPV for each geological model in the probable economic scenario.
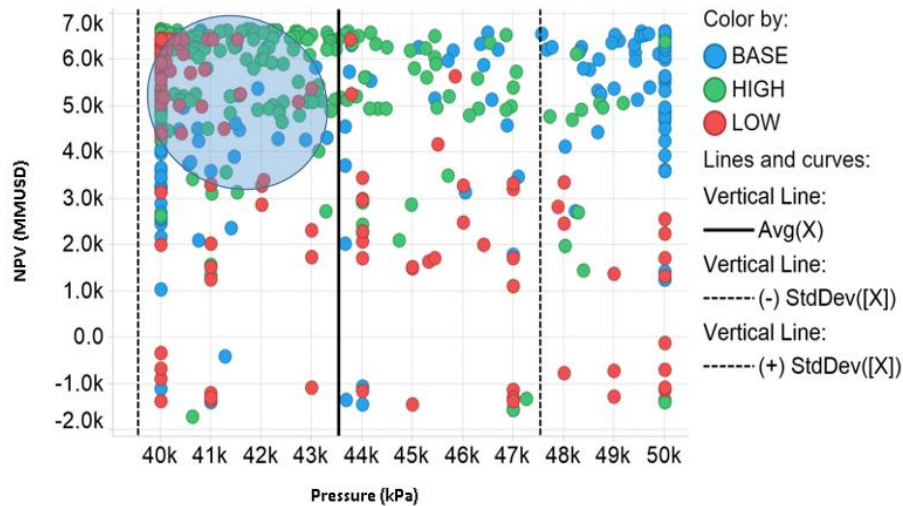
Source: Author, 2019

Figure 6.4.3.2-5 Water cut optimization at a probable economic scenario for all producers in the SP flooding.
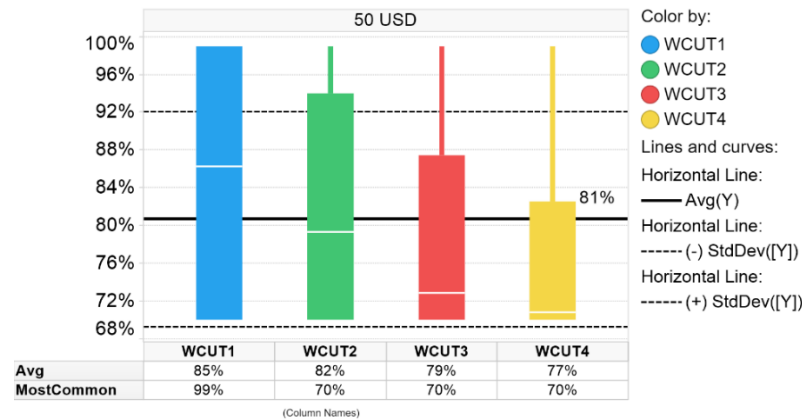
Source: Author, 2019

The surfactant and salt concentrations were clearer on the optimistic and pessimistic scenarios than for the probable. In **Figure 6.4.3.2-6** and **Figure 6.4.3.2-7**, it can be observed that higher surfactant concentrations were injected with brines with lower salt content, and the opposite applies. As mentioned in the Lula case, the preferable injection of salt according to the literature is a gradient injection which makes a contrast with the high salinity encountered in the reservoir. In **Figure 6.4.3.2-7** the high salinity brine with low surfactant concentration indicated that on the pessimist scenario the surfactant was not the main chemical agent, but the polymer was, as with higher salt concentrations the reduction of interfacial was not optimal (close to 60000 ppm). A reduction of surfactant cost was encountered, therefore on the pessimistic scenario.

Salt concentration per model can also be observed in **Figure *6.4.3.2-8***, where the average was found disregarding the economic scenario. Being on this graph where the tendency was clearer, the salt concentration was close to the optimal value mentioned on the input section and lab results of 60000 ppm NaCl (HIRASAKI; MILLER; PUERTO, 2011), where the IFT was minimal for all surfactant concentrations.

Figure 6.4.3.2-6 Surfactant concentration versus salt concentration injected on the Surfactant-polymer flooding for each geological model in the optimistic scenario.
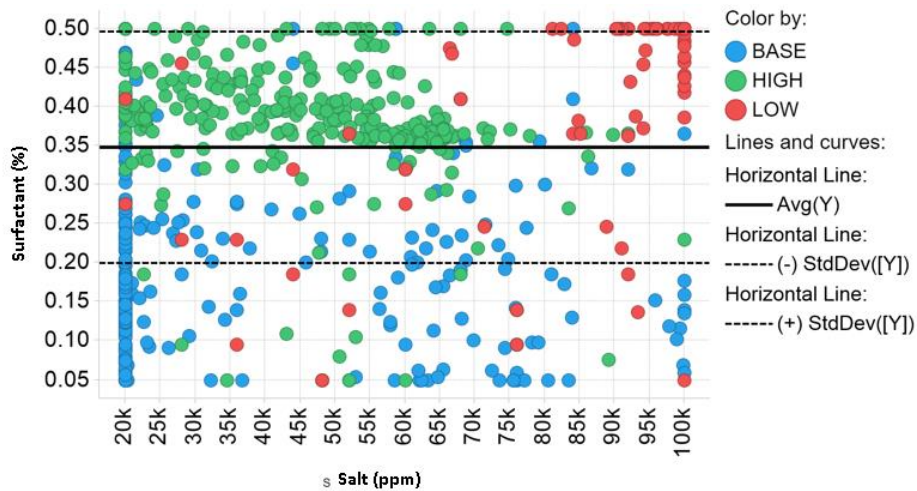
Source: Author, 2019

Figure 6.4.3.2-7 Surfactant concentration versus salt concentration injected on the Surfactant-polymer flooding for each geological model in the pessimistic scenario.
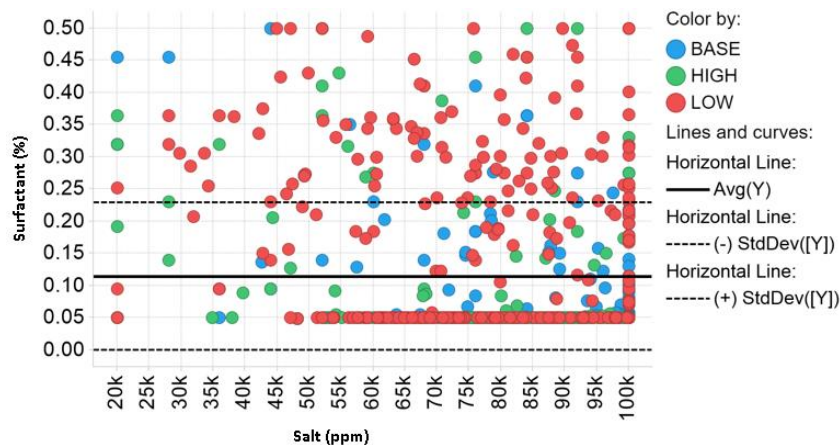
Source: Author, 2019

The surfactant concentration behavior also can be found in **Figure *6.4.3.2-9***, this time as a function of the economic scenario. The surfactant concentration depends on the economics of the project, and the higher concentrations were encountered in the optimistic scenario and the minimum percentages on the contrary, in the more pessimistic scenario. This can be confirmed as the average of the optimal surfactant concentration for the pessimistic scenario is 0.05%, for the probable scenario 0.16% and for the optimistic 0.32%. As mentioned before, at

higher oil prices, the economy of CEOR projects can compensate their costs and therefore higher concentrations on the brine injected.

Figure 6.4.3.2-8 Salt content tendency per model on the SP flooding.
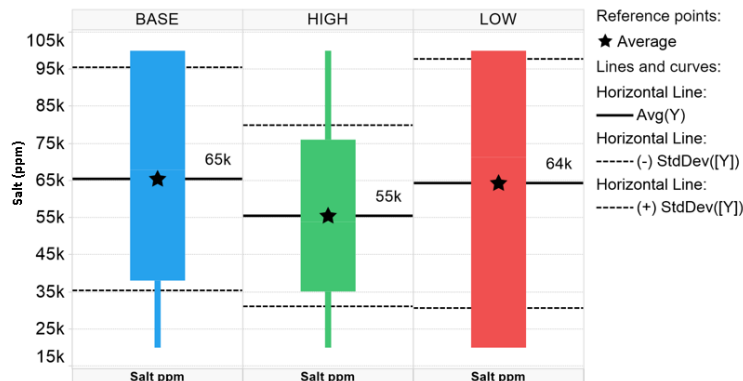
Source: Author, 2019

Figure 6.4.3.2-9 Surfactant concentration per economic scenario on the SP flooding.
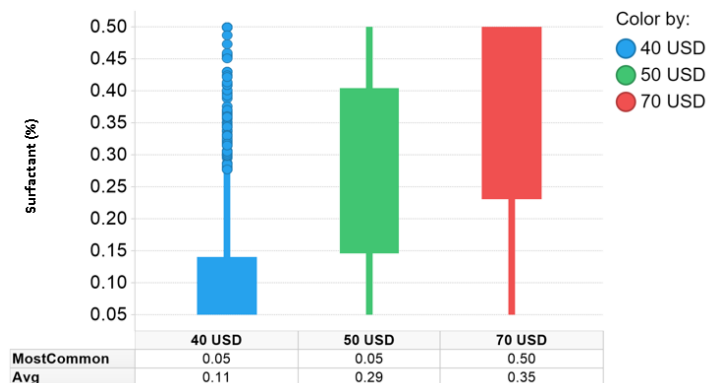
Source: Author, 2019

Finally, it must be noticed that despite the low injectivity of this chemical solution, there was sweep and effect of the surfactant addition in the models. In **Figure *6.4.3.2-10***, the (a) section cut shows the fraction of the surfactant that had been adsorbed in the layer observed for the low model, which was in average 1% while the (b) section cut shows the same layer for the high model, with an average of adsorption of 10%. First, it should be pointed out that higher permeability reservoirs do increase the oil recoveries and bring higher fluid rates, they require larger volumes of chemical injected to compensate the adsorption. With this results,

it can be discarded losses of surfactant as an issue on the performance of the technique inside of the reservoir, additionally, the area that covered went from the center to the producers indicating a good movement of the surfactant through the reservoir especially in the direction of producers 1 and 2. This movement indicated that in this wells, if a surface facility was built, they will be the first requiring microemulsion treatments because of the arrival of the emulsion front (LEVITT et al., 2013). Moreover, the incremental oil volumes given by the SP when compared to the PF were related to this IFT reduction.

Figure 6.4.3.2-10 Adsorption as a fraction of surfactant injected, for the SP flooding (a) optimistic scenario low permeability model, (b) probable scenario high permeability model.
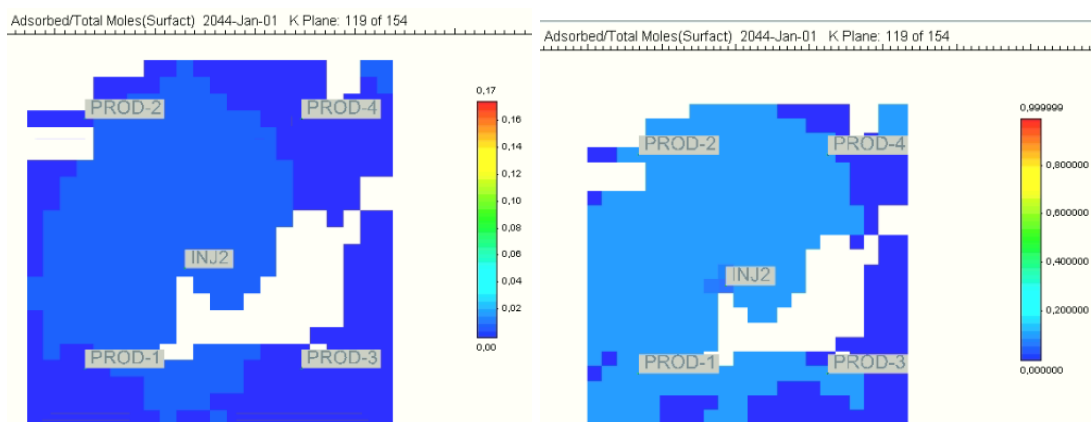
Source: Author, 2019

6.4.4. Expected Monetary Value (EMV) Cerena I

In **Table 6.4.4-1**, **Table 6.4.4-2** and **Table 6.4.4-3** have the EVM for each injection program according to the probability assigned for each case. As can be observed, the EMV for SP flooding was the higher of all three, followed by the PF.

In **Figure 6.4.4-1**, the optimized results for both chemical injections are shown, relating: cumulative oil production, final water cut, recovery factor, economic

model and NPV. It can be observed that the best economic results are obtained on the models where the final water cut after the 30 years of all the field production are between 50% and 65%, showing that optimizing the wells shut-in by its water cut can benefit the cash flow of a chemical recovery project. Moreover, the PF and the SP can increase the cumulative oil production overall models and scenarios, especially on a low barrel price scenario, when comparing against the WF. It can be noted that the NPV difference between methods gets higher on optimistic scenarios, meaning that higher oil prices benefit the implementation of chemical EOR programs such as PF and SP.

Figure 6.4.4-1 Results of optimal cases.
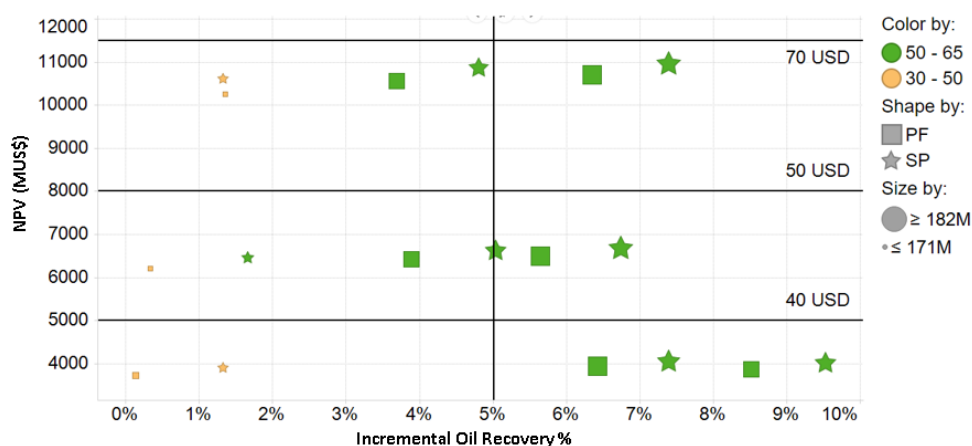
Source: Author, 2019

Table 6.4.4-1 NPVs and resulting EMVs for a water flooding program.

		Water flooding NPV (MMUSD)			
Model	Probability	Optimistic 30%	Probable 40%	Pessimistic 30%	
Base	40%	10,260	6,226	3,565	2,655
High	30%	10,239	6,235	3,744	2,007
Low	30%	10,069	6,175	3,710	1,981
				EMV (MMUSD)	6,643

Source: Author, 2019

Table 6.4.4-2 NPVs and resulting EMVs for a polymer flooding program.

Model	Probability	Optimistic 30%	Probable 40%	Pessimistic 30%	
Base	40%	10,558	6,416	3,860	2,757
High	30%	10,700	6,494	3,931	2,096
Low	30%	10,258	6,216	3,723	2,004
				EMV (MMUSD)	6,857

Source: Author, 2019

Table 6.4.4-3 NPVs and resulting EMVs for a Surfactant-Polymer flooding program.

Model	Probability	Optimistic 30%	Probable 40%	Pessimistic 30%	
Base	40%	10,868	6,614	4,015	2,844
High	30%	10,954	6,678	4,055	2,152
Low	30%	10,618	6,458	3,898	2,081
				EMV (MMUSD)	7,078

Source: Author, 2019

6.5. MODEL RESULTS VERSUS CARBONATE FIELD APPLICATION REPORTS

The results of this research for the Cerena-I model can be compared to findings of real field applications (the Lula model had an EMV lower for SP and PF than WF, therefore, is not compared). The most recent report of SP injection was the Single Well Tracer Test of an offshore carbonate reservoir in Abu Dhabi (AL-AMRIE et al., 2015). Both, their research and the present agreed on: salinity brine for the chemical injection lower than the one encountered at reservoir conditions it is preferential. Six of nine of the optimal scenarios on this research showed a salinity concentration under 70000 ppm (**Table 6.5-1)**, less than formation water, 104361 ppm (HIRASAKI; MILLER; PUERTO, 2011). Additionally, the objective reservoir

layers despite having a positive response on incremental recovery, the polymer solution presented injectivity problems reducing the injection rate to less than10% of its initial conditions with water. This flow resistance behavior has been observed in the Shengli pilot (ZHENQUAN et al., 2013) and other simulation reports (DANG et al., 2015).

However, the incremental oil recovery factor of the SP flooding despite being positive when compared to a conventional water injection, from 0.1 to 9.5%, the field results of some pilots are even higher, as an example the pilot performed on the Shengli field gave an incremental of 16.7% (ZHENQUAN et al., 2013) and the pilot on the Minas field (BOU-MIKAEL et al., 2000), an incremental of 20% — proving that field results can differ on from simulation results.

Table 6.5-1 Optimal salinity concentrations for SP flooding.

Model	Scenario	NaCl Content (ppm)
Base	Probable	66176
	Pessimistic	100000
	Optimistic	20000
High	Probable	45640
	Pessimistic	100000
	Optimistic	55653
Low	Probable	20000
	Pessimistic	64778
	Optimistic	100000

Source: Author, 2019

Regarding the performance of the PF, if compared against some field cases, it can be seen in **Figure 6.5-1** that this research result falls in a range of medium performance, having a low quantity of polymer injected and low and medium incremental recoveries compared with real field data (SHENG; LEONHARDT; AZRI, 2015). Better performance than the ones obtained for the Lula model explained as the oil encountered on it has higher API gravity resulting in less dense fluid with lower viscosities, a condition not favorable for the polymer flooding (NEEDHAM; DOE, 1987).

Figure 6.5-1 Polymer flooding performance of Cerena I against real field data.
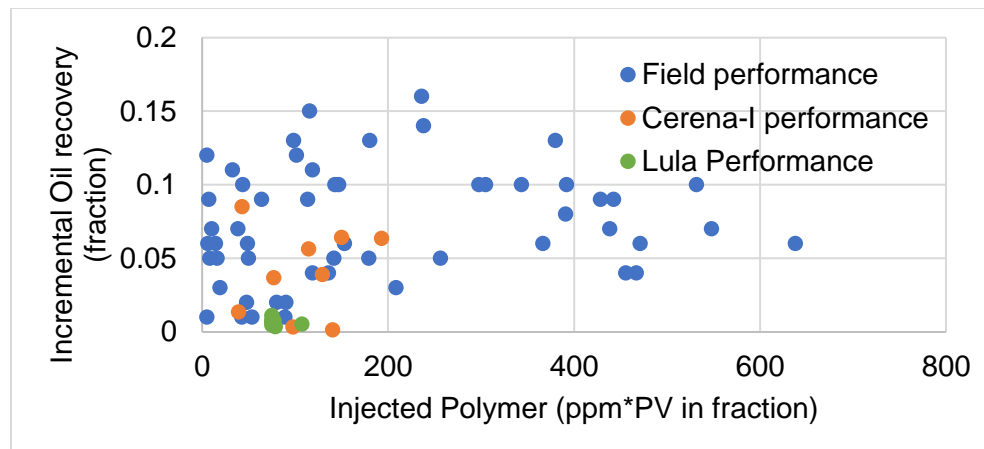
Source: Author, 2019; SHENG; LEONHARDT; AZRI, 2015

Regarding the performance of the SP, as was mentioned previously the PV injected was less than expected due to the low injectivity of the well. Additionally, it was desired to compare how the CEOR methodology performed against other projects. In **Figure 6.5-2**, it can be observed that the performance of the SP is far from being what would be expected as the incremental recoveries are not that high and the Surfactant quantity is less than some results of field applications. However, the results tend to increase rapidly with low quantities of surfactant, having a similarity to the laboratory results. This tendency indicates that by solving the injectivity issues and larger volumes of surfactant injected, a significant incremental oil could be recovered (DEBONS; BRAUN; LEDOUX, 2004).

Moreover, when comparing the results with the one obtained of Lula it can be mentioned that despite higher PV injected the incremental recovery is more or less the same, indicating that the Cerena cases may increase even higher the oil recovered and therefore the NPV if a solution for the low injectivity is defined.

Figure 6.5-2 Surfactant-Polymer flooding performance of Cerena-I against real data.
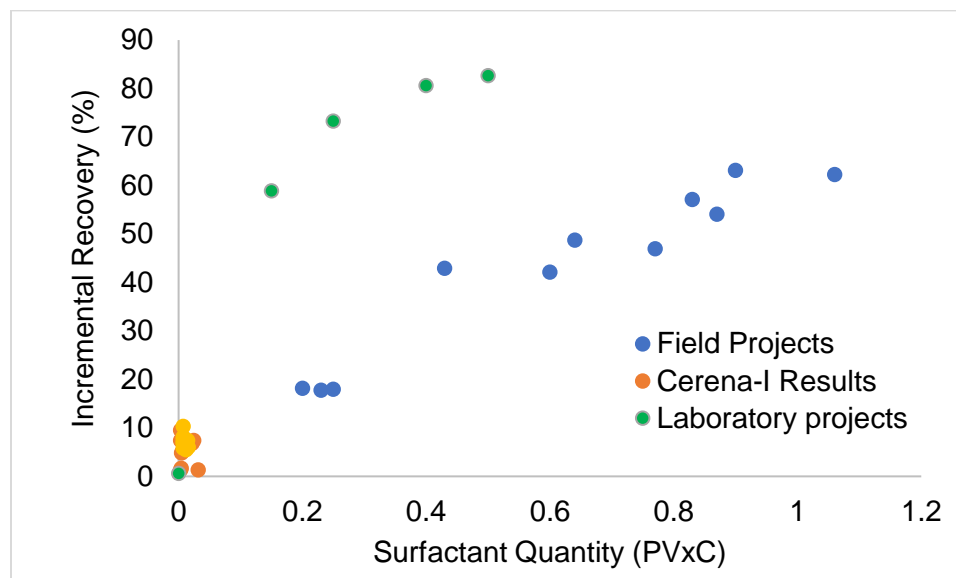
Source: Author, 2019; DEBONS; BRAUN; LEDOUX, 2004

CONCLUSIONS

Regarding the laboratory evaluation:

- Surfactants with low CMC, IFT, and adsorption are required for carbonate rocks, the type of surfactant; therefore, it is different than the anionic surfactants employed in sandstones. Non-ionic, cationic, or zwitterionic surfactants can be an answer to this requirement.
- The Xanthan gum behaves as expected on high salinity brines, generating a broad range of viscosities depending on its concentration.

Regarding the simulation evaluation of both models, Lula and Cerena-I:

- The economic cost of the chemical injection reduced the NPV of all scenarios in the Lula IFS, despite increasing the oil recovery factor. Therefore, the associated costs of CEOR program play a fundamental role in its applicability, a behavior observed previously by Bahrami et al. (2016) and Kamari et al. (2016) researches.

- Surfactant-Polymer flooding is the oil recovery mechanism which provided the in all the cases the largest incremental recovery for both models.

- When to close a producer well for a Chemical EOR program varies between economic scenario and models; however there is a tendency: the higher the oil price is, the higher the water cut shut-in can be as higher oil prices allow larger times producing per well.

- When to start a CEOR injection must be evaluated for each case. However, the Lula Model presents a tendency to start the project as early as possible, a statement previously visualized by Sheng (2011). In his research is observed that the main reason as to delay a CEOR injection based on the polymer is the economy of the project and the knowledge a company has over its reservoir.

- Average permeability over 100 md is the best option to inject polymer according to this results, which Dickson et al. (2010) in his screening recommendation highlights is the best option for this type of CEOR programs.

- The brine salinity required for a surfactant injection must be at/under the optimal concentration (~60000 ppm). Also, a negative gradient is the best recommendation, a behavior, and recommendation previously done by Hirasaki; Miller and Puerto (2011). This behavior is explained as in reservoir conditions the salt content of the formation brine is much higher than the optimal value; therefore the injection scheme must take into account the salinity mix between formation and injection waters, a mixture which reaches concentrations close to the optimal.

- During PF and SP flooding it is possible to observe problems related to injectivity of the solution on low permeability reservoirs, due to the high viscosity of the polymer. This was observed previously in a field pilot on a carbonate reservoir (AL-AMRIE et al., 2015) and previously in a laboratory level (SERIGHT; SEHEULT; TALASHEK, 2009).

- The associated treatment and chemical costs of a CEOR project impact its profitability under any economic scenario. It requires then an implementation that targets not only the incremental recovery of oil but also the overall cash flow of the project (SHENG, 2011).

- The risk curve graphs showed that WF, PF, and SP are close in space. Optimizing either one methodology and associated costs will increase the gap between them.

- For the Cerena-I models: the SP programs do increase the NPV and EMV when compared to the PF however, the increment is not significant either in profitability or recovery factor (comparing between both CEOR methodologies). This can be explained as an effect of low quantities of chemical injected due to injectivity problem in the injector. Assumption confirmed when evaluating its performance

against a pool of data relating surfactant quantities versus incremental recoveries and field results. Despite this result, it can be then expected on the other side that if the models have larger volumes injected the recovery factor and its cash flow may increase, as there was an incremental recovery with very low volumes of chemical.

- The Cerena-I sector presented injectivity problems when the chemical slug was injected regardless of the permeability model, as a result of high pressures and high viscosity fluid. It must be studied possible solutions to this phenomenon as it makes difficult achieving the quantity of surfactant required to have large increments of oil recovery by IFT reduction. One possibility not evaluated in this research it's changing the position of the vertical well or replacing it for a directional well avoiding the zones with lower injectivity.

- For the Cerena-I model: the surfactant concentration depends on the economics of the project, the higher concentrations are encountered on the optimistic scenarios, and the minimum percentages are on the contrary on the more pessimistic scenarios. This can be confirmed as the average of the optimal surfactant concentration for the pessimistic scenario is 0.05%, for the probable scenario 0.16% and for the optimistic 0.32%.

FUTURE WORKS

Next, a list of ideas for future works based on this research:

- Evaluate the performance of both CEOR methodologies in a real field model.
- Evaluate the performance of both CEOR injections in coreflooding tests and preliminary evaluation and screening of chemical based on state of the art.
- Evaluate the performance of other simulation alternatives such as proxy analysis, neural networks, and a combination of both as alternatives for CEOR evaluation.
- Evaluate the performance of vertical wells versus horizontal, directional wells and their placement.
- Evaluate the performance of other CEOR oil recovery mechanisms.

REFERENCES

ABDULLAH, M.; TIWARI, S.; PATHAK, A. Evolution of Chemical EOR (ASP) Program for a Carbonate Reservoir in North Kuwait. **SPE Middle East Oil & Gas Show and Conference, 8-11 March, Manama, Bahrain**, 2015.

ADAMS, W. T.; SCHIEVELBEIN, V. H. Surfactant Flooding Carbonate Reservoirs. **SPE Reservoir Engineering**, v. 2, n. 04, p. 619–626, 1987. Disponível em: <http://www.onepetro.org/doi/10.2118/12686-PA>.

AHMADI, M. A.; SHADIZADEH, S. R. Adsorption of a nonionic surfactant onto a silica surface. **Energy Sources, Part A: Recovery, Utilization and Environmental Effects**, v. 38, n. 10, p. 1455–1460, 2016.

AL-AMRIE, O. et al. The First Successful Chemical EOR Pilot in the UAE : One Spot Pilot in High Temperature , High Salinity Carbonate Reservoir. **Abu Dhabi International Petroleum Exhibition and Conference**, 2015.

AL-DOUSARI, M. M.; GARROUCH, A. A. An artificial neural network model for predicting the recovery performance of surfactant polymer floods. **Journal of Petroleum Science and Engineering**, v. 109, p. 51–62, 2013.

AL-SINANI, I. S. et al. Modified Surfactant Injection to Enhance Oil Production and Recovery , Case Study : Omani Carbonate Reservoir. **Spe-179851-Ms**, v. i, 2016.

AL ADASANI, A.; BAI, B. Analysis of EOR projects and updated screening criteria. **Journal of Petroleum Science and Engineering**, v. 79, n. 1–2, p. 10–24, 2011. Disponível em: <http://dx.doi.org/10.1016/j.petrol.2011.07.005>.

ALANIS, P. A. L. et al. Toward an Alternative Bio-Based SP Flooding Technology : I . Biosurfactant. 2015.

ALSOFI, A. M. et al. Numerical simulation of surfactant-polymer coreflooding experiments for carbonates. **Journal of Petroleum Science and Engineering**, v. 111, p. 184–196, 2013.

ALSOFI, A. M.; LIU, J. S.; HAN, M. SPE 1546 Numerica al Simula tion of Su urfactant r Coreflo oding Ex xperiment ts for Carbonat tes. **SPE Enhanced Oil Recovery Conference**, 2012.

ALZAHID, Y. A. et al. Toward an Alternative Bio-Based SP Flooding Technology : II . Biopolymer. 2016.

AMERICAN PETROLEUM INSTITUTE. **Recommended Practices for Evaluation of Polymers Used in Enhanced Oil Recovery Operations**. 1st Editio ed. [s.l: s.n.]

AMRAN, T. et al. Review : A New Prospect of Streaming Potential Measurement in Alkaline-Surfactant-Polymer Flooding. v. 56, n. 2010, p. 1183–1188, 2017.

ANDERSON, G. a et al. Optimization of Chemical Flooding in a Mixed-Wet Dolomite Reservoir. **Spe**, n. April, p. 1–9, 2006.

AYIRALA, S.; YOUSEF, A. A State-of-the-Art Review To Develop Injection-Water-Chemistry Requirement Guidelines for IOR/EOR Projects. **SPE Production & Operations**, v. 30, n. 01, p. 26–42, 2015. Disponível em: <https://www.onepetro.org/journal-paper/SPE-169048-PA>.

BAHRAMI, P. et al. A novel approach for modeling and optimization of surfactant/polymer flooding based on Genetic Programming evolutionary algorithm. **Fuel**, v. 179, n. April, p. 289–298, 2016. Disponível em: <http://dx.doi.org/10.1016/j.fuel.2016.03.095>.

BAKER, E. L.; ZAMAN, M. H. The biomechanical integrin. **Journal of Biomechanics**, v. 43, n. 1, p. 38–44, jan. 2010. Disponível em: <http://linkinghub.elsevier.com/retrieve/pii/S0021929009004989>.

BELTRAO, R. L. C. et al. SS: Pre-salt Santos basin - Challenges and New Technologies for the Development of the Pre-salt Cluster, Santos Basin, Brazil. **Offshore Technology Conference**, n. July 2014, 2009. Disponível em: <http://www.onepetro.org/doi/10.4043/19880-MS>.

BENT, V. J. Van Der. **Comparative study of foam stability in bulk and porous media**. 2014. 2014.

BOU-MIKAEL, S. et al. Minas Surfactant Field Trial Tests Two Newly Designed Surfactants with High EOR Potential. In: SPE Asia Pacific Oil and Gas Conference and Exhibition, **Anais**...Society of Petroleum Engineers, 4 abr. 2000. Disponível em: <http://www.onepetro.org/doi/10.2118/64288-MS>.

BOURGOYNE, A. T. et al. **Applied Drilling Engineering**. Richardson, TX: Society of Petroleum Engineers, 1986.

BOYD, A. et al. Presalt Carbonate Evaluation for Santos Basin , Offshore Brazil. **Petrophysics**, v. 56, n. 6, p. 577–591, 2015.

CARLISLE, C. et al. One-Spot Pilot Results in the Sabriyah-Mauddud Carbonate Formation in Kuwait Using a Novel Surfactant Formulation. **SPE Improved Oil Recovery Symposium, 12-16 April, Tulsa, Oklahoma, USA**, n. October 2013, p. 1–21, 2014.

CHACO, L. J. et al. ASP System Design for an Offshore Application in La Salina Field , Lake Maracaibo. n. June, p. 25–28, 2003.

CHAI, C. F. et al. St Joseph Chemical EOR Pilot – A Key De-risking Step Prior to Offshore ASP Full field Implementation. **SPE Enhanced Oil Recovery Conference**, n. SPE 144594, p. 1–8, 2011.

CHANG, H. L. et al. Advances in Polymer Flooding and Alkaline/Surfactant/Polymer Processes as Developed and Applied in the People's Republic of China. **Journal of Petroleum Technology**, v. 58, n. 02, p. 84–89, 2006. Disponível em: <https://www.onepetro.org/journal-paper/SPE-89175-JPT>.

CHAUHAN, P. D. **Data analysis and summary for surfactant-polymer flooding based on oil field projects and laboratory data**. 2014. MISSOURI UNIVERSITY OF SCIENCE AND TECHNOLOGY, 2014.

CHO, J. et al. Effects of relative permeability change resulting from interfacial tension reduction on vertical sweep efficiency during the CO 2 -LPG hybrid EOR process. **Energy Sources, Part A: Recovery, Utilization, and Environmental Effects**, v. 40, n. 10, p. 1242–1249, 19 maio 2018. Disponível em: <https://doi.org/10.1080/15567036.2018.1476619>.

CRAFT, T.; ABDELRAHIM, M. Measurement of Interfacial Tension in Hydrocarbon / Water / Dispersant Systems At Deepwater Conditions. n. May, p. 88, 2012.

DANG, T. Q. C. et al. Rheological Modeling and Numerical Simulation of HPAM Polymer Viscosity in Porous Media. **Energy Sources, Part A: Recovery, Utilization, and Environmental Effects**, v. 37, n. 20, p. 2189–2197, 18 out. 2015. Disponível em: <http://dx.doi.org/10.1080/15567036.2011.624156>.

DE MORAES CRUZ, R. O. et al. Lula NE Pilot Project - An Ultra-Deep Success in the Brazilian Pre-Salt. In: Offshore Technology Conference, **Anais**...Offshore Technology Conference, 2 maio 2016. Disponível em: <http://www.onepetro.org/doi/10.4043/27297-MS>.

DEBONS, F. E.; BRAUN, R. W.; LEDOUX, W. a. A Guide to Chemical Oil Recovery for the Independent Operator. In: SPE/DOE Symposium on Improved Oil Recovery, 200437, **Anais**...Society of Petroleum Engineers, 4 abr. 2004. Disponível em: <http://search.ebscohost.com/login.aspx?direct=true&db=pta&AN=843675&site=ehost-live>.

DICKSON, J. L.; LEAHY-DIOS, A.; WYLIE, P. L. Development Of Improved Hydrocarbon Recovery Screening Methodologies. In: SPE Improved Oil Recovery Symposium, 201036, **Anais**...Society of Petroleum Engineers, 4 abr. 2010. Disponível em: <http://www.onepetro.org/doi/10.2118/129768-MS>.

DU, K. et al. Evaluating Chemical EOR Potential of St Joseph Field, Offshore Malaysia. p. 1–10, 2011.

FABUSUYI, J. **Optimization of a Water Alternating Gas Injection Compositional fluid flow simulation with Water Alternating Gas Injection optimization on the upscaled synthetic reservoir CERENA-I**. 2015. 2015.

FARAJZADEH, R. et al. Foam – oil interaction in porous media : Implications for foam assisted enhanced oil recovery. **Advances in Colloid and Interface Science**, v. 184, p. 1–13, 2012. Disponível em: <http://dx.doi.org/10.1016/j.cis.2012.07.002>.

FORTENBERRY, R. et al. Interwell ASP Pilot Design for Kuwait ' s Sabriyah-Mauddud History of EOR Studies in SAMA. 2016.

FOSTER, W. R. A Low-Tension Waterflooding Process. **Journal of Petroleum Technology**, v. 25, n. 02, p. 205–210, 1 fev. 1973. Disponível em: <http://www.onepetro.org/doi/10.2118/3803-PA>.

FRASER, A. H.; SEBA, R. D. **Economics of worldwide petroleum production**. 3. ed. Tulsa, Oklahoma: OGCI Publications, 1993.

GASPAR, A. T. et al. Study Case for Reservoir Exploitation Strategy Selection based on UNISIM-I Field. **Research Group in Reservoir Simulation and Management**, 2015.

HENRIQUES, C. et al. Material Selection for Brazilian Presalt Fields. **Offshore Technology Conference**, v. 23320, n. May, p. 1–11, 2012.

HIRASAKI, G.; MILLER, C.; PUERTO, M. Recent Advances in Surfactant EOR. **SPE Journal**, v. 16, n. 4, p. 3–5, 2011.

HOLLEY, S. M.; CAYLAS, J. L. Design, Operation, and Evaluation of a Surfactant / Polymer Field Pilot Test. **SPE Reservoir Engineering**, v. 7, n. 01, p. 9–14, 1992. Disponível em: <https://doi.org/10.2118/20232-PA>.

HONGYAN, C. et al. Surfactant Derived from Natural Renewable Product for SP Flooding in High Temperature, Low Salinity Reservoir. **SPE Kingdom of Saudi Arabia Annual Technical Symposium and Exhibition**, 2016. Disponível em: <http://www.onepetro.org/doi/10.2118/182770-MS>.

HUBBARD, A. T. **Encyclopedia of Surface and Colloid Science -**. [s.l.] Taylor & Francis, 2002.

IZADI, M. et al. Assessing Productivity Impairment of Surfactant-Polymer EOR Using Laboratory and Field Data. **SPE Improved Oil Recovery Conference**, 2018.

JABBAR, M. Y. et al. Chemical Formulation Design in High Salinity, High Temperature Carbonate Reservoir for a Super Giant Offshore Field in Middle East. In: Abu Dhabi International Petroleum Exhibition & Conference, **Anais**...Society of Petroleum Engineers, 13 nov. 2017. Disponível em: <http://www.onepetro.org/doi/10.2118/188604-MS>.

JUNIOR, A. E. **Caracterização pvt de petróleo contendo CO2**. 2015. Universidade Estadual de Campinas, 2015.

KALN, P. E. **An introduction to applying surfactant simulation on the Norne field**. 2009. Norwegian University of Science and Technology, 2009.

KAMARI, A. et al. Integrating a robust model for predicting surfactant-polymer flooding performance. **Journal of Petroleum Science and Engineering**, v. 137, p. 87–96, 2016. Disponível em: <http://dx.doi.org/10.1016/j.petrol.2015.10.034>.

KASIMBAZI, G. **Polymer Flooding**. 2014. Norwegian University of Science and Technology, 2014.

KEMMOÉ TCHOMTÉ, S.; GOURGAND, M. Particle swarm optimization: A study of particle displacement for solving continuous and combinatorial optimization problems. **International Journal of Production Economics**, v. 121, n. 1, p. 57–67, 2009.

KENNEDY, J.; EBERHART, R. Particle swarm optimization. **Neural Networks, 1995. Proceedings., IEEE International Conference on**, v. 4, p. 1942–1948 vol.4, 1995.

KOVALEV, K. et al. North Sabah EOR ADP – Examining the Challenges of Offshore ASP Development. 2016.

KRÜSS GMBH. **Force Tensiometer – K6**. Disponível em: <https://www.kruss.de/products/tensiometers/force-tensiometer-k6/>.

KULAWARDANA, E. U. et al. Rheology and Transport of Improved EOR Polymers under Harsh Reservoir Conditions. **Improved Oil Recovery Symposium, Tulsa, Oklahoma,**

USA, p. 1–14, 2012.

LASKARIS, G. **Effect of Surfactant Concentration, WaterTreatment Chemicals, Fatty Acids and Alcohols on Foam Behavior in Porous Media and in Bulk**. 2015. Delft University of Technology, 2015.

LEVITT, D. et al. Identification and Evaluation of High-Performance EOR Surfactants. **SPE Reservoir Evaluation & Engineering**, v. 12, n. 02, p. 243–253, 1 abr. 2009. Disponível em: <http://aac.asm.org/cgi/doi/10.1128/AAC.01575-12>.

LEVITT, D. et al. Overcoming Design Challenges of Chemical EOR in High-Temperature, High Salinity Carbonates. **SPE Middle East Oil and Gas Show and Conference**, p. 1–15, 2013. Disponível em: <http://www.onepetro.org/doi/10.2118/164241-MS>.

LEVITT, D. et al. Designing and Injecting a Chemical Formulation for a Successful Off-Shore Chemical EOR Pilot in a High-Temperature , High-Salinity , Low-Permeability Carbonate Field. 2016.

LI, B. et al. SPE-190448-MS Polymeric Surfactant for Enhanced Oil Recovery- Microvisual , Core-Flood Experiments and Field Application. 2018.

LI, Y. et al. Mixtures of Anionic / Cationic Surfactants : A New Approach for Enhanced Oil Recovery in Low-Salinity , High-Temperature Sandstone Reservoir. 2016.

MADEIRA, P. T. **Dynamic simulation on the synthetic reservoir CERENA I Compositional fluid flow simulation with 4D seismic monitoring on a reservoir with a large content of CO 2**. 2014. 2014.

MANRIQUE, E. J.; MUCI, V. E.; GURFINKEL, M. E. EOR Field Experiences in Carbonate Reservoirs in the United States. **SPE Reservoir Evaluation & Engineering**, v. 10, n. 06, p. 667–686, 2007a. Disponível em: <http://www.onepetro.org/doi/10.2118/100063-PA>.

MANRIQUE, E.; MUCI, V.; GURFINKEL, M. EOR Field Experiences in Carbonate Reservoirs in the United States. **SPE Reservoir Evaluation & Engineering**, v. 10, n. 6, p. 667–686, 2007b.

MELLO, S. F. DE. **Caracterização de fluido e simulação de injeção alternada de agua e CO2 para reservatorios carbonaticos molhaveis a agua**. 2015. 2015.

MILLER, R. J.; RICHMOND, C. N. El Dorado Micellar-Polymer Project Facility. **Journal of Petroleum Technology**, v. 30, n. 01, p. 26–32, 1 jan. 1978. Disponível em: <http://www.onepetro.org/doi/10.2118/6469-PA>.

MOHAMID, S. et al. Screening of Polymers for EOR in High Temperature , High Salinity and. **International Petroleum Technology Conference**, 2015.

MOLLAEI, A.; LAKE, L. W.; DELSHAD, M. Application and variance based sensitivity analysis of surfactant-polymer flooding using modified chemical flood predictive model. **Journal of Petroleum Science and Engineering**, v. 79, n. 1–2, p. 25–36, 2011.

MOREL, D. et al. Polymer Injection in Deep Offshore Field : The Dalia Angola Case. **Polymer**, n. SPE 116672, p. 21–24, 2008.

MOREL, D. et al. Specific Procedure for an Offshore Chemical EOR One Spot Pilot in a

High Salinity High Temperature Environment. **SPE Annual Technical Conference and Exhibition**, 2016. Disponível em: <http://www.onepetro.org/doi/10.2118/181643-MS>.

MUKERJEE, P.; MYSELS, K. **Critical micelle concentrations of aqueous surfactant systemsJournal of Pharmaceutical Sciences**, 1971. . Disponível em: <http://doi.wiley.com/10.1002/jps.2600610254%5Cnhttp://oai.dtic.mil/oai/oai?verb=getRecord&metadataPrefix=html&identifier=ADD095344>.

NAVEIRO, J. T.; HAIMSON, D. Sapinhoá Field , Santos Basin Pre-Salt : From Conceptual Design to Project. **Offshore Technology Conference Brasil Brasil**, n. July 2014, p. 19, 2015.

NEEDHAM, R. B.; DOE, P. H. Polymer Flooding Review. **Journal of Petroleum Technology**, v. 39, n. 12, p. 1503–1507, 1987. Disponível em: <http://www.onepetro.org/doi/10.2118/17140-PA>.

OLAJIRE, A. A. **Review of ASP EOR (alkaline surfactant polymer enhanced oil recovery) technology in the petroleum industry: Prospects and challengesEnergy**Elsevier Ltd, , 2014. . Disponível em: <http://dx.doi.org/10.1016/j.energy.2014.09.005>.

PARK, S.; LEE, E. S.; SULAIMAN, W. R. W. Adsorption behaviors of surfactants for chemical flooding in enhanced oil recovery. **Journal of Industrial and Engineering Chemistry**, v. 21, p. 1239–1245, jan. 2015. Disponível em: <http://linkinghub.elsevier.com/retrieve/pii/S1226086X14002895>.

PEREIRA, A. D. F. et al. Santos Microbial Carbonate Reservoirs: A Challenge. **OTC Brasil**, n. October, p. 29–31, 2013. Disponível em: <http://www.onepetro.org/doi/10.4043/24446-MS>.

PINHEIRO, R. S. et al. Well Construction Challenges in the Pre-Salt Development Projects. **Offshore Technology Conference**, v. 4–7, n. May, p. 1–13, 2015.

RATERMAN, K. T. A Mechanistic Interpretation of the Torchlight Micellar/Polymer Pilot. **SPE Reservoir Engineering**, v. 5, n. 04, p. 459–466, 1 nov. 1990. Disponível em: <http://www.onepetro.org/doi/10.2118/18087-PA>.

ROMERO-ZERÓN, L. Advances in Enhanced Oil Recovery Processes. **Introduction to Enhanced Oil Recovery (EOR) Processes and Bioremediation of Oil-Contaminated Sites**, p. 1–43, 2012. Disponível em: <http://www.intechopen.com/books/introduction-to-enhanced-oil-recovery-eor-processes-and-bioremediation-of-oil-contaminated-sites/advances-in-enhanced-oil- recovery>.

ROSALAM, S.; ENGLAND, R. Review of xanthan gum production from unmodified starches by Xanthomonas comprestris sp. **Enzyme and Microbial Technology**, v. 39, n. 2, p. 197–207, 2006.

ROSEN, M. J. **Surfactants and Interfacial Phenomena**. [s.l: s.n.]

SAMPAIO, M. A. et al. Comparison Between Smart and Conventional Wells Optimized Under Economic Uncertainty. **OTC Brasil**, n. 3, 2013.

SCHIOZER, D. **Research Group in Reservoir Simulation and Management Study Case for Reservoir Exploitation Strategy Selection based on UNISIM-I Field**.

Disponível em: <http://www.unisim.cepetro.unicamp.br/benchmarks/br/unisim-i/unisim-i-d>.

SCHLUMBERGER LIMITED. **productivity index (PI)**. Disponível em: <https://www.glossary.oilfield.slb.com/en/Terms/p/productivity_index_pi.aspx>. Acesso em: 20 out. 2018.

SCHRAMM, L. L.; MARANGONI, G. Surfactants: Fundamentals and applications in the petroleum industry. **Chemical Engineering Journal**, v. 83, n. 1, p. 63, 2001.

SERIGHT, R. S.; SEHEULT, J.; TALASHEK, T. Injectivity Characteristics of EOR Polymers. **SPE Reservoir Evaluation & Engineering**, n. 783, p. 783–792, 2009.

SHAMSIJAZEYI, H.; HIRASAKI, G. J.; VERDUZCO, R. Sacrificial Agent for Reducing Adsorption of Anionic Surfactants. **Spe 164061**, n. April, p. 1–16, 2013.

SHENG, J. **Modern Chemical Enhanced Oil Recovery**. [s.l.] Elsevier, 2011.

SHENG, J. J. Surfactant-Polymer Flooding. **Enhanced Oil Recovery Field Case Studies**, p. 117–142, 2013a.

SHENG, J. J. Review of Surfactant Enhanced Oil Recovery in Carbonate Reservoirs. **Advances in Petroleum Exploration and Development**, v. 6, n. 1, p. 1–10, 2013b.

SHENG, J. J. A comprehensive review of alkaline-surfactant-polymer (ASP) flooding. **Asia-Pacific Journal of Chemical Engineering**, v. 9, n. 4, p. 471–489, 2014.

SHENG, J. J.; LEONHARDT, B.; AZRI, N. Status of polymer-flooding technology. **Journal of Canadian Petroleum Technology**, v. 54, n. 2, p. 116–126, 2015.

SHENG, J. J.; SHENG, J. J. Chapter 9 – Surfactant-Polymer Flooding. **Modern Chemical Enhanced Oil Recovery**, p. 371–387, 2011.

SRIVASTAVA, M. et al. A Systematic Study of Alkaline-Surfactant-Gas Injection as an EOR Technique. **Proceedings of SPE Annual Technical Conference and Exhibition**, 2009. Disponível em: <https://www.onepetro.org/conference-paper/SPE-124752-MS>.

STEGEMEIER, G. L. **MECHANISMS OF ENTRAPMENT AND MOBILIZATION**. [s.l.] ACADEMIC PRESS, INC., 1977.

TABARY, R. et al. SPE 155106 Design of a Surfactant / Polymer Process in a Hard Brine Context : A Case Study Applied to Bramberge Reservoir. 2012.

TABER, J. J. et al. EOR Screening Criteria Revisited - Part 1: Introduction to Screening Criteria and Enhanced Recovery Field Projects. **SPE Reservoir Engineering**, n. August, p. 10, 1997.

TABER, J. J.; MARTIN, F. D.; SERIGHT, R. S. EOR Screening Criteria Revisited—Part 2: Applications and Impact of Oil Prices. **Spe 39234**, v. 12, n. 3, p. 199–205, 1997a.

TABER, J. J.; MARTIN, F. D.; SERIGHT, R. S. EOR Screening Criteria Revisited - Part 1: Introduction to Screening Criteria and Enhanced Recovery Field Projects. **SPE Reservoir Engineering**, v. 12, n. 03, p. 189–198, 1997b. Disponível em: <http://www.onepetro.org/doi/10.2118/35385-PA>.

TALASH, a. W.; STRANGE, L. Summary of Performance and Evaluations in the West Burkburnett Chemical Waterflood Project. **Journal of Petroleum Technology**, v. 34, n. 11, 1982.

THOMAS, R. D. et al. Performance of DOE&apos;s Micellar-Polymer Project in Northwest Oklahoma. In: SPE Enhanced Oil Recovery Symposium, 198219, **Anais**...Society of Petroleum Engineers, 4 abr. 1982. Disponível em: <http://www.onepetro.org/doi/10.2118/10724-MS>.

THOMAS, S.; FAROUQ ALI, S. M. Micellar-Polymer Flooding : Status and Recent Advances. **Journal of Canadian Petroleum Technology**, v. 31, n. 8, p. 53–60, 1992.

WKFMNYER, R. Performance Evaluation of the Salem Unit Surfactant / Polymer Pilot. p. 1217–1226, 1982.

ZAITOUN, A. et al. New Surfactant for Chemical Flood in High-Salinity Reservoir. **Spe 80237**, 2003.

ZHANG, D. et al. Favorable Attributes of Alkali-Surfactant-Polymer Flooding. In: SPE/DOE Symposium on Improved Oil Recovery, **Anais**...Society of Petroleum Engineers, 4 abr. 2006. Disponível em: <http://www.onepetro.org/doi/10.2118/99744-MS>.

ZHANG, F. et al. A Novel Hydroxylpropyl Sulfobetaine Surfactant for High Temperature and High Salinity Reservoirs. **International Petroleum Technology Conference**, 2013.

ZHENQUAN, L. et al. A Successful Pilot of dilute Surfactant-Polymer Flooding in Shengli Oilfield. **SPE Improved Oil Recovery Symposium**, p. 1–6, 2013. Disponível em: <http://www.onepetro.org/doi/10.2118/154034-MS>.

ZHU, Y. et al. The research progress in the alkali-free surfactant-polymer combination flooding technique. **Petroleum Exploration and Development**, v. 39, n. 3, p. 371–376, 2012. Disponível em: <http://dx.doi.org/10.1016/S1876-3804(12)60053-6>.

ZHU, Y. et al. SPE 165208 Enhanced Oil Recovery by Chemical Flooding from the Biostromal Carbonate Reservoir. **Spe**, v. 165208, n. July, p. 1–8, 2013.

ZUBARI, H. K.; SIVAKUMAR, V. C. B. Single Well Tests to determine the Efficiency of Alkaline-Surfactant Injection in a highly. p. 1–6, 2003.

APPENDIX A – EXAMPLE OF SIMULATION FILE SP FLOODING LULA BASED MODEL

```
** ***********************************************************************
** Definition of grid and data results, Base model
** ***********************************************************************
INUNIT FIELD
WRST 0
WPRN GRID 0
WSRF GRID 0
WSRF WELL 1
WSRF GRID TIME
WSRF SECTOR TIME
OUTSRF GRID CAPN IFT MASDENO MASDENW MOLDENW PRES RFO RFW SG SO SW
        TEMP VELOCRC VISO VISW W X
OUTSRF WELL MASS COMPONENT ALL
OUTSRF SPECIAL MASSFRAC  'Injector Water' 'Polymer' WATER
        MASSFRAC  'Producer' 'Polymer' WATER
        MASSFRAC  'Producer2' 'Polymer' WATER
        MASSFRAC  'Producer3' 'Polymer' WATER
        MASSFRAC  'Producer4' 'Polymer' WATER
        MASSFRAC  'Injector Water' 'WATER' WATER
        VOLFRAC  'Injector Water' 'Polymer' WATER
        VOLFRAC  'Injector Water' 'WATER' WATER
        VOLFRAC  'Producer' 'Polymer' WATER
        VOLFRAC  'Producer2' 'Polymer' WATER
        VOLFRAC  'Producer3' 'Polymer' WATER
        VOLFRAC  'Producer4' 'Polymer' WATER
OUTSRF WELL LAYER NONE
WPRN GRID 0
OUTPRN GRID NONE
OUTPRN RES NONE
**  Distance units: ft
RESULTS XOFFSET          0.0000
RESULTS YOFFSET          0.0000
RESULTS ROTATION         0.0000  **  (DEGREES)
RESULTS AXES-DIRECTIONS 1.0 -1.0 1.0
** ***********************************************************************
** Definition of fundamental cartesian grid
** ***********************************************************************
GRID VARI 20 20 7
KDIR DOWN
DI IVAR
 20*200
DJ JVAR
 20*200
DK ALL
 2800*29
DTOP
 400*21100

NULL CON        1
*INCLUDE 'poro.inc'
*INCLUDE 'permx.inc'
*INCLUDE 'permy.inc'
*INCLUDE 'permz.inc'

PINCHOUTARRAY CON        1
END-GRID
***********************************************************************
** THE FOLLOWING KEYWORDS CAN BE USED IN THE INITIALIZATION SECTION IN STARS
***********************************************************************
** MFRAC_OIL 'CO2' CON  1.7844E-01
** MFRAC_OIL 'N2' CON  2.0004E-03
** MFRAC_OIL 'C1' CON  4.4829E-01
** MFRAC_OIL 'C2' CON  5.2811E-02
** MFRAC_OIL 'C3' CON  4.0708E-02
** MFRAC_OIL 'IC4toNC5' CON  3.3607E-02
** MFRAC_OIL 'C6 toC9' CON  6.0412E-02
** MFRAC_OIL 'C10toC14' CON  5.6511E-02
** MFRAC_OIL 'C15toC19' CON  3.4207E-02
** MFRAC_OIL 'C20+' CON  9.3019E-02
***********************************************************************
** THE FOLLOWING SECTION CAN BE USED FOR THE COMPONENT PROPERTY INPUT INTO STARS
***********************************************************************
** PVT UNITS CONSISTENT WITH *INUNIT *FIELD
** Model and number of components

** ***********************************************************************
** Definition of fluid, components and PVT
** ***********************************************************************

MODEL 14 14 14 4
COMPNAME 'WATER' 'Polymer' 'Salt' 'Surfact' 'CO2' 'N2' 'C1' 'C2' 'C3' 'IC4toNC5' 'C6 toC9' 'C10toC14' 'C15toC19' 'C20+'
**      -------- -------- -------- -------- -------- -------- -------- -------- -------- -------- --------
CMM
0 8000 58.4425 299.41 44.01 28.013 16.043 30.07 44.097 62.6744 102.725 160.019 231.564 451.282
PCRIT
0 0 0 0 1069.87 492.31 667.2 708.34 615.76 529.85 437.42 322.35 244.82 134.32
```

```
TCRIT
0.00 0.00 0.00 0.00 87.89 -232.51 -116.59 90.05 205.97 330.89 542.93 731.76 879.16 1350.91
** reference pressure,     corresponding to the density
PRSR 8520
** reference temperature,  corresponding to the density
TEMR 140
** pressure at surface,    for reporting well rates, etc.
PSURF 14.696
** temperature at surface, for reporting well rates, etc.
TSURF 60
K_SURF 'CO2' 68.328
K_SURF 'N2' 816.02
K_SURF 'C1' 171.09
K_SURF 'C2' 27.847
K_SURF 'C3' 7.0485
K_SURF 'IC4toNC5' 1.2414
K_SURF 'C6 toC9' 0.030584
K_SURF 'C10toC14' 0.00019433
K_SURF 'C15toC19' 6.4121e-007
K_SURF 'C20+' 1e-016
MOLDEN
0 0 0 0.790534 1.422 1.474 1.273 1.073 0.867801 0.669398 0.475 0.2978 0.2561 0.1199
CP
0 0 0 0 2.074e-005 2.36e-005 2.012e-005 1.668e-005 9.469e-006 7.187e-006 4.841e-006 3.046e-006 2.751e-006 9.574e-007
CT1
0 0 0 0 0.0006524 0.0008139 0.0005796 0.0003889 0.0002584 0.0001667 9.579e-005 5.251e-005 4.92e-005 3.019e-005
CT2
0 0 0 0 8.216e-007 7.201e-007 8.062e-007 8.325e-007 5.303e-007 4.545e-007 3.441e-007 2.283e-007 1.968e-007 5.815e-008
CPT
0 0 0 0 2.243e-007 -7.372e-006 1.292e-008 8.609e-008 4.938e-008 4.827e-008 6.131e-008 4.318e-008 6.313e-009 -3.021e-010
AVISC
0 163.426 0 0 0.5266 0.3455 0.3116 0.3726 0.3781 0.3793 0.3641 0.3022 0.246 0.1585
BVISC
0 0 0 0 328.74 107.39 154.62 281.88 366.11 466.46 676.16 955.74 1254.2 2259.82
VSMIXCOMP 'Polymer'
VSMIXENDP 0 6.77779e-006
VSMIXFUNC 0 0.29548 0.535752 0.667652 0.742474 0.789605 0.836735 0.881295 0.920863 0.960432 1


** Reaction specification
STOREAC
0 1 0 0 0 0 0 0 0 0 0 0 0 0
STOPROD
443.951 0 0 0 0 0 0 0 0 0 0 0 0 0
RPHASE
0 1 0 0 0 0 0 0 0 0 0 0 0 0
RORDER
0 1 0 0 0 0 0 0 0 0 0 0 0 0
EACT 0
FREQFAC 0.00385082


** The following is the complete WinProp fluid model description.

WINPROP *TITLE1    'Regression'
WINPROP *TITLE2    'Lumping Nitrogen and CO2 singles'
WINPROP *TITLE3    '10 components lumping'
WINPROP *INUNIT *FIELD
WINPROP *MODEL  *PR  *1978
WINPROP *NC     10   10
WINPROP *TRANSLATION 1
WINPROP *PVC3  0.0000000E+00
WINPROP *COMPNAME
WINPROP 'CO2    ' 'N2    ' 'C1   ' 'C2    ' 'C3    '
WINPROP 'IC4toNC5' 'C6 toC9 ' 'C10toC14' 'C15toC19' 'C20+    '
WINPROP *HCFLAG
WINPROP  3 0 1 1 1 1 1 1 1 1
WINPROP *SG
WINPROP  8.1800000E-01 8.0900000E-01 3.0000000E-01 3.5600000E-01 5.0700000E-01
WINPROP  5.9973671E-01 7.3651011E-01 8.0454854E-01 8.4854913E-01 9.4950000E-01
WINPROP *TB
WINPROP  -1.0921000E+02 -3.2035000E+02 -2.5861000E+02 -1.2757000E+02 -4.3690000E+01
WINPROP  5.5191319E+01 2.2687809E+02 4.0596799E+02 5.6276272E+02 9.9357400E+02
WINPROP *PCRIT
WINPROP  7.2800000E+01 3.3500000E+01 4.5400000E+01 4.8200000E+01 4.1900000E+01
WINPROP  3.6054179E+01 2.9764603E+01 2.1934463E+01 1.6659341E+01 9.1400041E+00
WINPROP *VCRIT
WINPROP  9.4000000E-02 8.9500000E-02 9.9000000E-02 1.4800000E-01 2.0300000E-01
WINPROP  2.7092603E-01 4.0418707E-01 6.1716790E-01 8.6552415E-01 1.5951000E+00
WINPROP *TCRIT
WINPROP  3.0420000E+02 1.2620000E+02 1.9060000E+02 3.0540000E+02 3.6980000E+02
WINPROP  4.3920044E+02 5.5700051E+02 6.6190469E+02 7.4379592E+02 1.0058772E+03
WINPROP *AC
WINPROP  2.2500000E-01 4.0000000E-02 8.0000000E-03 9.8000000E-02 1.5200000E-01
WINPROP  2.1002381E-01 3.3234061E-01 5.1758507E-01 7.1272938E-01 1.1641010E+00
WINPROP *MW
WINPROP  4.4010000E+01 2.8013000E+01 1.6043000E+01 3.0070000E+01 4.4097000E+01
WINPROP  6.2674425E+01 1.0272517E+02 1.6001947E+02 2.3156433E+02 4.5128197E+02
WINPROP *BIN
WINPROP  -2.0000000E-02
WINPROP  1.0300000E-01 3.1000000E-02
WINPROP  1.3000000E-01 4.2000000E-02
WINPROP  1.3500000E-01 9.1000000E-02
WINPROP  1.2837798E-01 9.5000000E-02
WINPROP  1.5000000E-01 1.2000000E-01
WINPROP  1.5000000E-01 1.2000000E-01
```

```
WINPROP   1.5000000E-01  1.2000000E-01
WINPROP   9.5652560E-02  1.2000000E-01
WINPROP *VSHIFT
WINPROP   0.0000000E+00  0.0000000E+00  0.0000000E+00  0.0000000E+00  0.0000000E+00
WINPROP   0.0000000E+00  2.6734950E-02 -8.8502198E-03  2.0050577E-01  2.4329367E-01
WINPROP *VSHIF1
WINPROP   0.0000000E+00  0.0000000E+00  0.0000000E+00  0.0000000E+00  0.0000000E+00
WINPROP   0.0000000E+00  0.0000000E+00  0.0000000E+00  0.0000000E+00  0.0000000E+00
WINPROP *TREFVS
WINPROP   6.0000000E+01  6.0000000E+01  6.0000000E+01  6.0000000E+01  6.0000000E+01
WINPROP   6.0000000E+01  6.0000000E+01  6.0000000E+01  6.0000000E+01  6.0000000E+01
WINPROP *ZRA
WINPROP   2.7360000E-01  2.9050000E-01  2.8760000E-01  2.7890000E-01  2.7630000E-01
WINPROP   2.7163661E-01  2.6617996E-01  2.5580644E-01  2.4931142E-01  2.1377354E-01
WINPROP *VISVC
WINPROP   9.4000000E-02  8.9500000E-02  9.9000000E-02  1.4800000E-01  2.0300000E-01
WINPROP   2.7124107E-01  4.0507947E-01  6.1856283E-01  8.6648830E-01  1.5951000E+00
WINPROP *VISCOR *MODPEDERSEN
WINPROP *VISCOEFF
WINPROP   1.3040000E-04  2.3030000E+00  7.3780000E-03  1.8470001E+00  5.1730000E-01
WINPROP *OMEGA
WINPROP   4.5723553E-01  4.5723553E-01  5.5383856E-01  4.5723553E-01  4.5723553E-01
WINPROP   4.5723553E-01  4.5723553E-01  4.5723553E-01  4.5723553E-01  5.0318781E-01
WINPROP *OMEGB
WINPROP   7.7796074E-02  7.7796074E-02  9.0025384E-02  7.7796074E-02  7.7796074E-02
WINPROP   7.7796074E-02  7.7796074E-02  7.7796074E-02  7.7796074E-02  7.4062583E-02
WINPROP *PCHOR
WINPROP   7.8000000E+01  4.1000000E+01  7.7000000E+01  1.0800000E+02  1.5030000E+02
WINPROP   2.0279702E+02  2.9680993E+02  4.4827009E+02  6.1837778E+02  1.0299000E+03
WINPROP *HREFCOR *HARVEY
WINPROP *IGHCOEF
WINPROP   4.7780500E+00  1.1443300E-01  1.0113200E-04 -2.6494000E-08  3.4706000E-12 -1.3140000E-16  0.0000000E+00
WINPROP  -6.8925000E-01  2.5366400E-01 -1.4549000E-05  1.2544000E-08 -1.7106000E-12 -8.2390000E-17  0.0000000E+00
WINPROP  -5.5811400E+00  5.6483400E-01 -2.8297300E-04  4.1739900E-07 -1.5255760E-10  1.9588570E-14  0.0000000E+00
WINPROP  -7.6005000E-01  2.7308800E-01 -4.2956000E-05  3.1281500E-07 -1.3898900E-10  2.0070230E-14  0.0000000E+00
WINPROP  -1.2230100E+00  1.7973300E-01  6.6458000E-05  2.5099800E-07 -1.2474610E-10  1.8935090E-14  0.0000000E+00
WINPROP   2.8037748E+01 -3.6806486E-05  3.2835604E-04 -8.1310899E-08  6.5514515E-12  6.8596856E-20  0.0000000E+00
WINPROP   0.0000000E+00 -3.7502741E-02  4.2416428E-04 -6.2592316E-08  0.0000000E+00  0.0000000E+00  0.0000000E+00
WINPROP   0.0000000E+00 -4.0590084E-02  4.2150667E-04 -6.2924870E-08  0.0000000E+00  0.0000000E+00  0.0000000E+00
WINPROP   0.0000000E+00 -3.3262702E-02  4.1341677E-04 -6.0912313E-08  0.0000000E+00  0.0000000E+00  0.0000000E+00
WINPROP   0.0000000E+00 -1.8199600E-02  3.9690000E-04 -5.6781800E-08  0.0000000E+00  0.0000000E+00  0.0000000E+00
WINPROP *HEATING_VALUES
WINPROP   0.0000000E+00  0.0000000E+00  8.4429000E+02  1.4784600E+03  2.1051600E+03
WINPROP   2.9198468E+03  4.9269295E+03  7.6602060E+03  1.0677765E+04  0.0000000E+00
WINPROP *COMPOSITION *PRIMARY
WINPROP   1.7843569E-01  2.0004000E-03  4.4828966E-01  5.2810562E-02  4.0708142E-02
WINPROP   3.3606721E-02  6.0412084E-02  5.6511301E-02  3.4206840E-02  9.3018604E-02


** *************************************************************************
** Definition of Surfactant and Salt
** *************************************************************************


ROCKFLUID
RPT 1 WATWET
INTCOMP 'Salt' WATER
IFTTABLE
** Weight percent Surface = 0.05
2CMPW 3.01067e-005
** Composition of component/phase  Interfacial tension
              1e-007          0.01  ** Salinity(Salt), ppm = 0
       0.006253247863       0.00531  ** Salinity(Salt), ppm = 20000
       0.01268442392        0.00359  ** Salinity(Salt), ppm = 40000
       0.01930123185        0.000923 ** Salinity(Salt), ppm = 60000
       0.02611182658        0.00206  ** Salinity(Salt), ppm = 80000
       0.03312484777        0.00318  ** Salinity(Salt), ppm = 100000
       0.04034945645        0.00589  ** Salinity(Salt), ppm = 120000
       0.04779537487        0.0116   ** Salinity(Salt), ppm = 140000
** Weight percent Surface = 0.1
2CMPW 6.02416e-005
** Composition of component/phase  Interfacial tension
              1e-007          0.007  ** Salinity(Salt), ppm = 0
       0.006253247863       0.00391  ** Salinity(Salt), ppm = 20000
       0.01268442392        0.00234  ** Salinity(Salt), ppm = 40000
       0.01930123185        0.000806 ** Salinity(Salt), ppm = 60000
       0.02611182658        0.00159  ** Salinity(Salt), ppm = 80000
       0.03312484777        0.00255  ** Salinity(Salt), ppm = 100000
       0.04034945645        0.00381  ** Salinity(Salt), ppm = 120000
       0.04779537487        0.00689  ** Salinity(Salt), ppm = 140000
** Weight percent Surface = 0.2
2CMPW 0.000120597
** Composition of component/phase  Interfacial tension
              1e-007          0.003  ** Salinity(Salt), ppm = 0
       0.006253247863       0.00186  ** Salinity(Salt), ppm = 20000
       0.01268442392        0.00135  ** Salinity(Salt), ppm = 40000
       0.01930123185        0.000722 ** Salinity(Salt), ppm = 60000
       0.02611182658        0.000891 ** Salinity(Salt), ppm = 80000
       0.03312484777        0.00283  ** Salinity(Salt), ppm = 100000
       0.04034945645        0.00319  ** Salinity(Salt), ppm = 120000
       0.04779537487        0.00588  ** Salinity(Salt), ppm = 140000
** Weight percent Surface = 0.3
2CMPW 0.000181066
** Composition of component/phase  Interfacial tension
              1e-007          0.007  ** Salinity(Salt), ppm = 0
       0.006253247863       0.00462  ** Salinity(Salt), ppm = 20000
```

```
        0.01268442392          0.00267  ** Salinity(Salt), ppm = 40000
        0.01930123185          0.000863 ** Salinity(Salt), ppm = 60000
        0.02611182658          0.00209  ** Salinity(Salt), ppm = 80000
        0.03312484777          0.00492  ** Salinity(Salt), ppm = 100000
        0.04034945645          0.00628  ** Salinity(Salt), ppm = 120000
        0.04779537487          0.0089   ** Salinity(Salt), ppm = 140000
INTLOG
KRINTRP 1
DTRAPW -5
DTRAPN -5

** ***************************************************************************
** Definition of Relative permeability curves
** ***************************************************************************


**     Sw     krw     krow
SWT
    0.187     0      0.956
    0.378   0.00973   0.41
    0.437   0.0164    0.271
    0.466   0.0214    0.222
    0.526   0.036     0.137
    0.575   0.0554    0.0889
    0.604   0.0699    0.065
    0.657   0.113     0.0318
    0.694   0.152     0.0132
    0.724   0.185     0.0131
    0.757   0.238     0.0129
    0.795   0.305     0

**     Sl      krg     krog
SLT
    0.398     0.833     0
     0.49     0.534    0.0049
    0.598     0.25     0.0245
    0.637  0.1933977011  0.0343
    0.672     0.137    0.0588
    0.745     0.0637   0.127
    0.803     0.0245   0.225
    0.846     0.0098   0.319
    0.884     0.0049   0.436
    0.992     0        0.956
KRINTRP 2
DTRAPW -2
DTRAPN -2
**     Sw     krw     krow
SWT
    0.187     0       1
    0.999     1       0
      1       1       0
**     Sl      krg     krog
**     Sl     krg     krog
SLT
    0.188     1       0
      1       0       1


** ***************************************************************************
** Definition of Surfactant adsorption
** ***************************************************************************


ADSCOMP 'Surfact' WATER
ADSTABLE
**    Mole Fraction  Adsorbed moles per unit pore volume
          0                        0
    0.0001205967384            0.001224409571
ADMAXT 0.00122441
INTERP_ENDS ON

** ***************************************************************************
** Definition of Initialization parameters
** ***************************************************************************


INITIAL
VERTICAL DEPTH_AVE

INITREGION 1
DWOC 21400
REFDEPTH 21300
REFPRES 8520
MFRAC_WAT 'WATER' CON     0.966875
MFRAC_WAT 'Salt' CON    0.0331248
MFRAC_WAT 'Polymer' CON         0
MFRAC_OIL 'N2' CON    0.0020004
MFRAC_OIL 'IC4toNC5' CON    0.033607
MFRAC_OIL 'CO2' CON      0.17844
MFRAC_OIL 'C6 toC9' CON     0.060412
MFRAC_OIL 'C3' CON     0.040708
MFRAC_OIL 'C20+' CON     0.093019
MFRAC_OIL 'C2' CON     0.052811
MFRAC_OIL 'C15toC19' CON     0.034207
MFRAC_OIL 'C10toC14' CON     0.056511
MFRAC_OIL 'C1' CON      0.17844
```

```
** ******************************************************************************
** Definition of Numerical solution Parameters
** ******************************************************************************


NUMERICAL
CONVERGE TOTRES TIGHTER
DTMAX 30
TFORM ZT
ISOTHERMAL
NEWTONCYC 20
NCUTS 10
SOLVER AIMSOL
RUN
DATE 2016 1 1
DTWELL 0.01
**
**

** ******************************************************************************
** Well Definitions
** ******************************************************************************

WELL  'Producer'
PRODUCER 'Producer'
OPERATE  MAX  STL  3000.0  CONT REPEAT
OPERATE  MIN  BHP  6000.0  CONT REPEAT
MONITOR  MIN  STO  100.0  STOP
MONITOR   GOR  1965.0  STOP
MONITOR   WCUT  0.99  STOP
**       rad  geofac  wfrac  skin
GEOMETRY  K  0.29  0.249  1.0  0.0
   PERF    GEOA 'Producer'
** UBA          ff       Status Connection
  20 20 1      1.0 OPEN  FLOW-TO 'SURFACE'
  20 20 2      1.0 OPEN  FLOW-TO 1
  20 20 3      1.0 OPEN  FLOW-TO 2
  20 20 4      1.0 OPEN  FLOW-TO 3
  20 20 5      1.0 OPEN  FLOW-TO 4
  20 20 6      1.0 OPEN  FLOW-TO 5
  20 20 7      1.0 OPEN  FLOW-TO 6 REFLAYER
**
WELL  'Producer2'
PRODUCER 'Producer2'
OPERATE  MAX  STL  3000.0  CONT REPEAT
OPERATE  MIN  BHP  6000.0  CONT REPEAT
MONITOR  MIN  STO  100.0  STOP
MONITOR   GOR  1965.0  STOP
MONITOR   WCUT  0.952558  STOP
**       rad  geofac  wfrac  skin
GEOMETRY  K  0.29  0.249  1.0  0.0
   PERF    GEOA 'Producer2'
** UBA          ff       Status Connection
  20 1 1       1.0 OPEN  FLOW-TO 'SURFACE'
  20 1 2       1.0 OPEN  FLOW-TO 1
  20 1 3       1.0 OPEN  FLOW-TO 2
  20 1 4       1.0 OPEN  FLOW-TO 3
  20 1 5       1.0 OPEN  FLOW-TO 4
  20 1 6       1.0 OPEN  FLOW-TO 5
  20 1 7       1.0 OPEN  FLOW-TO 6 REFLAYER
**
WELL  'Producer3'
PRODUCER 'Producer3'
OPERATE  MAX  STL  3000.0  CONT REPEAT
OPERATE  MIN  BHP  6000.0  CONT REPEAT
MONITOR  MIN  STO  100.0  STOP
MONITOR   GOR  1965.0  STOP
MONITOR   WCUT  0.942818  STOP
**       rad  geofac  wfrac  skin
GEOMETRY  K  0.29  0.249  1.0  0.0
   PERF    GEOA 'Producer3'
** UBA          ff       Status Connection
  1 20 1       1.0 OPEN  FLOW-TO 'SURFACE'
  1 20 2       1.0 OPEN  FLOW-TO 1
  1 20 3       1.0 OPEN  FLOW-TO 2
  1 20 4       1.0 OPEN  FLOW-TO 3
  1 20 5       1.0 OPEN  FLOW-TO 4
  1 20 6       1.0 OPEN  FLOW-TO 5
  1 20 7       1.0 OPEN  FLOW-TO 6 REFLAYER

**

WELL  'Producer4'
PRODUCER 'Producer4'
OPERATE  MAX  STL  3000.0  CONT REPEAT
OPERATE  MIN  BHP  6000.0  CONT REPEAT
MONITOR  MIN  STO  100.0  STOP
MONITOR   GOR  1965.0  STOP
MONITOR   WCUT  0.971235  STOP
**       rad  geofac  wfrac  skin
GEOMETRY  K  0.29  0.249  1.0  0.0
   PERF    GEOA 'Producer4'
** UBA          ff       Status Connection
  1 1 1        1.0 OPEN  FLOW-TO 'SURFACE'
```

```
  1 1 2      1.0 OPEN   FLOW-TO 1
  1 1 3      1.0 OPEN   FLOW-TO 2
  1 1 4      1.0 OPEN   FLOW-TO 3
  1 1 5      1.0 OPEN   FLOW-TO 4
  1 1 6      1.0 OPEN   FLOW-TO 5
  1 1 7      1.0 OPEN   FLOW-TO 6 REFLAYER

**
**
WELL  'Injector Water'
**COMPNAME                            'WATER'    'Polymer'   'Salt'              'Surfact'      'CO2' 'N2' 'C1' 'C2' 'C3' 'IC4toNC5' 'C6 toC9' 'C10toC14'
'C15toC19' 'C20+'
INJECTOR UNWEIGHT 'Injector Water'
INCOMP WATER 0.98601944 1.1623194e-006 0.01394834 3.1056261e-005 0.0 0.0 0.0 0.0 0.0 0.0 0.0 0.0 0.0 0.0
OPERATE MAX STW 12000.0 CONT REPEAT
OPERATE MAX BHP 8800.0 CONT REPEAT
**      rad geofac wfrac skin
GEOMETRY K 0.29 0.249 1.0 0.0
    PERF    GEOA 'Injector Water'
** UBA        ff       Status Connection
  10 10 1      1.0 OPEN   FLOW-FROM 'SURFACE'
  10 10 2      1.0 OPEN   FLOW-FROM 1
  10 10 3      1.0 OPEN   FLOW-FROM 2
  10 10 4      1.0 OPEN   FLOW-FROM 3
  10 10 5      1.0 OPEN   FLOW-FROM 4
  10 10 6      1.0 OPEN   FLOW-FROM 5
  10 10 7      1.0 OPEN   FLOW-FROM 6 REFLAYER

WELL  'Injector Water2'
**COMPNAME                            'WATER'    'Polymer'   'Salt'              'Surfact'      'CO2' 'N2' 'C1' 'C2' 'C3' 'IC4toNC5' 'C6 toC9'
'C10toC14' 'C15toC19' 'C20+'
INJECTOR UNWEIGHT 'Injector Water2'
INCOMP WATER 0.99374841 0.0 0.0062515926 0.0 0.0 0.0 0.0 0.0 0.0 0.0 0.0 0.0 0.0 0.0
OPERATE MAX STW 12000.0 CONT REPEAT
OPERATE MAX BHP 8800.0 CONT REPEAT
**      rad geofac wfrac skin
GEOMETRY K 0.29 0.249 1.0 0.0
    PERF    GEOA 'Injector Water2'
** UBA        ff       Status Connection
  10 10 1      1.0 OPEN   FLOW-FROM 'SURFACE'
  10 10 2      1.0 OPEN   FLOW-FROM 1
  10 10 3      1.0 OPEN   FLOW-FROM 2
  10 10 4      1.0 OPEN   FLOW-FROM 3
  10 10 5      1.0 OPEN   FLOW-FROM 4
  10 10 6      1.0 OPEN   FLOW-FROM 5
  10 10 7      1.0 OPEN   FLOW-FROM 6 REFLAYER
SHUTIN 'Injector Water2'
**

** ******************************************************************************
** Definition of Triggers to open and close injector
** ******************************************************************************

TRIGGER 'Injection'
ON_SECTOR 'Entire  Field' PAVE < 5500.0
 *OPEN 'Injector Water'
END_TRIGGER

TRIGGER 'Injection2'
ON_WELL 'Injector Water' 'Injector Water2' STW-CI > 1.14399e+007
 *OPEN 'Injector Water2'
 *SHUTIN 'Injector Water'
END_TRIGGER

DATE 2016 2  1.00000

** ******************************************************************************
** The final date is 2046 1 1.00000
** ******************************************************************************
```

APPENDIX B – EXAMPLE OF SIMULATION FILE SP FLOODING CERENA -I

```
** ***********************************************************************
** Definition of grid and data results, Base model
** ***********************************************************************
SRFORMAT SR3
INUNIT SI
WRST 0
WPRN GRID 0
WSRF GRID 0
WRST 0
WPRN GRID 0
WSRF GRID 0
WSRF WELL 1
WSRF GRID TIME
SR2PREC SINGLE
WPRN ITER MATRIX
OUTSRF GRID ADS 'Surfact' DENG DENO DENW MOLALITY 'Na+' MOLALITY 'Polymer' MOLALITY 'Surfact' PRES SG SIGMAOW
SO SW VISG VISO VISW
OUTSRF RES NONE
OUTSRF WELL WSTRMASDEN
WPRN GRID 0
OUTPRN GRID NONE
OUTPRN RES NONE
**  Distance units: m
RESULTS XOFFSET          0.0000
RESULTS YOFFSET          0.0000
RESULTS ROTATION          0.0000  **  (DEGREES)
RESULTS AXES-DIRECTIONS 1.0 1.0 1.0
** ***********************************************************************
** Definition of fundamental corner point grid
** ***********************************************************************
GRID CORNER 22 22 154

*INCLUDE 'corners.inc'

**  0 = null block, 1 = active block
NULL ALL
49368*1 374*0 1 21*0 1 21*0 1 21*0 1 21*0 1 21*0 24530*1 0 21*1 0 21*1 0 21*1 0 21*1 0 21*1 0 21*1 0 21*1

**
*INCLUDE 'poro.inc'
*INCLUDE 'permi.inc'
*INCLUDE 'permj.inc'
*INCLUDE 'permk.inc'
**
**  0 = pinched block, 1 = active block
PINCHOUTARRAY ALL
49368*1 374*0 1 21*0 1 21*0 1 21*0 1 21*0 1 21*0 24530*1 0 21*1 0 21*1 0 21*1 0 21*1 0 21*1 0 21*1 0 21*1
PRPOR 235
CPOR 0.00045

** ***********************************************************************
** Definition of fluid, components and PVT
** ***********************************************************************
MODEL PR
NC 8 8
COMPNAME 'CO2' 'C1' 'C2' 'C3' 'C4-6' 'C7+' 'Surfact' 'CO2T'
HCFLAG
0 0 0 0 0 0 0 0
TRES 100
VISCOR MODPEDERSEN
MW
4.401000000E+01 1.604300000E+01 3.003651882E+01 4.409700000E+01 7.023714980E+01 2.180000000E+02 427 44.01
AC
0.225 0.013 0.0976462 0.1524 0.224435 0.70397 1.14345 0.225
PCRIT
117.63520927708 73.324333925487 77.391917700469 67.934736787565 56.080118223538 27.185473861337 9.36 117.635
VCRIT
9.400075621E-02 9.800017929E-02 1.470534926E-01 1.999979608E-01 3.014148438E-01 8.499119437E-01 1.516 0.0940008
TCRIT
250.91111609 156.9532596 249.1099632 304.51896827 380.6181688 613.4226548 893.9 250.911
PCHOR
78 77 106.909 150.3 225.618 564.4 965.333 78
SG
0.777793 0.425434 0.552731 0.582594 0.625741 0.852369 0.915 0.777793
TB
-78.45 -161.45 -90.3932 -42.05 27.7747 293.746 471.85 -78.45
OMEGA
0.457236 0.457236 0.457236 0.457236 0.457236 0.457236 0.457236 0.457236
OMEGB
0.0777961 0.0777961 0.0777961 0.0777961 0.0777961 0.0777961 0.0777961 0.0777961
VSHIFT
-0.0453789 -0.182902 -0.126011 -0.105437 0.347695 -0.754778 0 0
HEATING_VALUES
0 844.29 1478.46 2105.16 3293.59 0 5250.01 0
BIN
1.000000000E-01
9.817700916E-02 3.701359105E-03
1.000000000E-01 6.214000000E-03 2.738293998E-03
1.000000000E-01 1.482207968E-02 7.750716921E-03 2.218453386E-03
```

```
1.000000000E-01 4.749600000E-02 3.439155849E-02 2.380100000E-02 1.318230040E-02
0.15 0 0 0 0 0
0 0 0 0 0 0 0

SOLUBILITY HENRY
TRACE-COMP 8
CHEM-EQUIL-SET ON
HENRYC
0 0 0 0 0 0 1e+007 0
REFPH
0 0 0 0 0 0 101.3 0
DER-CHEM-EQUIL ANALYTICAL
DER-REACT-RATE ANALYTICAL
ACTIVITY-MODEL B-DOT
** ***************************************************************************
** Definition of Surfactant
** ***************************************************************************
SALINITY-CALC ON
HENRY-MOD1-CO2
BIN-TDEP-CO2
COMPNAME-SFT 'Surfact'
MASSDENSITY-SFT 978.694
MW-SFT 427
CMC-SFT 6.20611e-006
FADSMAX-SFT 0.05
RM-THRESH-SFT 1e-006
IFTCMC-SFT 0.0116
CHIFT-SFT 0.3
VOLCHG-SFT ON

INTAQU 'Surfact'
** Optimum Salinity=23619.7 ppm
OPTSALIN-SFT 1.05225
** Surfactant concentration=0.05 wt%
INTAQU-VAL 0.00117155
SOLRATIO-SFT

**  Salinity    Ro      Rw
0.345183   7.51646    29.95
0.695888   9.14141   23.9893
1.05225   18.0285   18.0285
1.41441   26.9155   12.0678
1.7825    35.8025   9.71286
2.15667   44.6894   7.13679
2.53708   53.5764   5.08548
** Optimum Salinity=23619.7 ppm
OPTSALIN-SFT 1.05225
** Surfactant concentration=0.1 wt%
INTAQU-VAL 0.00234426
SOLRATIO-SFT
**  Salinity      Ro      Rw
0.345183   8.75936   30.4061
0.695888   11.3228   24.8494
1.05225   19.2927   19.2927
1.41441   27.2625   13.7361
1.7825    35.2324   10.8465
2.15667   43.2022   8.87357
2.53708    51.172   6.59859
** Optimum Salinity=23619.7 ppm
OPTSALIN-SFT 1.05225
** Surfactant concentration=0.2 wt%
INTAQU-VAL 0.00469323
SOLRATIO-SFT
**  Salinity      Ro      Rw
0.345183     12.7   24.4536
0.695888   14.9071   22.4189
1.05225   20.3841   20.3841
1.41441   25.8611   18.3494
1.7825    31.338   10.296
2.15667   36.8149   9.69762
2.53708   42.2919   7.14286
** Optimum Salinity=23619.7 ppm
OPTSALIN-SFT 1.05225
** Surfactant concentration=0.3 wt%
INTAQU-VAL 0.0070469
SOLRATIO-SFT
**  Salinity      Ro      Rw
0.345183   8.05823   31.9725
0.695888     10.6   25.3086
1.05225   18.6447   18.6447
1.41441   26.6893   11.9808
1.7825    34.7339   7.80869
2.15667   42.7785   6.91164
2.53708   50.8231   5.80585
** ***************************************************************************
** Definition of Aqueous components Polymer and Salt
** ***************************************************************************
NC-AQUEOUS 2
COMPNAME-AQUEOUS
'Polymer' 'Na+'
MW-AQUEOUS
8000 22.9898
ION-SIZE-AQUEOUS
4 4
```

```
CHARGE-AQUEOUS
0 1
COMPNAME-POLYMER
'Polymer'
COMPNAME-SAL 'Na+'
AQUEOUS-VISCOSITY POLYMER NONLIN1
VISCTABLE-AQUEOUS
**    temp
10   327.762 1.87031
20   254.014 1.44948
30   204.057 1.16441
40   168.536 0.961718
50   142.28 0.811895
60   122.253 0.697615
70   106.579 0.608174
80   94.0498 0.536677
90   83.8579 0.478519
100  75.4479 0.430529
110  68.4266 0.390463
120  62.5092 0.356697
130  57.4852 0.328028
140  53.196 0.303553
150  49.5206 0.28258
160  46.365 0.264573
170  43.6559 0.249114
180  41.3353 0.235872
190  39.3575 0.224586
200  37.6863 0.215049
VISCTABLE-H2O
**    temp
10   1.87031
20   1.44948
30   1.16441
40   0.961718
50   0.811895
60   0.697615
70   0.608174
80   0.536677
90   0.478519
100  0.430529
110  0.390463
120  0.356697
130  0.328028
140  0.303553
150  0.28258
160  0.264573
170  0.249114
180  0.235872
190  0.224586
200  0.215049
VSMIXENDP 'Polymer' 0 6.77779e-006
VSMIXFUNC 'Polymer' 0 0.350146 0.628434 0.765665 0.846371 0.899654 0.952937 0.989315 0.992877 0.996438 1
** ***************************************************************************
** Definition of Relative permeability curves
** ***************************************************************************
ROCKFLUID
INTERP_ENDS ON
RPT 1
INTCOMP LOGCAPNWO
KRINTRP 1
INTCOMP_VAL -5
**     Sw       krw        krow
SWT
0.200000    0.00000    0.900000
0.215909 3.818182E-05    0.859530
0.231818 7.636364E-05    0.819991
0.247727 1.145455E-04    0.781384
0.263636 1.527273E-04    0.743708
0.279545 1.909091E-04    0.706964
0.295455 2.290909E-04    0.671151
0.311364 6.559091E-04    0.636270
0.327273 1.238182E-03    0.602320
0.343182 1.820455E-03    0.569301
0.359091 2.402727E-03    0.537214
0.375000 2.985000E-03    0.506058
0.390909 3.567273E-03    0.475833
0.406818 4.997727E-03    0.446539
0.422727 7.559091E-03    0.418177
0.438636 1.012045E-02    0.390745
0.454545 1.268182E-02    0.364245
0.470455 1.524318E-02    0.338676
0.486364 1.780455E-02    0.314038
0.502273 2.095455E-02    0.290330
0.518182 2.763636E-02    0.267554
0.534091 3.431818E-02    0.245709
0.550000 4.100000E-02    0.224794
0.565909 4.768182E-02    0.204810
0.581818 5.436364E-02    0.185757
0.597727 6.104545E-02    0.167634
0.613636 7.427273E-02    0.150442
0.629545 8.859091E-02    0.134180
0.645455    0.102909    0.118849
0.661364    0.117227    0.104448
0.677273    0.131545 9.097787E-02
```

```
0.693182    0.145864  7.843752E-02
0.709091    0.166909  6.682727E-02
0.725000    0.193000  5.614701E-02
0.740909    0.219091  4.639664E-02
0.756818    0.245182  3.757605E-02
0.772727    0.271273  2.968509E-02
0.788636    0.297364  2.272364E-02
0.804545    0.328227  1.669152E-02
0.820455    0.371023  1.158854E-02
0.836364    0.413818  7.414476E-03
0.852273    0.456614  4.169057E-03
0.868182    0.499409  1.851921E-03
0.884091    0.542205  4.625563E-04
0.900000    0.585000     0.00000
0.915909    0.651023     0.00000
0.931818    0.717045     0.00000
0.947727    0.783068     0.00000
0.963636    0.849091     0.00000
0.979545    0.915114     0.00000
1.00000     1.00000      0.00000
**      Sl       krg        krog
SLT

0.200000    0.900000     0.00000
0.215909    0.859530  1.338467E-02
0.231818    0.819991  2.818149E-02
0.247727    0.781384  4.356276E-02
0.263636    0.743708  5.933628E-02
0.279545    0.706964  7.540807E-02
0.295455    0.671151  9.172161E-02
0.311364    0.636270     0.108239
0.327273    0.602320     0.124933
0.343182    0.569301     0.141783
0.359091    0.537214     0.158772
0.375000    0.506058     0.175888
0.390909    0.475833     0.193120
0.406818    0.446539     0.210459
0.422727    0.418177     0.227898
0.438636    0.390745     0.245429
0.454545    0.364245     0.263047
0.470455    0.338676     0.280747
0.486364    0.314038     0.298524
0.502273    0.290330     0.316375
0.518182    0.267554     0.334295
0.534091    0.245709     0.352283
0.550000    0.224794     0.370334
0.565909    0.204810     0.388446
0.581818    0.185757     0.406616
0.597727    0.167634     0.424843
0.613636    0.150442     0.443123
0.629545    0.134180     0.461456
0.645455    0.118849     0.479840
0.661364    0.104448     0.498272
0.677273  9.097787E-02     0.516752
0.693182  7.843752E-02     0.535277
0.709091  6.682727E-02     0.553846
0.725000  5.614701E-02     0.572459
0.740909  4.639664E-02     0.591114
0.756818  3.757605E-02     0.609809
0.772727  2.968509E-02     0.628544
0.788636  2.272364E-02     0.647318
0.804545  1.669152E-02     0.666129
0.820455  1.158854E-02     0.684977
0.836364  7.414476E-03     0.703861
0.852273  4.169057E-03     0.722780
0.868182  1.851921E-03     0.741733
0.884091  4.625563E-04     0.760720
0.900000    0.00000        0.779739
0.915909    0.00000        0.798791
0.931818    0.00000        0.817874
0.947727    0.00000        0.836988
0.963636    0.00000        0.856132
0.979545    0.00000        0.875306
1.00000     0.00000        0.900000
KRINTRP 2
INTCOMP_VAL -3.5
**      Sw       krw        krow
SWT

0.2        0        0.95
0.217045  6.5268e-005     0.907281
0.229829  0.000114219     0.87598
0.244744  0.000171329     0.840076
0.259659  0.000228438     0.804909
0.274573  0.000285547      0.77048
0.289489  0.00034266      0.736788
0.304404  0.000482797     0.703835
0.319319  0.00112121      0.671619
0.336364  0.00211655      0.635782
0.349148  0.00286307      0.609643
0.364063  0.00373395       0.57976
0.378977  0.00460487      0.550616
0.394805  0.00552915      0.520498
0.408807  0.00670923      0.494538
```

```
0.423721   0.00909049   0.467605
0.438636   0.0129215    0.441409
0.455681   0.0173       0.412453
0.468466   0.020584     0.391472
0.483381   0.0244148    0.367612
0.498296   0.0282459    0.344488
0.513211   0.0324543    0.3221
0.531169   0.040715     0.296156
0.54304    0.048669     0.279537
0.557955   0.0586636    0.259359
0.575      0.0700855    0.237282
0.589611   0.0798759    0.219201
0.602698   0.088646     0.203619
0.617614   0.0986409    0.186512
0.632529   0.112831     0.170141
0.648052   0.133955     0.153895
0.662358   0.154497     0.139611
0.677273   0.175913     0.125451
0.694319   0.200388     0.11025
0.707102   0.218744     0.0995875
0.722017   0.24016      0.0877594
0.736932   0.267327     0.0766678
0.751846   0.302038     0.0663126
0.766761   0.341064     0.0566935
0.784416   0.387258     0.0463137
0.79659    0.419115     0.0396636
0.813636   0.463715     0.0313342
0.830681   0.508315     0.0239861
0.842857   0.546        0.0194379
0.85625    0.59765      0.0149255
0.871164   0.661656     0.0105802
0.88608    0.72567      0.00697006
0.901298   0.790985     0.00405143
0.920779   0.87459      0.00153578
0.932955   0.926846     0.000488253
0.95       1            0
1          1            0
**         Sl    krg    krog
SLT

0.2        0.9          0
0.215909   0.85953      0.0141283
0.227841   0.829876     0.0258425
0.241761   0.795862     0.0398945
0.255682   0.762546     0.0543079
0.269602   0.729929     0.0689944
0.283523   0.698009     0.0839032
0.297443   0.666791     0.0989964
0.311364   0.63627      0.114253
0.327273   0.60232      0.131873
0.339205   0.577556     0.145214
0.353125   0.549247     0.160867
0.367045   0.521636     0.176625
0.381818   0.493103     0.193455
0.394886   0.468509     0.208425
0.408806   0.442994     0.224452
0.422727   0.418177     0.240559
0.438636   0.390745     0.259064
0.450569   0.370868     0.273012
0.464489   0.348264     0.289337
0.47841    0.326357     0.305726
0.49233    0.305148     0.322174
0.50625    0.284637     0.33868
0.52017    0.264824     0.35524
0.534091   0.245709     0.371855
0.55       0.224794     0.390908
0.563637   0.207664     0.407295
0.575852   0.192902     0.422013
0.589773   0.176695     0.438827
0.603693   0.161186     0.455682
0.618182   0.145796     0.47327
0.631534   0.132263     0.489519
0.645455   0.118849     0.506498
0.661364   0.104448     0.525954
0.673295   0.0943461    0.540583
0.687215   0.0831405    0.557681
0.701136   0.0726327    0.574814
0.715056   0.0628224    0.591982
0.728977   0.0537097    0.609185
0.742898   0.0452938    0.626421
0.756818   0.0375761    0.643688
0.772727   0.0296851    0.663463
0.78466    0.0244638    0.678327
0.8        0.0184149    0.697463
0.8125     0.01414      0.713084
0.82642    0.0100234    0.730506
0.840341   0.00660322   0.747958
0.854545   0.00383819   0.765792
0.868182   0.00185192   0.782941
0.884091   0.000462556  0.802982
0.9        0            0.823058
0.915909   0            0.843169
0.931818   0            0.863312
0.947727   0            0.883488
```

```
0.963637        0   0.903695
0.981818        0   0.926831
1        0     0.95
KRINTRP 3
INTCOMP_VAL -2
**      Sw     krw     krow
SWT

0.2      0      0.9
0.999      1      0
1      1      0
**      Sl      krg      krog
SLT

0.200000    0.900000      0.00000
0.215909    0.859530  1.338467E-02
0.231818    0.819991  2.818149E-02
0.247727    0.781384  4.356276E-02
0.263636    0.743708  5.933628E-02
0.279545    0.706964  7.540807E-02
0.295455    0.671151  9.172161E-02
0.311364    0.636270    0.108239
0.327273    0.602320    0.124933
0.343182    0.569301    0.141783
0.359091    0.537214    0.158772
0.375000    0.506058    0.175888
0.390909    0.475833    0.193120
0.406818    0.446539    0.210459
0.422727    0.418177    0.227898
0.438636    0.390745    0.245429
0.454545    0.364245    0.263047
0.470455    0.338676    0.280747
0.486364    0.314038    0.298524
0.502273    0.290330    0.316375
0.518182    0.267554    0.334295
0.534091    0.245709    0.352283
0.550000    0.224794    0.370334
0.565909    0.204810    0.388446
0.581818    0.185757    0.406616
0.597727    0.167634    0.424843
0.613636    0.150442    0.443123
0.629545    0.134180    0.461456
0.645455    0.118849    0.479840
0.661364    0.104448    0.498272
0.677273  9.097787E-02    0.516752
0.693182  7.843752E-02    0.535277
0.709091  6.682727E-02    0.553846
0.725000  5.614701E-02    0.572459
0.740909  4.639664E-02    0.591114
0.756818  3.757605E-02    0.609809
0.772727  2.968509E-02    0.628544
0.788636  2.272364E-02    0.647318
0.804545  1.669152E-02    0.666129
0.820455  1.158854E-02    0.684977
0.836364  7.414476E-03    0.703861
0.852273  4.169057E-03    0.722780
0.868182  1.851921E-03    0.741733
0.884091  4.625563E-04    0.760720
0.900000    0.00000    0.779739
0.915909    0.00000    0.798791
0.931818    0.00000    0.817874
0.947727    0.00000    0.836988
0.963636    0.00000    0.856132
0.979545    0.00000    0.875306
1.00000    0.00000    0.900000
** ************************************************************************
** Definition of Surfactant adsorption
** ************************************************************************
ADSORBTMAXA 'Surfact' 0.00168787
ADSTABA 'Surfact'
**    Mole Fraction    Adsorption
0        0
8.45648024e-005  0.00168618267
ROCKDEN CON        2710
** ************************************************************************
** Definition of Initialization parameters
** ************************************************************************
INITIAL
VERTICAL BLOCK_CENTER COMP
REFPRES
49299.6
REFDEPTH
209.999815687411
DWOC
300
SWOC
1
CDEPTH
209.999815687411
ZDEPTH
1
5.0 0.6377901971 0.2146591842 0.04769449603 0.0290114847 0.04028188729 0.02956275073 0.0 0.001
20.0 0.637534031 0.2140058359 0.04767402252 0.02906046498 0.04052327897 0.03020236656 0.0 0.001
50.0 0.6369442071 0.2126603864 0.04763201828 0.02916227853 0.04102589031 0.03157521937 0.0 0.001
```

90.0 0.6359634387 0.210768697 0.04757333909 0.02930763774 0.04174504015 0.03364184736 0.0 0.001
100.0 0.635676129 0.210274477 0.04755808399 0.02934604793 0.04193530526 0.0342099568 0.0 0.001
150.0 0.6339006329 0.2076308014 0.04747701015 0.02955461378 0.04296941727 0.03746752457 0.0 0.0009999999991
180.0 0.632458846 0.2058517074 0.04742291513 0.02969791938 0.04368022742 0.03988838462 0.0 0.001
190.0 0.6318870565 0.2052116983 0.04740353107 0.02975004401 0.04393868905 0.04080898109 0.0 0.001
200.0 0.6312560955 0.2045411146 0.04738325518 0.0298049763 0.04421098022 0.04180357824 0.0 0.001
209.9998156874110 0.548701511 0.1657320304 0.04467084796 0.03158315245 0.05703144588 0.1512810123 0.0 0.001
210.0 0.5487015024 0.1657320235 0.04467084702 0.03158315227 0.05703144762 0.1512810272 0.0 0.001
220.0 0.5482558752 0.1653645424 0.04462069346 0.03157362302 0.05712402298 0.1520612429 0.0 0.001
230.0 0.5478441308 0.1650113418 0.04457224772 0.03156421743 0.05721382259 0.1527942397 0.0 0.001
240.0 0.5474625582 0.1646708622 0.04452532995 0.03155493016 0.0573011809 0.1534851386 0.0 0.001
250.0 0.5471080754 0.1643418081 0.04447979028 0.03154575624 0.05738637412 0.1541381958 0.0 0.001
270.0 0.5464703973 0.1637137786 0.04439235808 0.03152773032 0.05755115374 0.1553445819 0.0 0.001
280.0 0.5461831036 0.1634130793 0.04435026476 0.03151887003 0.0576311 0242 0.1559035799 0.0 0.001
290.0 0.5459145688 0.163120301 0.04430914158 0.03151010646 0.05770962308 0.1564362591 0.0 0.001
300.0 0.5456633611 0.162834841 0.04426891786 0.03150143612 0.05778684055 0.1569446034 0.0 0.001
330.0 0.5450018214 0.1620173666 0.04415305448 0.03147595293 0.05801170162 0.1583401029 0.0 0.001
340.0 0.5448086849 0.1617564454 0.04411587075 0.03146762489 0.05808467636 0.1587666977 0.0 0.001

MOLALITY-AQUEOUS-PRIMARY
0 1.7825
DATUMDEPTH 209.999815687411 INITIAL
** **
** Definition of Numerical Solution Parameters
** **
NUMERICAL
DTMAX 5
DTMIN 1e-005
NEWTONCYC 20
AIM STAB AND-THRESH 1 0.005
NORM PRESS 200
NORM SATUR 0.1
NORM GMOLAR 0.1
MAXCHANGE PRESS 50000
MAXCHANGE SATUR 1
MAXCHANGE GMOLAR 1
CONVERGE MAXRES TIGHTER
NORTH 200
ITERMAX 200
RUN
DATE 2014 1 1
**
**
**
** **
** Well Definitions
** **
WELL 'PROD-1'
PRODUCER 'PROD-1'
OPERATE MAX STL 6359.49 CONT REPEAT
OPERATE MIN BHP 20000 CONT REPEAT
MONITOR MIN STO 10.0 STOP
MONITOR WCUT 0.99 STOP
**   rad geofac wfrac skin
GEOMETRY K 0.2 0.37 1.0 0.0
PERF   GEOA 'PROD-1'
** UBA   ff   Status Connection
4 4 1   1.0 OPEN   FLOW-TO 'SURFACE'
4 4 81   1.0 OPEN   FLOW-TO 1
4 4 82   1.0 OPEN   FLOW-TO 2
4 4 83   1.0 OPEN   FLOW-TO 3
4 4 84   1.0 OPEN   FLOW-TO 4
4 4 85   1.0 OPEN   FLOW-TO 5
4 4 86   1.0 OPEN   FLOW-TO 6
4 4 87   1.0 OPEN   FLOW-TO 7
4 4 88   1.0 OPEN   FLOW-TO 8
4 4 89   1.0 OPEN   FLOW-TO 9
4 4 90   1.0 OPEN   FLOW-TO 10
4 4 91   1.0 OPEN   FLOW-TO 11
4 4 92   1.0 OPEN   FLOW-TO 12
4 4 93   1.0 OPEN   FLOW-TO 13
4 4 94   1.0 OPEN   FLOW-TO 14
4 4 95   1.0 OPEN   FLOW-TO 15
4 4 96   1.0 OPEN   FLOW-TO 16
4 4 97   1.0 OPEN   FLOW-TO 17
4 4 98   1.0 OPEN   FLOW-TO 18
4 4 99   1.0 OPEN   FLOW-TO 19
4 4 100   1.0 OPEN   FLOW-TO 20
4 4 101   1.0 OPEN   FLOW-TO 21
4 4 102   1.0 OPEN   FLOW-TO 22
4 4 103   1.0 OPEN   FLOW-TO 23
4 4 104   1.0 OPEN   FLOW-TO 24
4 4 105   1.0 OPEN   FLOW-TO 25
4 4 106   1.0 OPEN   FLOW-TO 26
4 4 107   1.0 OPEN   FLOW-TO 27
4 4 108   1.0 OPEN   FLOW-TO 28
4 4 109   1.0 OPEN   FLOW-TO 29
4 4 110   1.0 OPEN   FLOW-TO 30
4 4 111   1.0 OPEN   FLOW-TO 31
4 4 112   1.0 OPEN   FLOW-TO 32
4 4 113   1.0 OPEN   FLOW-TO 33
4 4 114   1.0 OPEN   FLOW-TO 34
4 4 115   1.0 OPEN   FLOW-TO 35

```
4 4 116      1.0 OPEN   FLOW-TO 36
4 4 117      1.0 OPEN   FLOW-TO 37
4 4 118      1.0 OPEN   FLOW-TO 38
4 4 119      1.0 OPEN   FLOW-TO 39
4 4 120      1.0 OPEN   FLOW-TO 40
4 4 121      1.0 OPEN   FLOW-TO 41
4 4 122      1.0 OPEN   FLOW-TO 42
4 4 123      1.0 OPEN   FLOW-TO 43
4 4 124      1.0 OPEN   FLOW-TO 44
4 4 125      1.0 OPEN   FLOW-TO 45
4 4 126      1.0 OPEN   FLOW-TO 46
4 4 127      1.0 OPEN   FLOW-TO 47
4 4 128      1.0 OPEN   FLOW-TO 48
4 4 129      1.0 OPEN   FLOW-TO 49
4 4 130      1.0 OPEN   FLOW-TO 50
4 4 131      1.0 OPEN   FLOW-TO 51
4 4 132      1.0 OPEN   FLOW-TO 52
4 4 133      1.0 OPEN   FLOW-TO 53
4 4 134      1.0 OPEN   FLOW-TO 54
4 4 135      1.0 OPEN   FLOW-TO 55
4 4 136      1.0 OPEN   FLOW-TO 56
4 4 137      1.0 OPEN   FLOW-TO 57
4 4 138      1.0 OPEN   FLOW-TO 58
4 4 139      1.0 OPEN   FLOW-TO 59
4 4 140      1.0 OPEN   FLOW-TO 60
4 4 141      1.0 OPEN   FLOW-TO 61
4 4 142      1.0 OPEN   FLOW-TO 62
4 4 143      1.0 OPEN   FLOW-TO 63
4 4 144      1.0 OPEN   FLOW-TO 64
4 4 145      1.0 OPEN   FLOW-TO 65
4 4 146      1.0 OPEN   FLOW-TO 66
4 4 147      1.0 OPEN   FLOW-TO 67
4 4 148      1.0 OPEN   FLOW-TO 68
4 4 149      1.0 OPEN   FLOW-TO 69
4 4 150      1.0 OPEN   FLOW-TO 70 REFLAYER
OPEN 'PROD-1'
**
**
WELL 'PROD-2'
PRODUCER 'PROD-2'
OPERATE  MAX  STL 6359.49 CONT REPEAT
OPERATE MIN BHP 20000 CONT REPEAT
MONITOR  MIN STO 10.0 STOP
MONITOR WCUT 0.96137321 STOP
**      rad geofac wfrac skin
GEOMETRY K 0.2 0.37 1.0 0.0
PERF    GEOA 'PROD-2'
** UBA        ff       Status Connection
4 19 1       1.0 OPEN   FLOW-TO 'SURFACE'
4 19 81      1.0 OPEN   FLOW-TO 1
4 19 82      1.0 OPEN   FLOW-TO 2
4 19 83      1.0 OPEN   FLOW-TO 3
4 19 84      1.0 OPEN   FLOW-TO 4
4 19 85      1.0 OPEN   FLOW-TO 5
4 19 86      1.0 OPEN   FLOW-TO 6
4 19 87      1.0 OPEN   FLOW-TO 7
4 19 88      1.0 OPEN   FLOW-TO 8
4 19 89      1.0 OPEN   FLOW-TO 9
4 19 90      1.0 OPEN   FLOW-TO 10
4 19 91      1.0 OPEN   FLOW-TO 11
4 19 92      1.0 OPEN   FLOW-TO 12
4 19 93      1.0 OPEN   FLOW-TO 13
4 19 94      1.0 OPEN   FLOW-TO 14
4 19 95      1.0 OPEN   FLOW-TO 15
4 19 96      1.0 OPEN   FLOW-TO 16
4 19 97      1.0 OPEN   FLOW-TO 17
4 19 98      1.0 OPEN   FLOW-TO 18
4 19 99      1.0 OPEN   FLOW-TO 19
4 19 100     1.0 OPEN   FLOW-TO 20
4 19 101     1.0 OPEN   FLOW-TO 21
4 19 102     1.0 OPEN   FLOW-TO 22
4 19 103     1.0 OPEN   FLOW-TO 23
4 19 104     1.0 OPEN   FLOW-TO 24
4 19 105     1.0 OPEN   FLOW-TO 25
4 19 106     1.0 OPEN   FLOW-TO 26
4 19 107     1.0 OPEN   FLOW-TO 27
4 19 108     1.0 OPEN   FLOW-TO 28
4 19 109     1.0 OPEN   FLOW-TO 29
4 19 110     1.0 OPEN   FLOW-TO 30
4 19 111     1.0 OPEN   FLOW-TO 31
4 19 112     1.0 OPEN   FLOW-TO 32
4 19 113     1.0 OPEN   FLOW-TO 33
4 19 114     1.0 OPEN   FLOW-TO 34
4 19 115     1.0 OPEN   FLOW-TO 35
4 19 116     1.0 OPEN   FLOW-TO 36
4 19 117     1.0 OPEN   FLOW-TO 37
4 19 118     1.0 OPEN   FLOW-TO 38
4 19 119     1.0 OPEN   FLOW-TO 39
4 19 120     1.0 OPEN   FLOW-TO 40
4 19 121     1.0 OPEN   FLOW-TO 41
4 19 122     1.0 OPEN   FLOW-TO 42
4 19 123     1.0 OPEN   FLOW-TO 43
4 19 124     1.0 OPEN   FLOW-TO 44
4 19 125     1.0 OPEN   FLOW-TO 45
```

```
4 19 126     1.0 OPEN   FLOW-TO 46
4 19 127     1.0 OPEN   FLOW-TO 47
4 19 128     1.0 OPEN   FLOW-TO 48
4 19 129     1.0 OPEN   FLOW-TO 49
4 19 130     1.0 OPEN   FLOW-TO 50
4 19 131     1.0 OPEN   FLOW-TO 51
4 19 132     1.0 OPEN   FLOW-TO 52
4 19 133     1.0 OPEN   FLOW-TO 53
4 19 134     1.0 OPEN   FLOW-TO 54
4 19 135     1.0 OPEN   FLOW-TO 55
4 19 136     1.0 OPEN   FLOW-TO 56
4 19 137     1.0 OPEN   FLOW-TO 57
4 19 138     1.0 OPEN   FLOW-TO 58
4 19 139     1.0 OPEN   FLOW-TO 59
4 19 140     1.0 OPEN   FLOW-TO 60
4 19 141     1.0 OPEN   FLOW-TO 61
4 19 142     1.0 OPEN   FLOW-TO 62
4 19 143     1.0 OPEN   FLOW-TO 63
4 19 144     1.0 OPEN   FLOW-TO 64
4 19 145     1.0 OPEN   FLOW-TO 65
4 19 146     1.0 OPEN   FLOW-TO 66
4 19 147     1.0 OPEN   FLOW-TO 67
4 19 148     1.0 OPEN   FLOW-TO 68
4 19 149     1.0 OPEN   FLOW-TO 69
4 19 150     1.0 OPEN   FLOW-TO 70 REFLAYER
OPEN 'PROD-2'
**
**
WELL  'PROD-3'
PRODUCER 'PROD-3'
OPERATE MAX STL 6359.49 CONT REPEAT
OPERATE MIN BHP 20000 CONT REPEAT
MONITOR  MIN  STO 10.0 STOP
MONITOR WCUT 0.96722537 STOP
**       rad geofac wfrac skin
GEOMETRY K 0.2 0.37 1.0 0.0
PERF    GEOA 'PROD-3'
** UBA         ff       Status Connection
17 4 1       1.0 OPEN   FLOW-TO 'SURFACE'
17 4 81      1.0 OPEN   FLOW-TO 1
17 4 82      1.0 OPEN   FLOW-TO 2
17 4 83      1.0 OPEN   FLOW-TO 3
17 4 84      1.0 OPEN   FLOW-TO 4
17 4 85      1.0 OPEN   FLOW-TO 5
17 4 86      1.0 OPEN   FLOW-TO 6
17 4 87      1.0 OPEN   FLOW-TO 7
17 4 88      1.0 OPEN   FLOW-TO 8
17 4 89      1.0 OPEN   FLOW-TO 9
17 4 90      1.0 OPEN   FLOW-TO 10
17 4 91      1.0 OPEN   FLOW-TO 11
17 4 92      1.0 OPEN   FLOW-TO 12
17 4 93      1.0 OPEN   FLOW-TO 13
17 4 94      1.0 OPEN   FLOW-TO 14
17 4 95      1.0 OPEN   FLOW-TO 15
17 4 96      1.0 OPEN   FLOW-TO 16
17 4 97      1.0 OPEN   FLOW-TO 17
17 4 98      1.0 OPEN   FLOW-TO 18
17 4 99      1.0 OPEN   FLOW-TO 19
17 4 100     1.0 OPEN   FLOW-TO 20
17 4 101     1.0 OPEN   FLOW-TO 21
17 4 102     1.0 OPEN   FLOW-TO 22
17 4 103     1.0 OPEN   FLOW-TO 23
17 4 104     1.0 OPEN   FLOW-TO 24
17 4 105     1.0 OPEN   FLOW-TO 25
17 4 106     1.0 OPEN   FLOW-TO 26
17 4 107     1.0 OPEN   FLOW-TO 27
17 4 108     1.0 OPEN   FLOW-TO 28
17 4 109     1.0 OPEN   FLOW-TO 29
17 4 110     1.0 OPEN   FLOW-TO 30
17 4 111     1.0 OPEN   FLOW-TO 31
17 4 112     1.0 OPEN   FLOW-TO 32
17 4 113     1.0 OPEN   FLOW-TO 33
17 4 114     1.0 OPEN   FLOW-TO 34
17 4 115     1.0 OPEN   FLOW-TO 35
17 4 116     1.0 OPEN   FLOW-TO 36
17 4 117     1.0 OPEN   FLOW-TO 37
17 4 118     1.0 OPEN   FLOW-TO 38
17 4 119     1.0 OPEN   FLOW-TO 39
17 4 120     1.0 OPEN   FLOW-TO 40
17 4 121     1.0 OPEN   FLOW-TO 41
17 4 122     1.0 OPEN   FLOW-TO 42
17 4 123     1.0 OPEN   FLOW-TO 43
17 4 124     1.0 OPEN   FLOW-TO 44
17 4 125     1.0 OPEN   FLOW-TO 45
17 4 126     1.0 OPEN   FLOW-TO 46
17 4 127     1.0 OPEN   FLOW-TO 47
17 4 128     1.0 OPEN   FLOW-TO 48
17 4 129     1.0 OPEN   FLOW-TO 49
17 4 130     1.0 OPEN   FLOW-TO 50
17 4 131     1.0 OPEN   FLOW-TO 51
17 4 132     1.0 OPEN   FLOW-TO 52
17 4 133     1.0 OPEN   FLOW-TO 53
17 4 134     1.0 OPEN   FLOW-TO 54
17 4 135     1.0 OPEN   FLOW-TO 55
```

```
17 4 136    1.0 OPEN   FLOW-TO 56
17 4 137    1.0 OPEN   FLOW-TO 57
17 4 138    1.0 OPEN   FLOW-TO 58
17 4 139    1.0 OPEN   FLOW-TO 59
17 4 140    1.0 OPEN   FLOW-TO 60
17 4 141    1.0 OPEN   FLOW-TO 61
17 4 142    1.0 OPEN   FLOW-TO 62
17 4 143    1.0 OPEN   FLOW-TO 63
17 4 144    1.0 OPEN   FLOW-TO 64
17 4 145    1.0 OPEN   FLOW-TO 65
17 4 146    1.0 OPEN   FLOW-TO 66
17 4 147    1.0 OPEN   FLOW-TO 67
17 4 148    1.0 OPEN   FLOW-TO 68
17 4 149    1.0 OPEN   FLOW-TO 69
17 4 150    1.0 OPEN   FLOW-TO 70 REFLAYER
OPEN 'PROD-3'
**
**
WELL 'PROD-4'
PRODUCER 'PROD-4'
OPERATE  MAX  STL 6359.49  CONT REPEAT
OPERATE  MIN BHP 20000 CONT REPEAT
MONITOR  MIN  STO  10.0  STOP
MONITOR  WCUT 0.70876725 STOP
**      rad geofac wfrac skin
GEOMETRY K  0.2  0.37  1.0  0.0
PERF    GEOA 'PROD-4'
** UBA           ff      Status Connection
17 19 1      1.0 OPEN   FLOW-TO 'SURFACE'
17 19 81     1.0 OPEN   FLOW-TO 1
17 19 82     1.0 OPEN   FLOW-TO 2
17 19 83     1.0 OPEN   FLOW-TO 3
17 19 84     1.0 OPEN   FLOW-TO 4
17 19 85     1.0 OPEN   FLOW-TO 5
17 19 86     1.0 OPEN   FLOW-TO 6
17 19 87     1.0 OPEN   FLOW-TO 7
17 19 88     1.0 OPEN   FLOW-TO 8
17 19 89     1.0 OPEN   FLOW-TO 9
17 19 90     1.0 OPEN   FLOW-TO 10
17 19 91     1.0 OPEN   FLOW-TO 11
17 19 92     1.0 OPEN   FLOW-TO 12
17 19 93     1.0 OPEN   FLOW-TO 13
17 19 94     1.0 OPEN   FLOW-TO 14
17 19 95     1.0 OPEN   FLOW-TO 15
17 19 96     1.0 OPEN   FLOW-TO 16
17 19 97     1.0 OPEN   FLOW-TO 17
17 19 98     1.0 OPEN   FLOW-TO 18
17 19 99     1.0 OPEN   FLOW-TO 19
17 19 100    1.0 OPEN   FLOW-TO 20
17 19 101    1.0 OPEN   FLOW-TO 21
17 19 102    1.0 OPEN   FLOW-TO 22
17 19 103    1.0 OPEN   FLOW-TO 23
17 19 104    1.0 OPEN   FLOW-TO 24
17 19 105    1.0 OPEN   FLOW-TO 25
17 19 106    1.0 OPEN   FLOW-TO 26
17 19 107    1.0 OPEN   FLOW-TO 27
17 19 108    1.0 OPEN   FLOW-TO 28
17 19 109    1.0 OPEN   FLOW-TO 29
17 19 110    1.0 OPEN   FLOW-TO 30
17 19 111    1.0 OPEN   FLOW-TO 31
17 19 112    1.0 OPEN   FLOW-TO 32
17 19 113    1.0 OPEN   FLOW-TO 33
17 19 114    1.0 OPEN   FLOW-TO 34
17 19 115    1.0 OPEN   FLOW-TO 35
17 19 116    1.0 OPEN   FLOW-TO 36
17 19 117    1.0 OPEN   FLOW-TO 37
17 19 118    1.0 OPEN   FLOW-TO 38
17 19 119    1.0 OPEN   FLOW-TO 39
17 19 120    1.0 OPEN   FLOW-TO 40
17 19 121    1.0 OPEN   FLOW-TO 41
17 19 122    1.0 OPEN   FLOW-TO 42
17 19 123    1.0 OPEN   FLOW-TO 43
17 19 124    1.0 OPEN   FLOW-TO 44
17 19 125    1.0 OPEN   FLOW-TO 45
17 19 126    1.0 OPEN   FLOW-TO 46
17 19 127    1.0 OPEN   FLOW-TO 47
17 19 128    1.0 OPEN   FLOW-TO 48
17 19 129    1.0 OPEN   FLOW-TO 49
17 19 130    1.0 OPEN   FLOW-TO 50
17 19 131    1.0 OPEN   FLOW-TO 51
17 19 132    1.0 OPEN   FLOW-TO 52
17 19 133    1.0 OPEN   FLOW-TO 53
17 19 134    1.0 OPEN   FLOW-TO 54
17 19 135    1.0 OPEN   FLOW-TO 55
17 19 136    1.0 OPEN   FLOW-TO 56
17 19 137    1.0 OPEN   FLOW-TO 57
17 19 138    1.0 OPEN   FLOW-TO 58
17 19 139    1.0 OPEN   FLOW-TO 59
17 19 140    1.0 OPEN   FLOW-TO 60
17 19 141    1.0 OPEN   FLOW-TO 61
17 19 142    1.0 OPEN   FLOW-TO 62
17 19 143    1.0 OPEN   FLOW-TO 63
17 19 144    1.0 OPEN   FLOW-TO 64
17 19 145    1.0 OPEN   FLOW-TO 65
```

```
17 19 146    1.0 OPEN   FLOW-TO 66
17 19 147    1.0 OPEN   FLOW-TO 67
17 19 148    1.0 OPEN   FLOW-TO 68
17 19 149    1.0 OPEN   FLOW-TO 69
17 19 150    1.0 OPEN   FLOW-TO 70 REFLAYER
OPEN 'PROD-4'
**
**
**
WELL  'INJ'
INJECTOR 'INJ'
INCOMP AQUEOUS 0.0 0.0 0.0 0.0 0.0 0.0 0.0017517752 0.0 0.00037797 1.6091147
OPERATE MAX BHP 64121.2401 CONT
OPERATE MAX STW 28000.0 CONT
**     rad geofac wfrac skin
GEOMETRY K 0.1 0.37 1.0 0.0
PERF    GEOA 'INJ'
** UBA          ff       Status Connection
10 10 1      1.0 OPEN   FLOW-FROM 'SURFACE'
10 10 81     1.0 OPEN   FLOW-FROM 1
10 10 82     1.0 OPEN   FLOW-FROM 2
10 10 83     1.0 OPEN   FLOW-FROM 3
10 10 84     1.0 OPEN   FLOW-FROM 4
10 10 85     1.0 OPEN   FLOW-FROM 5
10 10 86     1.0 OPEN   FLOW-FROM 6
10 10 87     1.0 OPEN   FLOW-FROM 7
10 10 88     1.0 OPEN   FLOW-FROM 8
10 10 89     1.0 OPEN   FLOW-FROM 9
10 10 90     1.0 OPEN   FLOW-FROM 10
10 10 91     1.0 OPEN   FLOW-FROM 11
10 10 92     1.0 OPEN   FLOW-FROM 12
10 10 93     1.0 OPEN   FLOW-FROM 13
10 10 94     1.0 OPEN   FLOW-FROM 14
10 10 95     1.0 OPEN   FLOW-FROM 15
10 10 96     1.0 OPEN   FLOW-FROM 16
10 10 97     1.0 OPEN   FLOW-FROM 17
10 10 98     1.0 OPEN   FLOW-FROM 18
10 10 99     1.0 OPEN   FLOW-FROM 19
10 10 100    1.0 OPEN   FLOW-FROM 20
10 10 101    1.0 OPEN   FLOW-FROM 21
10 10 102    1.0 OPEN   FLOW-FROM 22
10 10 103    1.0 OPEN   FLOW-FROM 23
10 10 104    1.0 OPEN   FLOW-FROM 24
10 10 105    1.0 OPEN   FLOW-FROM 25
10 10 106    1.0 OPEN   FLOW-FROM 26
10 10 107    1.0 OPEN   FLOW-FROM 27
10 10 108    1.0 OPEN   FLOW-FROM 28
10 10 109    1.0 OPEN   FLOW-FROM 29
10 10 110    1.0 OPEN   FLOW-FROM 30
10 10 111    1.0 OPEN   FLOW-FROM 31
10 10 112    1.0 OPEN   FLOW-FROM 32
10 10 113    1.0 OPEN   FLOW-FROM 33
10 10 114    1.0 OPEN   FLOW-FROM 34
10 10 115    1.0 OPEN   FLOW-FROM 35
10 10 116    1.0 OPEN   FLOW-FROM 36
10 10 117    1.0 OPEN   FLOW-FROM 37
10 10 118    1.0 OPEN   FLOW-FROM 38
10 10 119    1.0 OPEN   FLOW-FROM 39
10 10 120    1.0 OPEN   FLOW-FROM 40
10 10 121    1.0 OPEN   FLOW-FROM 41
10 10 122    1.0 OPEN   FLOW-FROM 42
10 10 123    1.0 OPEN   FLOW-FROM 43
10 10 124    1.0 OPEN   FLOW-FROM 44
10 10 125    1.0 OPEN   FLOW-FROM 45
10 10 126    1.0 OPEN   FLOW-FROM 46
10 10 127    1.0 OPEN   FLOW-FROM 47
10 10 128    1.0 OPEN   FLOW-FROM 48
10 10 129    1.0 OPEN   FLOW-FROM 49
10 10 130    1.0 OPEN   FLOW-FROM 50
10 10 131    1.0 OPEN   FLOW-FROM 51
10 10 132    1.0 OPEN   FLOW-FROM 52
10 10 133    1.0 OPEN   FLOW-FROM 53
10 10 134    1.0 OPEN   FLOW-FROM 54
10 10 135    1.0 OPEN   FLOW-FROM 55
10 10 136    1.0 OPEN   FLOW-FROM 56
10 10 137    1.0 OPEN   FLOW-FROM 57
10 10 138    1.0 OPEN   FLOW-FROM 58
10 10 139    1.0 OPEN   FLOW-FROM 59
10 10 140    1.0 OPEN   FLOW-FROM 60
10 10 141    1.0 OPEN   FLOW-FROM 61
10 10 142    1.0 OPEN   FLOW-FROM 62
10 10 143    1.0 OPEN   FLOW-FROM 63
10 10 144    1.0 OPEN   FLOW-FROM 64
10 10 145    1.0 OPEN   FLOW-FROM 65
10 10 146    1.0 OPEN   FLOW-FROM 66
10 10 147    1.0 OPEN   FLOW-FROM 67
10 10 148    1.0 OPEN   FLOW-FROM 68
10 10 149    1.0 OPEN   FLOW-FROM 69
10 10 150    1.0 OPEN   FLOW-FROM 70 REFLAYER
SHUTIN 'INJ'

WELL  'INJ2'
INJECTOR 'INJ2'
INCOMP AQUEOUS 0.0 0.0 0.0 0.0 0.0 0.0 0.0 0.0 1.250125E-05 2.5351204
```

```
OPERATE MAX BHP 64121.2401 CONT
OPERATE MAX STW 28000.0 CONT
**      rad  geofac  wfrac  skin
GEOMETRY K  0.1  0.37  1.0  0.0
PERF    GEOA 'INJ2'
** UBA            ff        Status  Connection
10 10 1         1.0 OPEN   FLOW-FROM 'SURFACE'
10 10 81        1.0 OPEN   FLOW-FROM 1
10 10 82        1.0 OPEN   FLOW-FROM 2
10 10 83        1.0 OPEN   FLOW-FROM 3
10 10 84        1.0 OPEN   FLOW-FROM 4
10 10 85        1.0 OPEN   FLOW-FROM 5
10 10 86        1.0 OPEN   FLOW-FROM 6
10 10 87        1.0 OPEN   FLOW-FROM 7
10 10 88        1.0 OPEN   FLOW-FROM 8
10 10 89        1.0 OPEN   FLOW-FROM 9
10 10 90        1.0 OPEN   FLOW-FROM 10
10 10 91        1.0 OPEN   FLOW-FROM 11
10 10 92        1.0 OPEN   FLOW-FROM 12
10 10 93        1.0 OPEN   FLOW-FROM 13
10 10 94        1.0 OPEN   FLOW-FROM 14
10 10 95        1.0 OPEN   FLOW-FROM 15
10 10 96        1.0 OPEN   FLOW-FROM 16
10 10 97        1.0 OPEN   FLOW-FROM 17
10 10 98        1.0 OPEN   FLOW-FROM 18
10 10 99        1.0 OPEN   FLOW-FROM 19
10 10 100       1.0 OPEN   FLOW-FROM 20
10 10 101       1.0 OPEN   FLOW-FROM 21
10 10 102       1.0 OPEN   FLOW-FROM 22
10 10 103       1.0 OPEN   FLOW-FROM 23
10 10 104       1.0 OPEN   FLOW-FROM 24
10 10 105       1.0 OPEN   FLOW-FROM 25
10 10 106       1.0 OPEN   FLOW-FROM 26
10 10 107       1.0 OPEN   FLOW-FROM 27
10 10 108       1.0 OPEN   FLOW-FROM 28
10 10 109       1.0 OPEN   FLOW-FROM 29
10 10 110       1.0 OPEN   FLOW-FROM 30
10 10 111       1.0 OPEN   FLOW-FROM 31
10 10 112       1.0 OPEN   FLOW-FROM 32
10 10 113       1.0 OPEN   FLOW-FROM 33
10 10 114       1.0 OPEN   FLOW-FROM 34
10 10 115       1.0 OPEN   FLOW-FROM 35
10 10 116       1.0 OPEN   FLOW-FROM 36
10 10 117       1.0 OPEN   FLOW-FROM 37
10 10 118       1.0 OPEN   FLOW-FROM 38
10 10 119       1.0 OPEN   FLOW-FROM 39
10 10 120       1.0 OPEN   FLOW-FROM 40
10 10 121       1.0 OPEN   FLOW-FROM 41
10 10 122       1.0 OPEN   FLOW-FROM 42
10 10 123       1.0 OPEN   FLOW-FROM 43
10 10 124       1.0 OPEN   FLOW-FROM 44
10 10 125       1.0 OPEN   FLOW-FROM 45
10 10 126       1.0 OPEN   FLOW-FROM 46
10 10 127       1.0 OPEN   FLOW-FROM 47
10 10 128       1.0 OPEN   FLOW-FROM 48
10 10 129       1.0 OPEN   FLOW-FROM 49
10 10 130       1.0 OPEN   FLOW-FROM 50
10 10 131       1.0 OPEN   FLOW-FROM 51
10 10 132       1.0 OPEN   FLOW-FROM 52
10 10 133       1.0 OPEN   FLOW-FROM 53
10 10 134       1.0 OPEN   FLOW-FROM 54
10 10 135       1.0 OPEN   FLOW-FROM 55
10 10 136       1.0 OPEN   FLOW-FROM 56
10 10 137       1.0 OPEN   FLOW-FROM 57
10 10 138       1.0 OPEN   FLOW-FROM 58
10 10 139       1.0 OPEN   FLOW-FROM 59
10 10 140       1.0 OPEN   FLOW-FROM 60
10 10 141       1.0 OPEN   FLOW-FROM 61
10 10 142       1.0 OPEN   FLOW-FROM 62
10 10 143       1.0 OPEN   FLOW-FROM 63
10 10 144       1.0 OPEN   FLOW-FROM 64
10 10 145       1.0 OPEN   FLOW-FROM 65
10 10 146       1.0 OPEN   FLOW-FROM 66
10 10 147       1.0 OPEN   FLOW-FROM 67
10 10 148       1.0 OPEN   FLOW-FROM 68
10 10 149       1.0 OPEN   FLOW-FROM 69
10 10 150       1.0 OPEN   FLOW-FROM 70 REFLAYER
SHUTIN 'INJ2'

WELSEP 1, 2, 3, 4
STAGE
**  Stage Pres.  Stage Temp.
3203.99    23.8889
790.829    23.8889
101.325    15.5556
** ********************************************************************
** Definition of Triggers to open and close injector
** ********************************************************************
AIMWELL WELLNN
TRIGGER 'Injection'
ON_SECTOR 'FIELD' PAVE < 50000
*OPEN 'INJ'
DTWELL 0.001
```

END_TRIGGER

TRIGGER 'INJ2'
ON_WELL 'INJ' 'INJ2' STW-CI > 272044810
*OPEN 'INJ2'
*SHUTIN 'INJ'
DTWELL 0.001
END_TRIGGER

DATE 2014 2 1.00000
** ***
** The final date is 2044 1 1.00000
** ***

APPENDIX C – POLYMER VISCOSITY TABLES: LABORATORY DATA

Table C-1. Brine viscometer measurements

Polymer ppm	0		
Angle Torsion 300 rpm	1.5	n	0.999419586
Angle torsion 600 rpm	3	K	1.502493291
Rotor Speed	Shear rate (s^-1)	Dial reading (lb/100 ft^2)	Viscosity (cp)
100	10.47197551	3	1.5004
200	20.94395102	1.5	1.4998
300	31.41592654	1	1.4995
600	62.83185307	0.5	1.4989

Source: Author, 2019

Table C-2. Viscometer measurements for 500 ppm polymeric solution

Polymer ppm	500		
Angle 300	3	n	0.73653785
Angle 600	5	K	15.4823517
Rotor Speed	Shear rate (s^-1)	Dial reading (lb/100 ft^2)	Viscosity (cp)
100	10.4719755	1.5	8.3387
200	20.943951	2.5	6.9469
300	31.4159265	3	6.2430
600	62.8318531	5	5.2010

Source: Author, 2019

Table C-3. Viscometer measurements for 1000 ppm polymeric solution

Polymer ppm	1000		
Angle 300	6	n	0.58462298
Angle 600	9	K	79.8576137
Rotor Speed	Shear rate (s^-1)	Dial reading (lb/100 ft^2)	Viscosity (cp)
100	10.4719755	3	30.1037
200	20.943951	5	22.5725
300	31.4159265	6	19.0737
600	62.8318531	9	14.3019

Source: Author, 2019

Table C-4. Viscometer measurements for 2000 ppm polymeric solution

Polymer ppm	2000		
Angle 300	13	n	0.54717003
Angle 600	19	K	218.547979
Rotor Speed	Shear rate (s^-1)	Dial reading (lb/100 ft^2)	Viscosity (cp)
100	10.4719755	8	75.4479
200	20.943951	11	55.1229
300	31.4159265	13	45.8767
600	62.8318531	19	33.5179

Source: Author, 2019

Table C-5. Viscometer measurements for 3000 ppm polymeric solution

Polymer ppm	3000		
Angle 300	20	n	0.459164958
Angle 600	27.5	K	582.0874062
Rotor Speed	Shear rate (s^-1)	Dial reading (lb/100 ft^2)	Viscosity (cp)
100	10.4719755	8	163.4259
200	20.943951	11	112.3346
300	31.4159265	13	90.2147
600	62.8318531	19	62.0111

Source: Author, 2019